From the Department of Physiology and Pharmacology
Karolinska Institutet, Stockholm, Sweden

THE ROLE AND REGULATION OF NITRIC OXIDE AND OXIDATIVE STRESS IN CARDIOMETABOLIC DISEASE

FOCUS ON PREECLAMPSIA

Sarah McCann Haworth

Karolinska Institutet

Stockholm 2022

Published by Karolinska Institutet.
Printed by Universitets service US-AB, 2022

ISBN 978-91-8016-651-5

The role and regulation of nitric oxide and oxidative stress in cardiometabolic disease

Focus on preeclampsia

THESIS FOR DOCTORAL DEGREE (Ph.D.)

By

Sarah McCann Haworth

The thesis will be defended in public at Karolinska Insitutet, Inghesalen, Widerström Huset, Tomtebodavägen 18a, Solna, 20th of May 2022

Principal Supervisor:
Prof. Mattias Carlström, PhD, PharmD
Karolinska Institutet
Department of Physiology & Pharmacology
Division of Renal-Cardio-Metabolic Research

Co-supervisor(s):
Prof. Eddie Weitzberg, MD, PhD
Karolinska Institutet
Department of Physiology & Pharmacology
Division of Anaesthesiology & Intensive Care

Prof. Jon Lundberg, MD, PhD
Karolinska Institutet
Department of Physiology & Pharmacology
Division of Pharmacological Nitric Oxide Research

Rafael Krmar, MD, PhD
Karolinska Institutet
Department of Physiology & Pharmacology
Division of Renal-Cardio-Metabolic Research

Opponent:
Prof. Giovanni E. Mann
King's College London
Department of Vascular Biology & Inflammation
Division of Vascular Physiology

Examination Board:
Associate Prof. Malou Friederich Persson
Uppsala University
Department of Medical Cell Biology (MCB)

Prof. Thomas Kahn, MD, PhD
Karolinska Institutet
Department of Clinical Sciences
Division of Cardiology

Prof. Ganesh Acharya, MD, PhD
Karolinska Institutet
Department of Clinical Science, Intervention and Technology (CLINTEC)
Division of Obstetrics & Gynecology

In honour of Richard Bruce Flavell

ABSTRACT

Cardiovascular (CVD) and metabolic diseases account for significant morbidity and mortality. Over the last decades, despite significant research and clinical effort, their global prevalence is estimated to further increase. This trend is similarly observed in the pregnant population, which increases the risk of cardiometabolic complications of pregnancy, such as preeclampsia (PE), which in turn, predisposes both the mother and offspring to increased future cardiovascular and metabolic risk. Disruption of the delicate balance between nitric oxide (NO) and reactive oxygen species (ROS) leads to a vicious pathogenic cycle which results in oxidative stress and systemic vascular dysfunction, key features of numerous CVD and metabolic diseases. In the vasculature, NO is predominantly synthesised via endothelial nitric oxide synthase (eNOS), although the nitrate-nitrite-NO pathway can serve as an additional source. The latter can be stimulated by dietary inorganic nitrate, found in leafy green vegetables and beetroot.

The present thesis aimed to further explore the role of NO deficiency and oxidative stress in the pathogenesis of cardiometabolic disease, with focus on PE. We sought to dissect the mechanisms underlying the beneficial metabolic effects of dietary nitrate, investigate the role and mechanisms underlying erythrocrine function on endothelial homeostasis, assess the feasibility of conducting a clinical dietary nitrate intervention RCT in PE women and finally, examine how monocyte-derived factors perpetuate endothelial oxidative stress in PE.

In **study I**, models of diet-induced metabolic syndrome and liver steatosis demonstrated a novel therapeutic role of dietary nitrate, mediated via modulation of AMPK signalling and NADPH oxidase-derived oxidative stress. In **studies II, III**, and **IV**, *ex vivo* incubations of red blood cells (RBCs) and healthy murine aortas were utilised to specifically evaluate functional RBC-endothelial interactions. In **study II**, a lack of RBC eNOS induced endothelial dysfunction (ED), in part mediated via vascular arginase, elevated endothelial oxidative stress, and reduced NO bioavailability. In **studies III** and **IV**, RBCs isolated from PE patients, but not healthy pregnant women, induced ED, mediated via elevated arginase activity, reduced NO bioavailability, and elevated oxidative stress, in a contact-dependent manner. **Study IV** demonstrated that short term (7-day) dietary nitrate supplementation was well accepted and not associated with any adverse events. No significant differences in blood pressure changes were observed. Beneficial nitrate-independent effects on RBC-endothelial communication were observed *ex vivo*. In **Study V** an *in vitro* approach demonstrated that peripheral blood mononuclear cells (PBMCs) isolated from PE women increase oxidative stress and reduce NO bioavailability in the endothelium, which was prevented by antioxidant treatment (Silibinin).

The balance between NO bioavailability and oxidative stress governs endothelial homeostasis. Beneficially targeting this delicate balance can be achieved via dietary inorganic nitrate, which holds safe, therapeutic promise for cardiometabolic disease. The RBC is a central player in mediating this balance in the vascular microenvironment, dysregulated erythrocrine function results in ED. Further investigation regarding RBC-endothelial signalling may provide insight into previously discarded therapeutic approaches for cardiometabolic diseases.

LIST OF SCIENTIFIC PAPERS

I. **AMP-activated protein kinase activation and NADPH oxidase inhibition by inorganic nitrate and nitrite prevent liver steatosis**

Cordero-herrera, I., Kozyra, M., Zhuge, Z., **McCann Haworth, S. M.,** Moretti, C., Peleli, M., Caldeira-dias, M., Jahandideh, A., Huirong, H., Cruz, J. D. C., Kleschyov, A. L., Montenegro, M. F., Ingelman-sundberg, M., Weitzberg, E., Lundberg, J. O. & Carlstrom

Proc Natl Acad Sci USA. 2019 Jan;116(1):217-226.

II. **Endothelial Nitric Oxide Synthase-Deficient Mice Induce Vascular Dysfunction mediated in part via elevated oxidative stress and endothelial Arginase I**

Zhuge, Z*., **McCann Haworth, S. M***., Nihlén, C., Carvalho, L., Leo, F., Kleschyov, A. L., Cortese-Krott, M. M., Weitzberg, E., Lundberg, J. O. & Carlström, M.

Manuscript

III. **Red blood cells from patients with preeclampsia induce endothelial dysfunction**

McCann Haworth, S. **M***., Zhuge, Z*., Nihlén, C., Von Rosen, M. F., Weitzberg, E., Lundberg, J. O., Krmar, R. T., Nasiell, J. & Carlström, M.

J. Hypertens. 2021 Feb; 39(8): 1628–1641

IV. **Effects of dietary nitrate supplementation on blood pressure and gestational outcomes in preeclamptic women: a randomised, double-blind, placebo-controlled pilot study (NITBEETPE)**

McCann Haworth, S. M., Zhuge, Z., Nihlén, C., Von Rosen, M. F., Nasiell, J. & Carlstrom, M.

Manuscript

V. **Monocytes from preeclamptic women previously treated with silibinin attenuate oxidative stress in human endothelial cells**

Gomes, V. J., Rezeck Nunes, P., **McCann Haworth, S. M.,** Sandrim, V. C., Peraçoli, J. C., Peraçoli, M. T. S. & Carlström, M.

Hypertens. Pregnancy. 2021 Jan; 40(2): 124–132

**equal contribution*

ADDITIONAL PAPERS NOT INCLUDED IN THIS THESIS

I. **The novel organic mononitrate NDHP attenuates hypertension and endothelial dysfunction in hypertensive rats**

Paulo, L. L., Cruz, J. C., Zhuge, Z., Carvalho-Galvão, A., Brandão, M. C. R., Diniz, T. F., **McCann Haworth, S. M**. C., Athayde-Filho, P. F., Lemos, V. S., Lundberg, J. O., Montenegro, M. F., Braga, V. A. & Carlström, M.

Redox Biol. 2018 Dec; 15: 182–191

II. **Maternal androgen excess induces cardiac hypertrophy and left ventricular dysfunction in female mice offspring**

Manti, M., Fornes, R., Pironti, G., **McCann Haworth, S**. **M**., Zhengbing, Z., Benrick, A., Carlström, M., Andersson, D. & Stener-Victorin, E.

Cardiovasc. Res. 2019 Jul; 116(3): 619-632

III. **The obligatory role of host microbiota in bioactivation of dietary nitrate**

Moretti, C., Zhuge, Z., Zhang, G., **McCann Haworth, S**, Paulo, L. L., Guimarães, D. D., Cruz, J. C., Montenegro, M. F., Cordero-Herrera, I., Braga, V. A., Weitzberg, E., Carlström, M. & Lundberg, J. O.

Free Radic. Biol. Med. 2019 Jul; 145:342-348

IV. **Dietary nitrate attenuates high-fat diet-induced obesity via mechanisms involving higher adipocyte respiration and alterations in inflammatory status.**

Peleli, M., Ferreira, D. M. S., Tarnawski, L., **McCann Haworth, S. M.,** Xuechen, L., Zhuge, Z., Newton, P. T., Massart, J., Chagin, A. S., Olofsson, P. S., Ruas, J. L., Weitzberg, E., Lundberg, J. O. & Carlström, M.

Redox Biol. 2019 Nov; 28: 101387

V. **Head-to-head comparison of inorganic nitrate and metformin in a mouse model of cardiometabolic disease**

Cordero-Herrera, I., Guimarães, D. D., Moretti, C., Zhuge, Z., Han, H., **McCann Haworth, S. M.,** Uribe Gonzalez, A. E., Andersson, D. C., Weitzberg, E., Lundberg, J. O. & Carlström, M.

Nitric Oxide. 2020 Jan; 97: 48-56

CONTENTS

LIST OF ABBREVIATIONS

A2B receptor	Adenosine A2B receptor
ACADM	Gene encoding acyl-coenzyme A dehydrogenase
ACOG	The American College of Obstetricians and Gynaecologists
Akt	Protein kinase B (PKB)
AMP	Adenosine monophosphate
AMPK	5' adenosine monophosphate-activated protein kinase
Ang II	Angiotensin II
AP-1	Activator protein 1
APO	Adverse pregnancy outcomes
ATP	Adenosine triphosphate
AUC	Area under the curve
BH_4	Tetrahydrobiopterin
BMI	Body mass index
CAD	Coronary heart disease
CaMK-II	Calcium/calmodulin-dependent protein kinase II
cGMP	Cyclic guanosine monophosphate
CMD	Cardiometabolic disease
CO	Carbon monoxide
CRP	C-reactive protein
CV	Cardiovascular
CVD	Cardiovascular disease
DAF	4-amino-5-methylamino-2',7'-difluorofluorescein
DBP	Diastolic Blood pressure
DetaNONOate	2-(N,N-Diethylamino)-diazenolate 2-oxide sodium salt hydrate
DEXA	Dual-emission x-ray absorptiometry
DHE	Dihydroethidium
DNIC	Dinitrosyl iron complex
EC	Endothelial cells
ED	Endothelial dysfunction
EDHF	Endothelial-derived hyperpolarization factor
EDRF	Endothelial-derived relaxation factor
EDTA	Ethylenediaminetetraacetic acid
ELISA	Enzyme-linked immunosorbent assay
eNOS	Endothelial nitric oxide synthase
EO-PE	Early-onset PE
EPR	Electron paramagnetic resonance
ERK1/2	Extracellular signal-regulated kinases 1/2
ET-1	Endothelin 1
FAD/FMN	Flavin adenine dinucleotide
FMD	Flow mediated dilatation
GLUT-4	Glucose transporter type 4
GPx	Glutathione peroxidase
GTN	Glyceryl trinitrate
H_20_2	Hydrogen peroxide
Hb	Haemoglobin
HbA1c	Glycated haemoglobin
HbFe(II)NO	Nitrosyliron(II)haemoglobin
HFD	High fat diet
HNO_2	Nitrous acid
HO-1	Heme oxygenase-1
HP	Healthy pregnant women
HPLC	High-performance liquid chromatography
IHC	Immunohistochemistry

IPGTT	Intraperitoneal glucose tolerance test
IPITT	Insulin tolerance test
ISSHP	The International Society for the Study of Hypertension in Pregnancy
KO	Knock-out
L-NAME	NG-Nitro-L-arginine-methyl ester
LDLs	Low-density lipoproteins
LO-PE	Late-onset PE
MAP	Mean arterial pressure
MOA	Mechanism of action
mRNA	Messenger ribonucleic acid
NADPH	Nicotinamide adenine dinucleotide phosphate
NAFLD	Non-alcoholic fatty liver disease
NfκB	Nuclear factor-κb
NiRs	Nitrite reductase enzymes
NO	Nitric oxide
NO_2^-	Nitrite
NO_3^-	Nitrate
Nor-NOHA	Nω-Hydroxy-nor-L-arginine acetate
NOS	Nitric oxide synthase
NOX	NADPH oxidases
Nrf2	Nuclear factor E2-related factor-2
O_2^-	Superoxide
$OH^{\bullet -}$	Hydroxyl radical
$ONOO^-$	Peroxynitrite
OxyHb	Oxyhaemoglobin
p-ACC	Phosphorylated Acetyl-CoA Carboxylase
PBMCs	Peripheral blood mononuclear cells
PDE5	Phosphodiesterase inhibitor 5
PE	Preeclampsia
PETN	Pentaerythritol tetranitrate
PGI2	Prostacyclin
PVAT	Perivascular adipose tissue
RBCs	Erythrocytes
RNS	Reactive nitrogen species
$ROO^{\bullet}$	Peroxyl radical
ROS	Reactive oxygen species
RT-PCR	Reverse transcription polymerase chain reaction
Sb	Silibinin
SBP	Systolic Blood pressure
Ser615/633/1177	Serine 615/633/1177
sFLT1	Soluble fms-like tyrosine kinase 1
sGC	Soluble guanylyl cyclase
SIRT3	Sirtuin 3
SNO	S-nitrosothiols
SNO-Hb	S-nitrosated Hb
SOD	Superoxide dismutase
sPE	Severe preeclampsia
SREBP1c	Sterol regulatory element-binding protein 1
T2D	Type 2 diabetes
TBARS	Thiobarbituric acid reactive substances
TEMPOL	4-hydroxy-2,2,6,6-tetramethylpiperidine-N-oxyl
Thr495	Threonine 495
TXA2	Thromboxane
VSMCs	Vascular smooth muscle cells
vWF	Von Willebrand factor

1 INTRODUCTION

1.1 CARDIOMETABOLIC DISEASE

Cardiometabolic diseases are a group of common, often preventable, non-communicable conditions which include myocardial infarction, stroke, heart failure, diabetes, and non-alcoholic fatty liver disease (NAFLD). This interrelationship between cardiovascular (CVD) and metabolic diseases is complex and the result of robust epidemiological evidence, accumulated over the 20th century, demonstrating increased morbidity and mortality rates of CVD in the setting of dysmetabolic morbidities[1,2]. More recently, over an 8-year period, metabolic syndrome was associated with 33.7% of male cardiovascular events, and 46.9% of T2D diagnoses[3].

Importantly, these studies identified shared causal risk factors which predispose individuals to develop these diseases, and by extension, the targets for preventative treatment. This resulted in a clinical focus shift towards prediction and identification of at-risk and prodromal patients via screening of individual cardiometabolic risk scores. This concept encompasses traditional risk factors, such as hypertension, dyslipidaemia, dysglycaemia, smoking, age, sex, and family history, as well as emerging risk factors, such as abdominal obesity, insulin resistance, systemic inflammation, diet, exercise, and stress.

CVD remains the overall global leading cause of mortality, accounting for 23.9% of hospital admissions and 40% of all deaths between 2005-2016[4]. Indeed, global CVD mortality is estimated by WHO to exceed 23.6 million by 2030. Between 1990 and 2019, the global prevalence of total CVD doubled, concomitant with significantly increased prevalence of modifiable cardiovascular risk factors[5,6] .

Concurrently, prevalence of obesity (body mass index (BMI) >30kg/m^2) and type 2 diabetes (T2D) has significantly increased[3,7]. Between 1980-2015 global obesity rates have doubled[8], and in 2017 an estimated 462 million individuals had T2D worldwide[9]. In 2015, 4 million deaths were associated with a high BMI, with CVD being the leading cause of death (2.7 million) and diabetes being the second (0.6 million deaths)[8]. In 2019, the CAPTURE study reported that ~1 in 3 individuals with T2D had a diagnosed CVD[10].

These trends are mirrored in pregnant women globally. The presence of cardiometabolic morbidity pre-pregnancy increases the risk of adverse pregnancy outcomes (APOs)[11,12]. The significant physiological adaptations of pregnancy burden the cardiovascular system, rendering pregnant women particularly vulnerable to either development or exacerbation of existing CMD, both in the peri- and post- partum periods. Cardiometabolic complications of pregnancy (PE, gestational diabetes, and gestational hypertension) increase the risk of APOs and future cardiovascular risk of both mother and offspring[13–16], such that addition of cardiometabolic complications of pregnancy to traditional risk scores improves future CVD risk prediction of mothers[17].

CMD morbidity and mortality is predicted to increase over the next decade, despite implementation of improved preventative and therapeutic interventions. These contemporary epidemiological shifts in CMD incidence and mortality rates pose significant challenges for healthcare, therefore identification of novel therapeutic targets for the prevention of future CMD are urgently required. This is particularly important in high-risk populations, such as pregnant women, where treatment options are limited.

1.2 VASCULAR HOMEOSTASIS & DYSFUNCTION

Vascular homeostasis is crucial for optimal control of vascular tone to ensure adequate tissue perfusion. It is precisely regulated by crosstalk between multiple cellular compartments, including endothelial cells (ECs), vascular smooth muscle cells (VSMCs), and adventitial tissues containing inflammatory cells, autonomic nervous innovation, and the vasa vasorum. These are arranged into three distinct layers of the vascular wall, the intima, the tunica media, and the tunica externa. More recently, the role of local deposits of abluminal adipose tissue (perivascular adipose tissue; PVAT) in paracrine vascular regulation has been established[18,19]. Together, these cells/tissues interact to precisely orchestrate homeostasis and morphogenesis of the vascular wall.

Across differing vascular beds, the organisation of layers within the vascular wall differs depending on function, location, and size. Understanding these unique properties informs site-specific diagnostics and therapeutics. Briefly, the transition from artery to arteriole is characterised by a progressive thinning of elastic tissue within the tunica media, decreased lumen diameter and loss of definitive distinction between the three layers. Arterioles predominantly consist of VSMCs and are highly innervated by sympathetic nerves, this facilitates optimal regulation of blood flow relative to tissue requirements. To facilitate optimal tissue perfusion, capillary walls are composed of a single layer of ECs, which enhances gas, metabolite, and nutrient transfer between blood and tissues. Notably, the endothelial cell monolayer persists throughout.

Vascular dysfunction, specifically endothelial dysfunction (ED), is a crucial early predictor of future cardiovascular risk, correlates with disease progression and is a central mechanism which underpins cardiometabolic pathologies, including stroke[20,21], hypertension[22,23], coronary artery disease (CAD)[24], heart failure[25,26], peripheral artery disease[27,28], T2D[29,30], NAFLD[31,32], gestational diabetes mellitus and PE[33,34].

1.2.1 Endothelial function & dysfunction

The vascular endothelium is a highly dynamic, multi-functional monolayer of endothelial cells, with heterogeneity in structure and function across the vascular tree[35]. Its position enables it to play a key sentinel role in maintaining vascular homeostasis via acting as both a semipermeable physical barrier between blood and tissues, and rapidly responding to physical, chemical and hormonal signals via the local synthesis of endocrine mediators which regulate processes such as inflammation, vasomotion, vascular permeability, haemostasis, angiogenesis and fibrinolysis[36]. Its importance in the regulation of local vascular tone was seminally

demonstrated by Furchgott and Zawadzki in 1980, whereby removal of the endothelial layer from isolated arteries prevented *in vitro* acetylcholine-induced vasorelaxation, suggesting the release of an endothelial-derived relaxation factor (EDRF)[37].

Physiologically, the quiescent endothelium regulates the above processes via maintaining balanced production of vasoactive factors. These include vasodilatory, anti-thrombotic and anti-proliferative factors, such as NO, prostacyclin (PGI_2) and endothelium-derived hyperpolarizing factor (EDHF), or vasoconstrictive, pro-inflammatory and pro-thrombotic factors, such as thromboxane (TXA_2), endothelin-1 (ET-1), angiotensin II (Ang II), ROS, and von Willebrand factor (vWF).

ED is classically viewed as the disruption to this balance, which alters its ability to regulate the above processes in response to chronic exposure to several deleterious stimuli. These include the individual or cumulative effects of dysregulatory cardiovascular risk factors[38]. However, the exact influential interplay of cardiovascular risk factors on ED pathogenesis is complex and is only beginning to be elucidated. In 2020, EC heterogeneity across vascular beds and tissues was evidenced in single-cell RNA-seq murine analyses, which observed 78 sub-clusters of EC transcriptomes across 11 tissues, with tissue source dictating EC heterogeneity rather than type of vascular bed[39]. More recently, Pinheiro-de-Sousa *et al*[40] investigated the specific influence of CV risk factors on endothelial molecular architecture. *In vitro* exposure of human carotid artery ECs to surrogate CV risk factors, modelled the differentially expressed genes observed in human coronary artery plaques, in a hierarchical pattern of influence. Interestingly, the authors found that a combination of stimuli, as observed clinically in CV patients, induced a different global gene expression response vs the sum of each individual stimulus[40]. These studies highlight that the pathophysiological mechanisms underlying ED varies between diseases and patients, such that the definition and evaluation of ED must be context dependent.

1.3 NITRIC OXIDE (NO)

Following the discovery of an EDRF, substantial research effort was focused on its identification. Subsequent studies revealed that EDRF was unstable, mediated vasorelaxation via stimulation of soluble guanylate cyclase, inactivated by the superoxide (O_2^-) anion and other compounds with redox activity and haemoglobin (Hb), which culminated in Furchgott and Ignarro proposing nitric oxide as EDRF[41]. In 1998, Furchgott, Ignarro and Murad were awarded the Nobel Prize in Physiology and Medicine for their discoveries concerning “nitric oxide as a signalling molecule in the cardiovascular system”.

NO is a diatomic, colourless, gaseous signalling molecule and a free radical. Its characteristics (highly reactive, uncharged, small size, and lipid soluble) facilitate it to play a crucial homeostatic role in multiple physiological systems, as well as in several pathophysiological processes, via autocrine and paracrine actions. This is especially true for the cardiovascular system as NO governs cardiovascular homeostasis via mechanisms including regulation of vascular tone, platelet aggregation and overall cardiac function. Further, irregular NO synthesis and/or bioavailability is associated with several CV risk factors and is observed prior to

cardiovascular events and throughout cardiovascular pathogenesis. Indeed, reduced NO bioavailability is a crucial early mechanism in the pathogenesis of endothelial dysfunction[42].

1.3.1 NO signalling

The diverse biological properties of NO are mediated through a complex, redox-sensitive network of signalling pathways, such that it acts as both a substrate for oxidant formation and in an antioxidant capacity. Its three key reactions are with transition metals in enzymes, other free radical species and oxidation reactions which form reactive nitrogen species (RNS).

Reactions of NO with transition metals within enzymes, directly regulate their function. NO activates soluble guanylyl cyclase (sGC) via binding to its heme moiety. In the vasculature, this generates the second messenger cyclic guanosine monophosphate (cGMP) in VSMCs, which triggers a signalling cascade involving intracellular protein kinases, resulting in vasodilation, angiogenesis, and nerve signalling. Additionally, these reactions regulate mitochondrial and metabolic functions via reversible inhibition of the heme-copper oxygen binding site of cytochrome C oxidase, the terminal enzyme in the mitochondrial electron transport chain, and the oxidation of the iron-sulphur cluster within aconitase, respectively[43].

NO reacts with free radical species, including O_2^-, resulting in instant inactivation of NO, scavenging of O_2^- or formation of other RNS, such as peroxynitrite ($ONOO^-$). RNS can also be formed during oxidation of NO and have the capacity to post-translationally modify proteins or small molecules, thereby regulating their function. For example, via nitrosation of cysteine residues or nitration of tyrosine residues. Depending on the basal redox state and target of these reactions, their outcome can be protective (antioxidant, immunomodulatory), regulatory (vascular tone and permeability), or deleterious (DNA damage, lipid peroxidation, protein inhibition)[43].

1.3.2 1.2.1 NO generation pathways

1.3.2.1 NO synthase (NOS) pathway

The canonical NO synthesis pathway is nitric oxide synthase (NOS)-dependent, whereby NOS enzymes convert L-arginine to NO in an oxygen-dependent manner, as summarised in Figure 1A. There are three NOS isoforms: endothelial NOS (eNOS, NOS3), inducible NOS (iNOS, NOS2) and neuronal NOS (nNOS, NOS1). Structurally, they possess multiple binding sites, which are crucial for their function. These include sites for L-arginine, the co-factor tetrahydrobiopterin (BH_4) and a reductase domain which allows for interaction with electron donors (nicotinamide adenine dinucleotide phosphate; NADPH and flavin adenine dinucleotide; FAD/FMN)[43]. eNOS and nNOS are constitutively expressed and their activity is regulated by calcium. In contrast, iNOS is commonly induced via inflammatory stimuli and generates higher amounts of NO relative to the other NOS isoforms.

eNOS is highly abundant in blood vessels, primarily the endothelium. It accounts for the majority of NOS-dependent NO synthesis in this system and as such, is crucial for its

homeostasis. Mechanistic outcomes of reduced eNOS-derived NO include increased platelet aggregation[44], VSMC proliferation[45] and amelioration of endothelium-derived relaxation[46]. Indeed, eNOS dysregulation has been associated with an array of cardiovascular and metabolic disorders, including pro-atherogenic[47] and hypertensive[46] phenotypes, increased risk of thrombosis[48] and stroke[49,50], T2D[51,52], metabolic syndrome[53,54], and NAFLD[55,56].

Regulation of eNOS activity and expression is complex and involves several mechanisms, including dynamic transcriptional and post-translational regulation, as well as substrate and enzymatic co-factor availability. BH_4 depletion or L-Arginine deficiency result in uncoupling of eNOS, whereby the enzyme switches from a NO to O_2^- source, which in turn, triggers a cascade of detrimental redox reactions, as discussed further below (*section 1.4*). Multisite phosphorylation of eNOS regulates its activity. Phosphorylation of Ser615, 633 and 1177 of eNOS results in its activation, and phosphorylation of Thr495 reduces its activity. Ser1177 phosphorylation is governed by several kinases including AMP-activated protein kinase (AMPK), Akt, ERK1/2 and CaMK-II, the activation of which has been observed to be beneficial in several models of cardiometabolic pathologies[57,58]. Due to the diversity in signalling pathways that converge to regulate eNOS, and in turn bioavailability of eNOS-derived NO, it has been suggested as a crucial integration point which underlies the ED observed across cardiovascular and metabolic disorders[59].

1.3.2.2 NOS-independent nitrate-nitrite-NO pathway

Dietary nitrate (NO_3^-) and nitrite (NO_2^-) have long been considered unwanted residues in the food chain due to concerns related to the formation of carcinogenic nitrosamines, which drove substantial anti-nitrite sentiment[60]. Following the discovery of endogenously produced NO_3^-[61], and the role as a stable end-product of NO oxidation[62], the effects and physiological importance of NO_3^- and NO_2^- were reconsidered. In 1994, two independent research groups demonstrated that NO_3^- and NO_2^- could endogenously be reduced to NO in the stomach, providing the first indication of a NOS-independent NO synthesis pathway (i.e., nitrate-nitrite-NO pathway). The following year, direct reduction of NO_2^- to NO was evidenced during myocardial ischemia, which was not completely blocked by NOS inhibitors[63]. These observations triggered the development of a new research field focused on stimulation of the nitrate-nitrite-NO pathway as a source of NO *in vivo*.

A short half-life (milliseconds to seconds) and rapid scavenging reactions via other radical species and transition metals, limit the bioactivity of NO. In contrast, NO_2^- and NO_3^- anions are more stable, with intravascular half-lives of ~ 20 min and ~ 5-8 hours, respectively, and thus have widely been used a surrogate measure of NO. Leafy green vegetables (spinach, lettuce, rucola) and beetroot are rich sources of NO_3^-. Sources of NO_3^- and NO_2^- also include the oxidation of NOS-derived NO in blood and tissues, with fasting levels ranging from 20-40uM and 0.05-0.3uM, respectively[64]. Circulating levels of these anions are dynamic, key influential factors include timing of dietary NO_3^- ingestion, which induces peak nitrate levels after 15-30 mins[65], and NOS activity and expression.

The nitrate-nitrite-NO pathway utilises NO_3^- and NO_2^- to produce NO and other bioactive nitrogen oxide species via serial reduction catalysed by native mammalian and commensal bacteria proteins[64], as summarised in Figure 1B. Digestion of dietary nitrate occurs via an enterosalivary mechanism. Following efficient absorption in the gut, nitrate enters the circulation. The majority of circulating nitrate is renally excreted, however up to 25% is taken up by salivary glands, concentrated and excreted into the oral cavity. For the conversion of nitrate to nitrite, oral commensal anaerobic bacteria are required. This is due to the abundance of nitrate reductase (NiRs) enzymes in some of these bacteria, which mammalian cells are functionally lacking. NiRs refer to a wide variety of enzymes which catalyse the reduction of nitrite. In the acidic environment of the stomach, the nitrite in the saliva is either immediately protonated to form nitrous acid (HNO_2), which subsequently decomposes to NO and other nitrogen oxides via non-enzymatic dehydration and disproportionation reactions or absorbed in the small intestine to reach the circulation. In less acidic pH environments, circulating and intratissue nitrite is reduced to NO and other reactive nitrogen oxide species, via both non-enzymatic and enzymatic (NiR) systems (*e.g.* low pH/hypoxia, ferrous globins (Hb and MyoHb), xanthine oxidase (XO), cytochrome P450s, mitochondrial electron transport chain complexes)[64]. Both the NOS-dependent and independent NO synthesis pathways can work in parallel. Both function under normoxic conditions, however, the latter is oxygen-independent, and is downregulated in hypoxic/ischemic and acidic environments, when function of the NOS enzymes are compromised. Interestingly, evidence of a potential crosstalk between these pathways was demonstrated *in vivo*, whereby long-term dietary nitrate supplementation reduced aortic eNOS Ser1177 phosphorylation in a dose-dependent manner and increased eNOS Thr495 phosphorylation. These observations were concomitant with a reduction in eNOS-dependent vasoreactivity and, at a higher nitrate dose, elevated blood pressure and plasma cGMP levels vs controls. However, following pharmacological inhibition of NOS, the higher nitrate dose significantly reduced blood pressure vs controls[66].

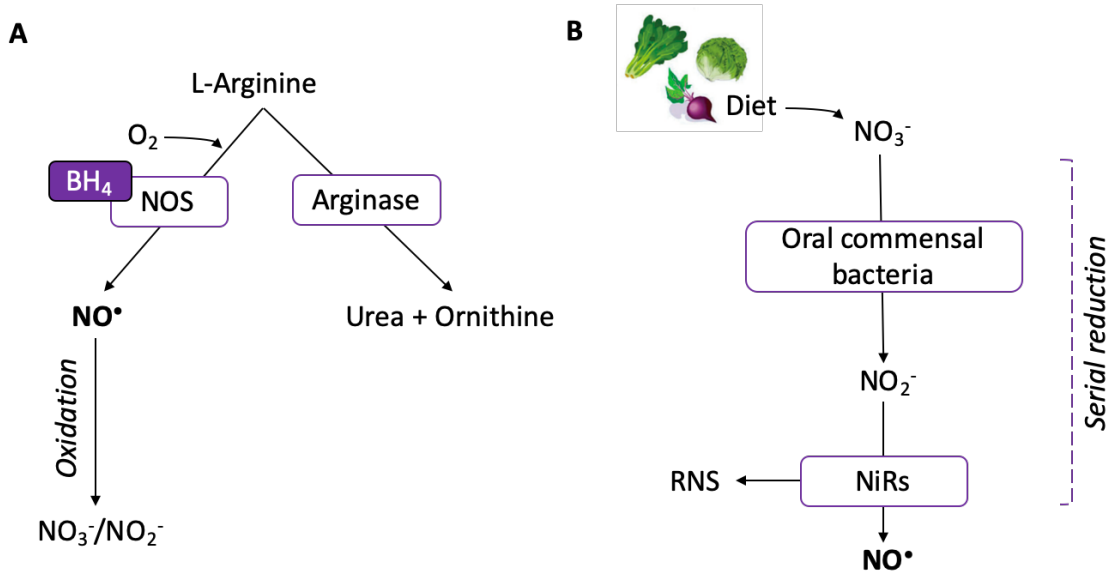

Figure 1. Comparison of pathways of NO generation and metabolism. (A) Endogenously generated NO from NOS enzymes, which use L-Arginine and molecular oxygen as substrates. Cofactor BH_4 enables dimerization of eNOS and L-Arginine binding. Arginase competes with NOS for the substrate L-Arginine. **(B)** Ingested dietary inorganic nitrates are serially reduced during an entero-salivary circulation, by oral commensal bacteria and nitrite reductase enzymes (NiRs) to NO and other RNS.

1.3.3 Therapeutic aspects of the nitrate-nitrite-NO pathway

1.3.3.1 Modulation of cardiovascular function

In 2006, Larsen *et al*[67] were the first to present a short-term vasodilatory effect of nitrite-derived NO, whereby inorganic nitrate supplementation (0.1 mmol/kg for 3 days) in healthy normotensive participants decreased diastolic blood pressure (DBP) by 3.7mmHg compared to placebo. Subsequently, Webb *et al*[68] demonstrated similar vasodilatory effects following ingestion of beetroot juice (0.3 mmol/kg nitrate). The peak difference in systolic blood pressure (SBP) was -10.4mmHg vs control, 2.5 hours post ingestion. This effect was maintained at 24hrs post ingestion, with a 4.4mmHg reduction in SBP vs control. However, disruption of the enterosalivary circulation post ingestion (via spitting out saliva for 3 hours) prevented decreases in SBP and increases in plasma nitrite[68]. Later, similar findings (-7.7 mmHg SBP, -5.2 mmHg DBP vs placebo) were demonstrated in hypertensive patients following a 4 week daily ingestion of beetroot juice (6.5 mM nitrate)[68]. Since then, numerous studies have demonstrated a blood pressure lowering effect of dietary nitrate ingestion[69,70].

In humans, endothelial function correlates with plasma nitrite concentration. Accordingly, elevations in plasma nitrite via dietary supplementation has been shown to improve endothelial function[71]. Concomitant to the BP observations, Webb *et al*[68] observed prevention of ischemia-reperfusion induced reduction in flow-mediated dilatation (FMD) following ingestion of beetroot juice. Following a single dose of dietary nitrate (0.15 mM/kg in 150ml, post 1.5 hours), FMD of the brachial artery was improved in healthy volunteers, which was associated with

increased abundance of circulating endothelial progenitor cells[72], thus suggesting a mechanistic role of nitrate in vascular regeneration.

In an *in vivo* model of diet-induced hypercholesterinaemia, nitrite supplementation (33 mg/L nitrite for 3 weeks) prevented development of endothelial dysfunction, vascular leukocyte recruitment and emigration, and elevations in circulating C-reactive protein (CRP), suggesting an anti-inflammatory vascular role of nitrite. Additionally, a nitrite-induced elevation in hepatic BH_4 levels was observed vs control[73]. Carotid arterial ED and aortic pulse wave velocity was reduced in aged mice following nitrate supplementation (50 mg/L) for 3 weeks, to levels comparable to young mice. In the same study, scavenging of free radicals via 4-hydroxy-2,2,6,6-tetramethylpiperidine-N-oxyl (TEMPOL) and NADPH oxidase (NOX) inhibition via apocynin treatment restored endothelial function in control aged mice, suggesting nitrate mediates a reduction in NOX-derived O_2^- production[74]. More recently, a meta-analysis confirmed these findings demonstrating that dietary nitrate supplementation via beetroot juice significantly decreased arterial pulse wave velocity by 0.27 m/s and increased FMD by 0.62%, compared with controls[75].

1.3.3.2 Modulation of metabolic function

Following the discovery of NO signalling, eNOS knock-out (KO) mice were demonstrated to be hypertensive, insulin resistant and exhibit hallmark features of metabolic syndrome, including dyslipidaemia, glucose intolerance, and increased abdominal fat[46,76], thus highlighting the crucial role of eNOS in metabolic homeostasis. Similar findings were observed following a 14-day pharmacological inhibition of eNOS *in vivo*[77]. Utilising this model, Carlström *et al*[78] first demonstrated the beneficial metabolic potential of dietary nitrate. eNOS KO mice supplemented with dietary nitrate (1mM in drinking water; 8-10 weeks), at similar concentrations to replace physiologically generated eNOS-derived NO[79]**,** exhibited improved glucose tolerance, and reduced plasma triglycerides, lower levels of glycated haemoglobin (HbA1c,) weight gain and visceral fat. Thus, highlighting the capacity of dietary nitrate to partially compensate for the dysfunctional metabolic sequalae of deficiency in eNOS-dependent signalling. Later results expanded the beneficial effects of dietary nitrate in other *in vivo* models of metabolic syndrome and T2D, including increased insulin secretion and islet blood flow, increased skeletal muscle glucose uptake and mitochondrial efficiency, and increased browning of fat[80–84].

In accordance with the significant prevalence of liver steatosis patients with metabolic comorbidities[85], the beneficial metabolic effects of dietary nitrate are conferred to the liver. *In vivo* induction of hepatic steatosis via a calorie dense diet and ovariectomy was suppressed by 150 mg/L nitrite supplementation for 18 weeks[86]. In healthy mice, supplementation with 0.5mM sodium nitrate for 7 months decreased hepatic lipid deposition[87]. Interestingly, after 18 months consumption of a nitrate-depleted diet (<4.8 μmol/kg vs 548.3 μmol/kg in regular diet), control mice exhibited endothelial dysfunction, hypertension, and features of metabolic syndrome[88]. This demonstrated that sufficient long-term intake of dietary nitrate is crucial for maintenance of metabolic homeostasis.

Despite this, supporting evidence from clinical trials is lacking. Gilchrist *et al*[89] investigated dietary nitrate supplementation (via beetroot juice) on insulin sensitivity in T2D patients (n=27), which failed to observe beneficial effects. Of note, these patients maintained their hypoglycaemic medications, including metformin. The mechanism of which is thought to be mediated via AMPK activation, similarly to the mechanism of action of dietary nitrate, as discussed below.

The identification and interplay of mechanisms underlying the observed beneficial metabolic effects of dietary nitrate supplementation remain to be fully elucidated. Thus far, evidence supports modulation of mitochondrial function, AMPK activation, glucose transporter type 4 (GLUT-4) translocation, elevated insulin release, reduction of NOX-derived oxidative stress and immune cell regulation, as mechanistic candidates[84].

The serine/threonine kinase AMPK complex is an important sensor of cellular metabolism, which facilitates rapid metabolic adaptation to meet intracellular energy requirements and respond to availability of nutrients. AMPK responds to an increased intracellular [AMP]/[ATP] ratio via phosphorylating specific targets to induce ATP generation and reduce ATP consumption. This 'energy switch' regulates multiple cellular processes including lipid and glucose metabolism[90]. However, in diet-induced obesity and T2D, AMPK activation is repressed[91,92], therefore it is a desirable therapeutic target for these diseases. Dietary nitrate treatment increased AMPK phosphorylation, thus activation, in liver[93] and skeletal muscle[94] in *in vivo* models of metabolic syndrome, as well as in skeletal muscle biopsies from patients with metabolic syndrome[94]. Amongst other mechanisms, AMPK increases cellular glucose utilisation via promoting trafficking of GLUT-4 to the plasma membrane, where it facilitates transport of glucose into the cell[90]. Exposure to nitrite was demonstrated to increase GLUT-4 translocation *in vitro* facilitated via a proposed mechanism of nitrite derived-NO mediation of GLUT-4 nitrosation[95]. Similarly, *in vivo* models of T2D supplemented with dietary nitrate demonstrated increased GLUT-4 protein expression on the cell membrane of soleus muscle, epididymal adipose tissue[96] and skeletal muscle[94,97]. However, Lai *et al*[94] suggested an alternative mechanism of a nitrite-driven activation of SIRT3-AMPK signalling, and downstream GLUT4 translocation.

Evidence is mounting in support of dietary nitrate supplementation reducing NOX activity, specifically in metabolic *in vivo* models*,* thus reducing NOX-derived ROS and elevating NO bioavailability. In aged rats (22 months), supplementation with nitrate (10mM in drinking water, 14 days) significantly reduced NOX activity in cardiac and renal tissues, concomitant to improved glucose clearance and insulin release[98]. In a genetic model of metabolic syndrome, A2B receptor knockout mice ($A^{-/-}$), nitrate treatment improved the metabolic phenotype and hepatic NOX activity both before and after acute glucose supplementation[93].

In summary, the therapeutic scope of stimulating the nitrate-nitrite-NO pathway via dietary interventions to boost NO bioavailability in cardiometabolic pathologies is vast. Further exploration of the specific targets and mechanisms underlying these beneficial effects is warranted.

1.4 VASCULAR OXIDATIVE STRESS

Oxidative stress arises due to an imbalance between pro- and antioxidant systems. It is induced in pathophysiological states via an abundance of ROS, and decreased synthesis and dysfunction of antioxidant protective pathways[99].

ROS are short-lived, reactive molecules and ions, derived from partially reduced molecular oxygen, which play critical signalling roles in the regulation of various physiological and pathophysiological processes. ROS are classified as either free radical, containing an unpaired electron, or nonradical. Free radicals include $O_2^{\bullet-}$, the hydroxyl radical ($OH^{\bullet-}$) and peroxyl radical ($ROO^{\bullet}$), they are highly unstable and thus have short biological half-lives. In comparison, nonradicals have relatively longer half-lives and are more stable, these include hydrogen peroxide (H_2O_2) and $ONOO^-$. Physiological functions of ROS, where low levels of ROS are present, include regulation of host defence, vascular homeostasis, immunity and cellular growth, senescence, apoptosis, oxygen tension. However, excessive accumulation of ROS, can lead to states of oxidative stress and result in cellular damage.

In the vasculature, the major sources of ROS are NOXs, especially isoforms NOX1, NOX2, NOX4 and NOX5, XO, the mitochondrial electron transport chain, and uncoupled eNOS[100]. Vascular antioxidant systems consist of various enzymes, including superoxide dismutase (SOD), catalase and glutathione peroxidase (GPx), which act to stabilise or deactivate ROS and in turn, reduce the oxidative burden. In addition, dietary or endogenously synthesised compounds, such as vitamin C, vitamin E, uric acid, flavonoids, and thiol compounds, neutralise ROS[101]. Importantly, the capacity/efficiency of these antioxidant systems to provide redox homeostasis may be impaired by excessive ROS, thus propagating their imbalance.

Vascular oxidative stress contributes to the pathogenesis of multiple cardiometabolic diseases, such as atherosclerosis, hypertension, and diabetes[102]. This oxidative stress is propagated systemically in the vasculature and contributes to development of vascular injury via multiple mechanisms, including inducing an imbalance between vasodilatory and vasocontractile factors, promotion of VSMC hypertrophy, deposition of collagen and fibronectin in the vascular wall, oxidation of low-density lipoproteins (LDLs) leading to foam cell formation and platelet activation[103].

Excessive ROS crucially mediates sustained damage to the endothelium, resulting in endothelial dysfunction. As aforementioned, NO can act as an antioxidant via reacting with free radical species, whereby O_2^- can react rapidly with NO to produce $ONOO^-$. However, this results in a reduction in NO bioavailability and propagation of $ONOO^-$ induced cellular damage. This process becomes pathological in environments with excessive ROS, resulting in NO bioavailability being significantly compromised. This results in a dysregulation of NO homeostasis, and in turn, endothelial dysfunction.

NOS enzymes compete with arginase for the common substrate L-arginine. Increased arginase activity is stimulated by a variety of stimuli, including H_2O_2, $ONOO^-$ and NOX. This results in the shunting of L-arginine into ornithine and urea production (Figure 1A), resulting in reduced

NO formation concomitant with eNOS uncoupling[104]. As outlined above, eNOS uncoupling significantly reduces eNOS-derived NO bioavailability. BH_4 is particularly sensitive to oxidation by $ONOO^-$, resulting in its depletion, which leads to further uncoupling of eNOS. Uncoupled eNOS produces $O_2^{\bullet-}$, which is catalytically converted by SOD to form hydrogen peroxide, which can be eliminated by catalase-mediated decomposition to oxygen and water. Under oxidative stress conditions, these antioxidant defence systems may become overwhelmed. Further redox regulation of eNOS activity includes oxidative disruption of in the binding region of the eNOS dimer, S-Glutathionylation of the eNOS reductase domain, and phosphorylation of Thr495[105]. Overall, this results in a viscous cycle of a progressive increase in ROS and decrease in NO bioavailability, thus propagating oxidative stress.

Heme oxygenase-1 (HO-1) is an endogenous cytoprotective enzyme which plays a role in maintaining homeostasis during oxidative stress via catabolism of pro-oxidant heme into carbon monoxide (CO), biliverdin and free iron (Fe^{2+}). Both HO-1 *per se* and heme metabolites exhibit antioxidant and anti-inflammatory properties, both of which are crucial for preservation of vascular NO. HO-1 expression is upregulated by multiple stimuli including oxidative stress and cytokines. Oxidative stress activates various transcription factors including nuclear factor E2-related factor-2 (Nrf2), activator protein-1 (AP-1), and nuclear factor-κB (NfκB), which promote HO-1 expression. HO-1 deficiency has been demonstrated to render the endothelium more susceptible to systemic damage via mechanisms including acceleration of atherosclerotic lesion formation, increased lipid accumulation, VSMC proliferation and elevated ROS[106–108]. HO-1 has been demonstrated to mediate its protective endothelial effects via preserving bioavailability of NO, mechanistically via prevention of eNOS uncoupling[109], suppression of NOX activity[110], and upregulating SOD and catalase[111]. Therefore HO-1 is a promising target for protection against oxidative stress, whilst concomitantly preserving eNOS-derived NO.

1.5 RED BLOOD CELLS IN CARDIOMETABOLIC DISEASE

Canonically, red blood cells (RBCs) play a critical physiological role via gaseous (O_2 and CO_2) transportation between the lungs and peripheral tissues, this is governed by complex inter- and intracellular mechanisms. The close proximity of RBCs to other blood cells and adjacent vascular beds, promotes their dynamic interaction which can influence their function. RBCs synthesise, store and export vasoactive molecules, including NO-like bioactivity and adenosine triphosphate (ATP), which enables them to induce vasorelaxation under hypoxia[112,113]. Changes in RBC structure and function have been described in cardiometabolic disease, a phenomenon entitled 'erythropathy'[114]. These include increased ROS formation, a reduction in antioxidant capacity and increased vascular wall adhesion, as well as altered protein levels and expression, morphology, and deformability[114,115].

1.5.1 RBC-derived NO bioactivity

RBCs generate NO bioactivity, however questions regarding the specific source, molecular form and export of RBC-derived NO remain. As a result of the high levels of Hb in RBCs facilitating the ultrarapid scavenging of NO by oxyhaemoglobin (oxyHb), the functional

importance of RBC export of NO has long been debated. Proposed sources of RBC-derived NO bioactivity include the export of S-nitrosothiols (SNO) from intraerythrocytic S-nitrosated Hb (SNO-Hb)[116], nitrosyliron(II)haemoglobin (HbFe(II)NO)[117], mobile nitrosyl-heme[118], and nitrite[119–121].

Catalytically active eNOS is expressed in RBCs at low levels, localised to the plasma membrane and cytoplasm[122]; however, its physiological role remains the subject of debate[123]. Interestingly, even in the presence of high Hb levels, studies have evidenced that RBC eNOS influences plasma nitrite concentration[124], blood pressure[119, 120] and mediates cardioprotection in ischemia-reperfusion injury[126,127]. Further, recent evidence suggests that RBC eNOS modulates levels of circulating NO metabolites and blood pressure, independently of EC eNOS[125].

1.5.2 Redox signalling in RBCs

RBCs are supersaturated with Hb (~10mM heme), which is maintained in its reduced Fe^{2+} state to facilitate oxygen binding via coordinated network of antioxidant and reducing enzymes, including SOD, catalase, glutathione, and glutathione peroxidase. These enable RBCs to maintain cell function and integrity and, via conferring their protection to peripheral tissues, provide systemic redox buffering[128]. The dominant source of ROS in RBCs is the continuous autooxidation of $HbFe^{2+}$, which produces methaemoglobin (MetHb; Fe^{3+}) and O_2^-, and in turn, hydrogen peroxide. Enzymatic sources include NOX[129] and XO[130]. Oxidative stress in RBCs has been linked with T2D, whereby elevations in RBC-derived ROS deleteriously impact the cardiovascular system, including induction of endothelial oxidative stress and reduced endothelial function[131–133].

1.5.3 RBC arginase

Findings suggest a tight regulation of RBC-derived NO bioactivity via arginase which is dependent on RBC eNOS[126]. Studies have highlighted dysregulation of RBC arginase in cardiac function[126] and T2D[132,134]. In an *ex vivo* model of myocardial-ischemia-reperfusion injury, inhibition of RBC arginase in perfused RBCs significantly improved cardiac function post-ischemia. Additionally, export of NO metabolites (nitrate and nitrite) from isolated RBCs was increased following arginase inhibition[126]. In a separate study, co-incubation of RBCs from T2D patients with wild-type rat aortas induced ED when compared with healthy RBCs. This dysfunction was alleviated when RBCs were pre-incubated with a pharmacological arginase inhibitor[132]. In addition, arginase activity and expression was upregulated in human T2D RBCs vs healthy, with concomitant increased NOX1 and NOX2 expression[132].

Together, these observations suggest that RBC eNOS is biologically active, and has the capacity to influence cardiovascular function. Additionally, that RBC-derived ROS are linked to the development of cardiometabolic disease. Further, RBC arginase downregulates export of RBC-derived NO bioactivity in pathological cardiometabolic states. Further investigation into whether this phenomenon is mirrored across other cardiometabolic diseases is warranted. Additionally, further detailed insight into the specific functional interaction(s) between RBC

eNOS and the endothelium would be valuable in elucidating the specific mechanisms by which RBCs mediate cardiometabolic disease. In future, these could be developed into novel therapeutic strategies for CMD.

1.6 PREECLAMPSIA

PE is a major multisystem obstetric disorder, clinically characterised by a new-onset maternal hypertension (≥140 mmHg SBP and/or ≥90 mmHg DBP), and *de novo* proteinuria or evidence of other renal or liver dysfunction, a low platelet count or new-onset headaches or visual disturbances, after 20 weeks of gestation[135]. PE with severe features (sPE) is characterised via severe range hypertension (≥160 mmHg SBP and/or ≥110 mmHg DBP) or any other severe features. Estimated global PE incidence ranges from 3.4-4.6% of all pregnancies[136,137], and it is a major cause of foetal and maternal mortality[138]. Incidence of PE is associated with increased risk of adverse maternal complications. Between 2010-2011, 16.3% of severe maternal outcomes were attributed to PE globally[139].

Further, the outcomes of PE extend beyond the gestational period for both the mother and offspring. A history of PE is independently associated with a 1.97-fold increased risk of CVD[140] and development of CVD risk factors[141]. Post-PE, women have a 3.13-fold greater risk of hypertension[142], and a 2.25-fold increased risk of T2D[143] vs women with normal pregnancies. *In utero* exposure to PE was associated with hypertension (+2.39/+1.35 mmHg SBP/DBP vs controls), increased BMI[144], and increased fasting glucose[145] during childhood and young adulthood.

1.6.1 PE Pathogenesis

PE represents a complex, heterogenous disorder which is associated with multiple pathogenic mechanisms; however, the exact cause is unknown. In 1991, Redman[146] was the first to associate the placenta with PE, proposing the classical two-stage model of PE pathogenesis; pre-clinical placental dysfunction (Stage 1), and subsequent induction of the clinical maternal syndrome (Stage 2) via release of factors from the hypoxic placenta. Later seminal findings confirmed this, and in 1989, ED was first suggested to underlie the clinical manifestations of PE[146]. Since then, the 2-stage model has evolved to integrate maternal risk factors, the two main placental dysfunction pathways (extrinsic vs intrinsic) and the mediators which link stage 1 and 2 (illustrated in Figure 2)[147].

PE patients are classified by the time of delivery, either early-onset PE (EO-PE; <34 weeks), intermediate onset (34-37 weeks) or late-onset PE (LO-PE; >37 weeks). EO-PE is largely a result of dysfunction of placentation and unmodeled spiral arteries (the extrinsic placenta). This results in increased uterine-circulation resistance and uteroplacental hypoperfusion, thus creating an ischaemic/hypoxic placental environment. Subsequently, this induces a state of oxidative stress and the placental release of multiple pro-inflammatory and anti-angiogenic factors into the systemic circulation[148]. LO-PE pathogenesis has more recently been postulated to be due to placental capacity being exceeded as gestation advances (the intrinsic placenta).

This induces a state of placental inflammation and oxidative stress, which triggers the systemic manifestations[147].

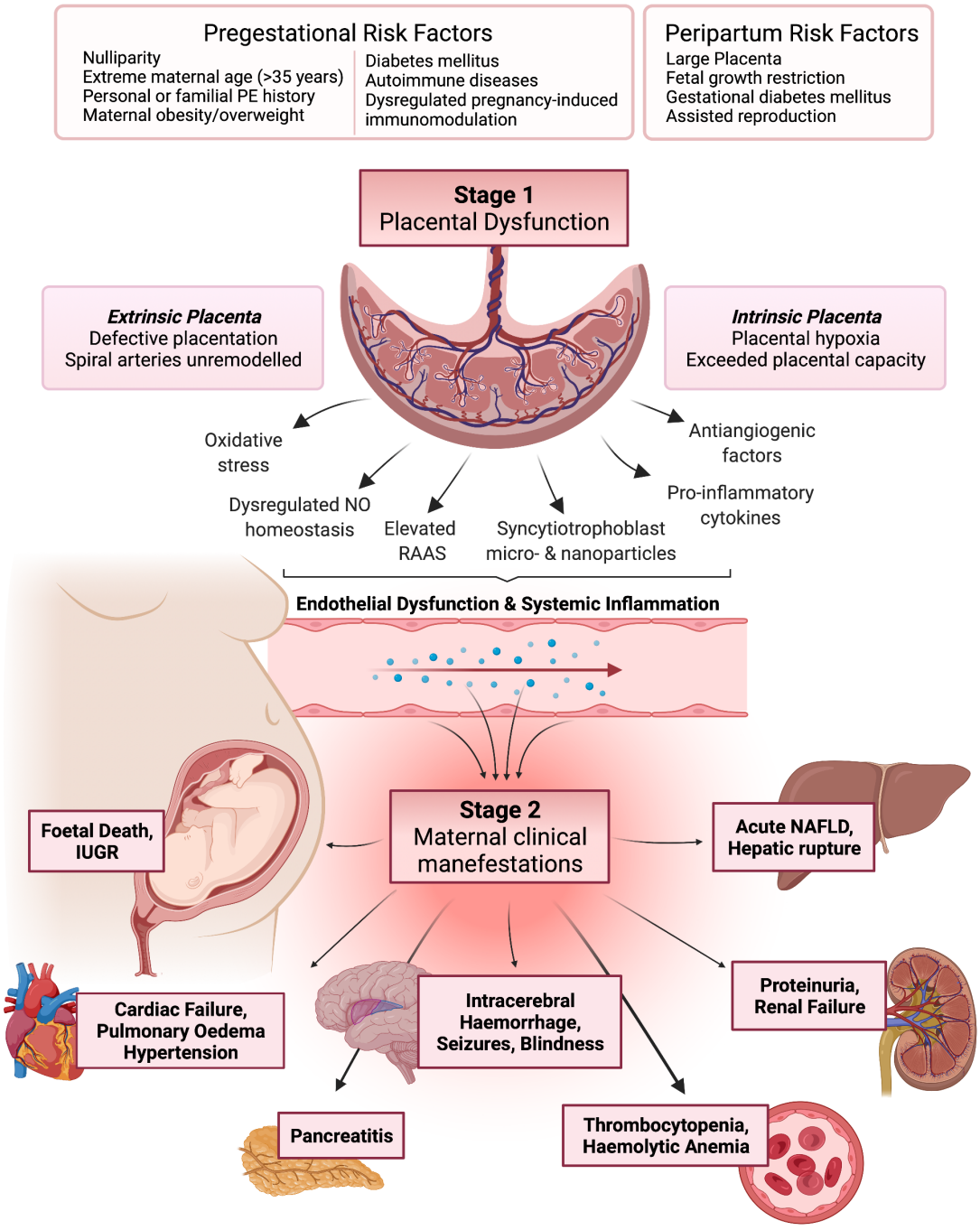

Figure 2. Two-stage model of PE pathogenesis, integrating maternal risk factors, placental pathways, and clinical manifestations. NO; nitric oxide, PE; preeclampsia, IUGR; intrauterine growth restriction, NAFLD; non-alcoholic fatty liver disease, RAAS; renin-angiotensin-aldosterone system. Created with BioRender.com.

1.6.2 PE Treatment Approaches

Development of pharmacological approaches for pregnant populations is complex due to the interdependent maternal and fetal safety concerns and ethical considerations. This issue is compounded by the elusive aetiology and complex pathophysiology of PE. Despite its prevalence, aspirin (75-150 mg/day for 11-14 weeks) is the only approved preventative strategy

for PE, having been associated with lower incidence vs placebo[149]. Currently, despite a significant research effort, there are no approved available treatment options for pre-eclamptic patients, aside from delivery of the placenta[150]. Therapeutic options for PE are limited to the treatment of hypertension, expectant management of seizures, and close foetal monitoring. Current clinical recommendations include administration of magnesium sulphate for the prevention and treatment of seizures, and anti-hypertensive and anti-thrombotic medications[135]. However, there is a lack of consensus regarding the associated maternal and foetal risks of employing antihypertensive agents[151–155].

1.6.3 PE-associated vascular endothelial dysfunction

Importantly, it is the progression of the diverse systemic manifestations of the disease (stage 2) which accounts for its severe clinical manifestations and maternal and fetal mortality. The vasculature is central to this progression, and as such, is consistently exposed to deleterious circulating factors. This results in systemic ED, characterised by oxidative stress and dysregulation of angiogenic signalling and inflammatory processes[147]. Therefore, therapeutic approaches aiming to protect the endothelium, via targeting the pathogenic mediators, may provide prophylaxis for women at high risk for PE.

1.6.3.1 Oxidative stress in PE

Oxidative stress is a central pathogenic contributor to the ED observed in PE. The ischemic/hypoxic and inflammatory environment of the utero-placental circulation induced by placental dysfunction is reported to be the initial stimulus of excessive ROS. Indeed, studies have reported multiple placental sources of ROS including; mitochondria[156], NADPH oxidases[157–159], XO[160] and uncoupled eNOS[161]. As gestation progresses, in addition to placental sources, ROS production is also propagated by maternal circulating factors such as cytokines[158], oxidised low-density lipoproteins[162] and lipid peroxides[163]. Concomitantly, insufficiency in placental and vascular antioxidant capacities has been reported *in vitro*[164], however clinical studies have failed to report beneficial therapeutic effects of vitamin C and E supplementation in PE[165,166].

1.6.3.2 NO metabolism in PE

During pregnancy, NO is crucial in mediating the diverse response to the systemic increases in blood volume, cardiac output and decreased vascular resistance, therefore in healthy pregnancy, endogenous NO is elevated[167]. Whereas in PE, although there have been conflicting reports, dysregulated maternal NO homeostasis has been evidenced clinically via reduced urinary[168] and plasma[169] nitrate/nitrite levels, increased NO consumption[170] and reduced FMD[171] in PE vs healthy pregnancies.

In vivo studies utilising eNOS KO and NOS inhibited pregnant mice have demonstrated a role of dysfunctional eNOS in the development of a pre-eclamptic phenotype[172]. *Ex vivo* studies observed reduced endothelium-dependent relaxation in vessels incubated with plasma from PE vs healthy pregnant (HP) women[173,174]. In addition, the anti-platelet aggregative properties of

NO are reduced in women with PE as evidenced by elevated systemic activation of platelets[175]. Proposed mechanisms underlying reduced endogenous NO bioavailability in PE include scavenging via ROS and/or ferric heme, upregulation of arginase, vascular endothelial growth factor deficiency, upregulation of endogenous NOS inhibitors such as asymmetric dimethylarginine[176], and upregulation of soluble fms-like tyrosine kinase 1 (sFLT1)[172].

1.6.4 Boosting NO in PE

Therapeutics aiming to boost endogenous NO in PE are of great interest, although findings have been inconclusive. In a pilot study, the NO donor pentaerythritol tetranitrate (PETN) improved uteroplacental blood flow and reduced APOs. A larger RCT is currently being conducted to confirm these findings[177]. A Cochrane systematic review failed to establish a reliable conclusion regarding the efficacy of NO donors (glyceryl trinitrate; GTN) or precursors (L-arginine) in the reduction of PE complications[178]. Sildenafil is a selective inhibitor of the cGMP-specific phosphodiesterase (PDE5). A small meta-analysis reported an association between sildenafil and increased fetal weight[179]. More recently, the UK arm of the STRIDER trial failed to observe beneficial effects of sildenafil to prolong pregnancy or improve pregnancy outcomes[180]. Later, the Dutch arm was suspended due to unexplained fetal mortality[181]. As outlined above, low dose aspirin prophylaxis (60-150 mg/day) reduces PE incidence and outcomes[149]. Alongside its anti-aggregant and anti-inflammatory properties, aspirin has been shown to boost HO-1 protein expression in a NO-dependent manner *in vitro*[182], and vasodilate uterine arcuate and mesenteric arteries *ex vivo* in an endothelial and NOS-dependent manner[183]. Together these findings suggests that aspirin in part mediates prevention of reduced NO bioavailability in PE. However, the beneficial effects of aspirin are solely preventative, as they are only observed when initiated before 16 weeks of gestational age.

1.6.5 The nitrate-nitrite-NO pathway in PE

Importantly, metabolism of nitrite to NO via the NOS-independent pathway is enhanced under hypoxic conditions, therefore, has the potential to alter NO bioavailability in the hypoxic utero-placental circulation during PE. Thus, supplementation with nitrate or nitrite may provide beneficial effects for both the mother and foetus. More recent efforts have focused on investigating the therapeutic potential of boosting NO via the nitrate-nitrite-NO pathway in hypertensive diseases of pregnancy. Dietary nitrite (vs placebo) was demonstrated to reduce SBP, preserve plasma antioxidant function and prevent negative gestational outcomes in an *in vivo* NG-Nitro-L-arginine-methyl ester (L-NAME) induced hypertension-in-pregnancy model[184]. Levels of maternal nitrate supplementation were linearly related to vitality of piglets from HP sows[185]. In HP women, a single dose of 140 ml beetroot juice (8.95 mmol/L nitrate; equal to 77.69 mg nitrate) improved endothelial function (FMD) by 5.48%, whereas placebo juice remained comparable to baseline[186]. In a clinical feasibility study, safety, and acceptability of dietary nitrate supplementation via 70 ml concentrated beetroot juice (92.4 ± 11.9 mmol/L; equal to 400 mg nitrate) in borderline hypertensive pregnant women (>22 weeks gestation) was demonstrated. Although no significant difference in blood pressure was demonstrated between nitrate and placebo groups, this was attributed to the lack of dietary

control and in turn, increased plasma nitrate and nitrite variability. Although, changes in plasma nitrite levels were linearly correlated to decreases in DBP[187]. More recently, a nitrate-independent blood pressure lowering effect of beetroot juice was demonstrated in an *in vivo* pregnant $eNOS^{-/-}$ mouse model of hypertension-in-pregnancy, although this was concomitant with variable increases in plasma nitrate and nitrite concentrations[188]. Further investigation is required to confirm the effects of nitrate on hypertension-in-pregnancy, crucially with tighter dietary control.

The lack of effective therapeutic approaches for PE, concomitant with the evidenced dysfunctional NO homeostasis and hypoxic utero-placental circulation, provides considerable scope for the evaluation of dietary nitrate supplementation in the reduction of blood pressure and improvement of gestational outcomes, that may reduce both the mortality, as well as acute and chronic cardiovascular morbidity, associated with PE.

RESEARCH AIMS

The overall aim of the present thesis was to explore the role and regulation of NO and oxidative stress in cardiometabolic disease. Special focus was devoted to investigating the interplay between NO bioactivity, oxidative stress, and endothelial homeostasis in the pathogenesis of ED in PE.

The specific aims were as follows:

I) Explore the effects of dietary nitrate on liver steatosis observed in a model of diet-induced cardiometabolic dysfunction

II) Investigate the specific role of RBC eNOS *per se* on endothelial function

III) Explore the importance of RBCs in mediating the ED observed in PE and the role of RBC-derived NO bioactivity and oxidative stress in the interaction

IV) Investigate the feasibility of short-term (7 days) supplementation with dietary nitrate on reducing blood pressure, improving gestational outcomes in PE, and restoring the deleterious crosstalk between PE RBCs and adjacent vessels.

V) Examine whether monocytes mediate endothelial oxidative stress and inflammation in PE and the potential protective effect of antioxidant (Silibinin) treatment

2 MATERIALS AND METHODS

A brief description of the methodology used in the present thesis are described below. For further detailed information, please see the materials and methods sections of each scientific paper.

2.1.1 Overview

Table 1. Overview of the studies conducted in the present thesis.

Study	Title	Studied Population	Intervention(s)	Primary endpoint(s)	Secondary endpoint(s)	Methods
I	AMP-activated protein kinase activation and NADPH oxidase inhibition by inorganic nitrate and nitrite prevent liver steatosis	Control vs Liver Steatosis vs Liver Steatosis + Nitrate mice	Control, HFD +/- L-NAME +/- Nitrate	Metabolic: IPGTT, IPITT CV: MAP, *ex vivo* vascular reactivity	Plasma/Liver NO_3^- & NO_2^- Blood iron-nitrosylated Hb Liver DNIC	IPGTT, IPITT, blood pressure, Myography, DEXA, HPLC, NOX activity, EPR, RT-PCR, WB
II	Endothelial Nitric Oxide Synthase-Deficient Mice Induce Vascular Dysfunction mediated in part via elevated oxidative stress and endothelial Arginase I	WT vs global eNOS KO mice	RBCs +/- TEMPOL, NOX inhibitors, DetaNONOate, Nor-NOHA	*Ex vivo* Vascular reactivity	ROS production Arginase Activity	Myography, DHE IHC, Arginase activity, Drapkin's Method
III	Red blood cells from patients with preeclampsia induce endothelial dysfunction	HP vs PE	RBCs +/- Nitrite, TEMPOL, Nor-NOHA	*Ex vivo* Vascular reactivity	Plasma NO_3^- & NO_2 Plasma cGMP RBC Arginase activity	Myography, HPLC, cGMP ELISA, Arginase activity, WB, ELISAs
IV	Effects of dietary nitrate supplementation on blood pressure and gestational outcomes in preeclamptic women: a double-blind, randomised-controlled pilot study (NITBEETPE)	PE (Placebo vs Treatment)	Beetroot Juice +/- Nitrate	Blood pressure (Office)	Plasma and Saliva NO_3^- & NO_2 *Ex vivo* Vascular reactivity	Office blood pressure, HPLC, cGMP ELISA, myography, EPR,
V	Monocytes from preeclamptic women previously treated with silibinin attenuate oxidative stress in human endothelial cells.	HP vs PE	Monocyte supernatant +/- Silibinin	*In vitro* oxidative stress and cytokine secretion	NO species Cellular NO_3^- & NO_2	Cytokine & HO-1 ELISA, TBARS, DAF, HPLC

Abbreviations: AMP; Adenosine monophosphate, cGMP; Cyclic guanosine monophosphate , DAF; 4-Amino-5-Methylamino-2',7'-Difluorofluorescein, DetaNONOate; 2-(N,N-Diethylamino)-diazenolate 2-oxide sodium salt hydrate, DEXA; dual-emission x-ray absorptiometry , DHE; dihydroethidium, DNIC; dinitrosyl iron complex, ELISA; enzyme-linked immunosorbent assay, eNOS; endothelial nitric oxide synthase, EPR; Electron paramagnetic resonance , Hb; Haemoglobin, HFD; High fat diet , HO-1; Heme oxygenase-1 , HPLC; High-performance liquid chromatography, HP; Healthy pregnant women, IHC; Immunohistochemistry, IPGTT; Intraperitoneal Glucose Tolerance Test, IPITT; Insulin Tolerance Test , L-NAME ; NG-Nitro-L-arginine-methyl ester , NADPH; nicotinamide adenine dinucleotide phosphate, NO; Nitric oxide, Nor-NOHA; Nω-Hydroxy-nor-L-arginine acetate, NOX ; NADPH oxidases, PE; Preeclampsia, RBCs; Erythrocytes, ROS; Reactive oxygen species, RT-PCR; Reverse transcription polymerase chain reaction, TBARS; Thiobarbituric acid reactive substances , TEMPOL; 4-hydroxy-2,2,6,6-tetramethylpiperidine-N-oxyl, WB; Western Blot, WT; Wild-type

2.1.2 Study subjects

Healthy (HP), preeclamptic (PE) and severe (sPE) preeclamptic pregnant women in **study III** were recruited from Karolinska University Hospital Huddinge and Solna, and Danderyd Hospital between 2017-2020. Diagnoses and severity classification was according to the American College of Obstetricians and Gynaecologists (ACOG) criteria[135]. **Study III** recruitment differed according to downstream experimental application. During *part I*, PE patients were recruited immediately prior to delivery. Recruitment of HP patients was matched by delivery date and gestational age. During *part II*, PE patients were recruited at diagnosis, recruitment of matched HP patients was according to sampling time and gestational age.

In **study IV**, preeclamptic patients were recruited at the pre-natal care unit at Danderyd Hospital, Stockholm, between 2021-2022, according to the ACOG criteria[135]. **Study IV** exclusion criteria were pre-existing type I diabetes, use of proton-pump inhibitors or antacids, a vegetarian or vegan diets, incidence of smoking. A smaller cohort of HP patients (gestational week >20) were recruited for baseline sampling only, for use in experimental analyses.

PE women were recruited in **study V**, between 2018-2019 at the obstetric unit of Botucatu Medical School, Sao Paulo, Brazil, according to the International Society for the Study of Hypertension in Pregnancy (ISSHP) 2018 guidelines[189]. HP women were matched for gestational age for use as controls. Exclusion criteria were previous history of hypertension or adverse medical or obstetric complications, multiparity, and illicit drug use.

Study Design (Study IV)

Study IV was a double-blind, randomised, single-centre, placebo-controlled pilot study. Participants participated in two study visits, baseline (day 0), and follow-up (day 7). Prior to recruitment, block randomisation (Block size of 6, 1:1 allocation) using an online programme was conducted by an independent researcher. Following inclusion, participants were assigned a study number and provided a bag of either placebo (<0.043g nitrate) or nitrate-rich (~400mg nitrate) beetroot juices (70mL, James White Drinks Ltd.). All other research members were blinded. Participants were instructed to drink one juice before breakfast, for 7 days. At each study visit, participants were instructed to be fasted, with the exception of the last juice which was ingested 2 hours prior to the post-intervention visit.

2.1.3 Clinical sampling & handling

Blood

In **study III**, during *part I* blood venous maternal blood and neonatal blood from the umbilical cord was sampled in nitrate or nitrite free EDTA-containing Eppendorf tubes (2mM; Sigma-Aldrich, Merck, Sweden). Blood components were immediately separated by centrifugation (5mins x 900G), and plasma was isolated and immediately stored at -80ºC until further analyses. During *part II*, venous maternal blood was sampled at recruitment in lithium heparin containing BD vacutainers® (368497; BD Biosciences). Samples were placed on ice (+4ºC)

and delivered to Karolinska Biomedicum. Within 1hr of delivery, blood samples were isolated and washed (*see below*) for further experimental analyses.

At each study visit for **study IV**, venous maternal blood was sampled in 1x BD lithium heparin, 1x BD EDTA and 3x BD sodium heparin vacutainers (368497; 366643; 1245647, respectively. BD Biosciences, Stockholm, Sweden), for standard clinical PE blood tests and experimental analyses, respectively. In addition, blood was collected in a vacuette tube containing EDTA (250 mM; 455007; Greiner Bio-one, Austria), free from nitrate and nitrite contamination, and plasma was immediately separated via centrifugation (5mins x 900G) and snap-frozen. Blood in sodium heparin vacutainers was processed via the same protocol as **study III** *part II.*

In **study V**, venous peripheral blood (10mL) was collected upon PE diagnosis, into EDTA (5%)-containing vacuette tubes and centrifuged for separation of blood components and isolation of peripheral blood mononuclear cells (PBMCs) (*see below*).

Saliva & Urine

In **study IV**, urine was immediately assessed for proteinuria via a urine dipstick test (Multistix 7, SIEMENS healthcare diagnostics, Germany). In addition, a 1.5mL Eppendorf tube of saliva and 2x 2mL Eppendorf tubes of urine were collected and immediately frozen (-80^{o}C) at each study visit.

Clinical blood pressure

In **study IV,** office blood pressure was collected at each research visit. SBP and DBP (mmHg) were systematically measured with an automatic blood pressure monitor (OmronM10-IT; Omron Corporation). Following 15 minutes of seated rest, 3 measurements were taken from the left arm. The mean of the last two measurements constituted the blood pressure result.

2.1.4 Animals

Study I

Commercially available 12-week-old male C57BL/6J mice (Janvier Labs, France) were housed at the Karolinska Institute animal facility and provided standard rodent chow *ad libitum* (R34, 4% fat, Lantmannen, Sweden) for a 10-day acclimatisation period. On the 10th day, baseline cardiovascular and metabolic parameters were collected. Subsequently, a 7-week high fat diet (HFD; fat 60 kcal%; carbohydrate 20 kcal%, protein 20% kcal; D12492, Research Diet Inc., USA) +/- inorganic sodium nitrate in drinking water ($NaNO_3$; 1.0mmol/kg/day) +/- NOS inhibitor (L-NAME; 1g/L drinking water) was initiated. Control mice were maintained on standard chow. NOS inhibition was included to induce a hypertensive phenotype, in aim to mirror the metabolic syndrome, as well as to dissect the input of nitrate and nitrite vs endogenous NOS generated NO underlying any observed therapeutic effect. To investigate the role of the commensal bacteria within the enterosalivary circulation required for the nitrate-nitrite-NO pathway, in separate experiments, germ-free mice were fed irradiated HFD (fat 40 kcal%, carbohydrate 43 kcal%, protein 17 kcal%, D12079B, Research Diets Inc., USA) +/- L-

NAME (1g/L drinking water) for 7 weeks. GF status was continually confirmed via aerobic and anaerobic faecal sample cultures. Body weight and food intake was continually monitored. An intraperitoneal insulin tolerance test (IPGTT), intraperitoneal glucose tolerance test (IP-GTT) and blood pressure were conducted at weeks 5 and 6 (*see below*). Post 7-weeks of diet, animals were euthanized, and tissues were collected for further downstream analyses (*see below*).

Study II

Male and female commercially available wildtype mice (C57BL/6J; Janvier Labs, France) and global eNOS KO mice (C57BL/6J/ B6.129P2-Nos3tm1Unc/J homozygous $eNOS^{-/-}$; Jackson Labs, USA) were utilised for experiments. In collaboration with the Cortese-Krott group at the university of Düsseldorf, Germany, Arginase 1 conditional endothelial cell-specific knockout mice (EC-Arg1 KO; EC $Arg1^{lox/flox}$ Cdh5-Cre/$ERT2^{pos}$ +TAM) were generated via tamoxifen-dependent (5 days; 33mg/kg/day) activation of Cre recombinase targeting endothelial Arginase 1, and characterised (Cortese-Krott *et al. Unpublished data*).

Study III & IV

Aortic rings for *ex vivo* preparations were isolated from the thoracic aorta of commercially available wild type mice (C57BL/6J; Janvier Labs, France).

2.1.5 *In vivo* experiments

Tail Cuff Blood pressure

After a period of training, murine SBP, DBP, and mean arterial blood pressure were measured in **study I** using a Coda High Throughput Non-invasive Tail Monitoring System (Kent Scientific, USA), according to the manufactures protocol. Measurements were repeated daily for 3x days and the mean value for each mouse was utilised for analysis.

Body Composition Measurements

To quantify fat and lean mass dual-emission x-ray absorptiometry (DEXA; Lunar PIXImus densitometer; USA) was utilised in **study I** on mice anaesthetized with isoflurane (Forene; Abbott Scandinavia AB, Solna, Sweden).

Intraperitoneal Glucose Tolerance Test (IP-GTT)

In **study I,** after 6 weeks on a HFD, an IP-GTT was performed on mice, after a 5 hour fasting period. Mice were intraperitoneally injected with a D-Glucose solution (2g/kg body weight). Blood glucose was measured 15, 30, 60 and 120 minutes post-initial glucose load, in tail vein blood samples via a portable glucose meter (FreeStyle Lite; Abbott Diabetes Care Inc, Canada).

Intraperitoneal Insulin Tolerance Test (IP-ITT)

IP-ITT was performed on non-fasted mice following an insulin bolus (0.75IU/kg body weight; Novorapid 100IU/ml; Novo Nordisk, Denmark in 0.2IU/ml saline) in **study I**. Glucose was measured in tail vein blood samples at 15, 30, 60 and 120 minutes post-initial insulin load.

Animal euthanasia and sample collection

In **study I, II** and **III,** mice were anaesthetized using isoflurane. Blood samples were collected via the inferior vena cava and immediately placed into 1.5mL EDTA-containing Eppendorf tubes (0.5mmol; Sigma-Aldrich, Sweden). Blood was immediately centrifuged (**Study I,** 5mins x 6000Gx 4ºC; **study II,** 5mins x 900Gx 4ºC) to separate blood components. Plasma was immediately snap frozen and stored at -80ºC for later analyses. In **study II**, the buffycoat was aspirated and RBCs were washed via adding 1mL PBS, mixed gently, and further centrifuged (5mins x 900Gx 4ºC). This was repeated for a total of 3x, and subsequently, washed RBC were co-incubated with murine aortae (*see below*). In **study I**, organs of interest were snap frozen and the mesenteric arteries were maintained in ice cold physiological salt solution (PSS, composition in mmol/L: NaCl, 130; KCl, 4.7; CaCl2, 1.6; KH2PO4, 1.18; MgSO4·7H2O, 1.17; NaHCO3, 14.9; glucose, 5.5; and EDTA, 0.026) buffer until later vascular myography analyses. In **study II** and **III**, thoracic aortae were isolated and dissected into 2mm aortic rings for subsequent vascular myography experiments (*see below*).

2.1.6 *Ex vivo* experiments

Human-murine tissue co-incubation

Washed RBCs from eNOS KO and WT mice (**study II**), and PE and HP patients (**study III; IV**) were diluted in Dulbecco's Modified Eagle Medium containing 10% fetal bovine serum (FBS), penicillin and streptomycin (50mg/L) to 10% haematocrit (DMEM; 17.mM D-Glucose; Gibco, Sweden). 200uL of washed RBC dilutions were incubated with murine aortic rings in a 96-well cell-culture plate (CLS3598; Sigma, Germany) for 18hrs overnight at 37°C with 5% CO_2 in a tissue culture incubator.

In addition, acute (1hr) RBC-aorta co-incubations at 37°C with 5% CO_2 in a tissue culture incubator in **study III**. Further, in **study III**, plasma samples were pooled (5 patients per pool) and diluted to a final concentration of 5% in DMEM media, and co-incubated with WT murine aortic rings for 18hrs overnight at 37°C with 5% CO_2 in a tissue culture incubator. For all experiments, controls were aortic rings incubated in DMEM.

To investigate the role of arginase, oxidative stress, NOXs, and NO bioavailability, the following compounds were added to the co-incubation preparations; N(omega)-hydroxy-nor-L-arginine (Nor-NOHA; 10uM, Bachem), TEMPOL (1mM, Merck), the NOX inhibitors GLX7013114 (NOX4; 3 uM, Glucox Biotech AB, Stockholm) and GLX481304 (NOX2/4; 30 uM, Glucox Biotech AB, Stockholm), DetaNONOate (30 uM, Sigma), and sodium nitrite (NaNO2; 10uM, Sigma), respectively.

In separate experiments within **study III,** to assess whether direct contact of RBCs (lower chamber) and vessels (upper chamber) was required in the observed dysfunctional phenotype, transwell plates (pore size; 0.4μm; Corning) were utilised.

Vascular Myography

Following co-incubation, aortic rings (**studies II, III & IV**) or third-order branches of mesenteric arteries (**study I**) were thoroughly washed (3x in PSS) and mounted onto a multi wire myograph system (Model 620M; Danish Myo Technology, Denmark). Vessels were left to equilibrate (45 mins) in 8mL PSS, which was continuously bubbled with carbogen gas (95% O_2; 5% CO_2). Contractile forces were measured via a PowerLab system (PowerLab 4/30). Resting tension of vessels was achieved via normalization in aim to mimic the internal circumference at which the vessel is relaxed under a transmural pressure of 100mmHg, to enable comparison across vessels. To test their functional integrity, vessels were exposed to potassium chloride (KCl; 120 mM) solution, then washed (3x) and left to equilibrate for 30 mins. Non-responsive vessels to KCl were excluded. Vessels were precontracted to ~80% (aortic rings) or ~50% (mesenteric arteries) of KCl-induced maximal contraction via increasing concentrations of phenylephrine (Phe, 0.1nM to 10μM) until a stable plateau was reached. Subsequently, endothelium dependent (EDR) and independent (EIR) responses were determined via increasing concentrations of acetylcholine (ACh, 1 nM to 100 μM) and sodium nitroprusside (SNP, 1 nM to 100 μM), respectively. Between each dose-response curve, vessels were washed 3x with PSS and left to equilibrate for 40 mins. In separate experiments within **study II**, after mounting vessels, TEMPOL (300 uM; Sigma) was acutely added to the chamber and incubated for 30 mins, followed by washing (3x, PSS) and the above myography protocol.

2.1.7 *In vitro* experiments

Liver steatosis HepG2 *in vitro* model (Study I)

Human HepG2 cells were cultured in DMEM medium (5.5mM glucose; Gibco) containing 10% FBS, penicillin and streptomycin (50 mg/L). To induce steatosis *in vitro*, cells were treated with a *'steatosis cocktail'*; serum starved DMEM media containing 25 mM glucose, 10 nM insulin and 240 μM FFA (i.e., Palmitic acid and Oleic acid mixture 1:1) +/- sodium nitrite (10 uM) for 24, 48 or 72 hours. In addition, the following compounds were included in the treatment media; TEMPOL (100 μM), NOX2/4 inhibitor (GLX481304, 1- 50 μM), GLX7013114, 0.2-2 μM), DETA-NONOate (5 μM) or cGMP analogue 8-pCPT-cGMP (10 μM). In separate experiments, cells were pre-incubated with the following compounds for 30mins before steatosis treatment; Febuxostat (50 nM), Raloxifene (50 nM), ODQ (10 μM) or Compound C (20 μM).

Isolation and culture of PBMCs (Study V)

Peripheral blood samples were centrifuged (1200g x 10mins x 4^{o}C), the plasma was removed and PBMCs were obtained by Ficoll-Paque® PREMIUM (1.077 g/mL Density Max; GE Healthcare, Sweden) density gradient centrifugation (400g x 30 mins at room temperature).

Specifically, solution from the diluted plasma/Ficoll-Paque® PREMIUM interface layer was collected. PBMCs were resuspended in Gibco Roswell Park Memorial Institute 1640 Medium (RPMI; Sigma, USA) supplemented with FBS (10%; Gibco, Sweden). The Tryphan Blue dye exclusion test was utilised to determine cell viability, and cell counting was performed using the Neutral Red Uptake Assay (0.02%; Sigma, USA). Subsequently, PBMCs were seeded at a density of $5x10^5$ cells/mL in RPMI medium (+10% FBS) in 24-well cell culture plates (NalgeNunc, USA). Following 2 hours incubation a cell culture incubator (37ºC, 5% CO_2), non-adherent PBMCs were aspirated and adherent PBMCs were washed (2x) with RPMI medium (+10% FBS). To investigate the therapeutic effect of Silbinin (Sb), when PBMCs reached 90% confluence, cells were treated +/- 50 μM Sb (Sigma, USA) and incubated in a cell culture incubator (37ºC, 5% CO_2) for 18hrs. Subsequently, supernatants were collected, immediately snap-frozen and stored until later analyses.

HUVEC and PBMC supernatant co-incubation (Study V)

Pooled human umbilical venous endothelial cells (HUVECs; LONZA; Switzerland) from at least three donors, were maintained on gelatin (1% v/v)-coated cell culture flasks in complete growth medium 199 (M199, supplemented with 20 % fetal bovine serum (FCS), 2mM L-glutamine, 100 IU/ml penicillin and 0.1 mg/ml streptomycin (Invitrogen, Paisley, UK). HUVEC were used between passage 3 to 6. HUVEC were treated with PBMC supernatants (20% v/v in M199 media) from PE vs HP patients +/- Sb (*see above*) for 24hrs, followed by further analyses (*see below*).

Cell Viability was determined utilising the Tryphan blue exclusion assay (**Study I & V**) or the PrestoBlue™ Cell Viability reagent (**Study V**), according to manufacturer's protocols.

2.1.8 Biochemical Assays

Immunohistochemistry with the cell-permeable, fluorescence dye, **dihydroethidium (DHE)** was utilised for ***in situ*** **quantification of cellular $O_2^{\bullet-}$** in aortic rings post co-incubation with RBCs vs controls (**Study II**). DHE can be oxidised by intracellular $O_2^{\bullet-}$, which generates either ethidium (E^+) or 2-hydroxyethidium (2-OH-E+), via ($O_2^{\bullet-}$)-specific hydroxylation and non-specific oxidation of DHE, respectively. Both are red fluorescent products. Post co-incubation, aortic rings were washed (3x) with PSS, stabilised in PSS (37 °C x 60 mins), then fixed in optical cutting temperature compound (OCT; Tissue-Tek® O.C.T.TM) and snap frozen. Rings were cryosectioned (8 μm) and mounted on histological slides (duplicate). Replicates were either incubated with DHE (5 μM; Sigma, Germany) or PSS (control) for 15 mins in darkness, then washed (2x) with deionized water. Samples were visualised by excitation via a xenon lamp (magnification 10x) at 570-645 nm emission (TRITC Filter) and captured using a Nikon fluorescence microscope (TE2000-U, Japan) with a digital microscope camera (Nikon DS-5M, Japan). Images were quantified utilising ImageJ 2.0 software, DHE-derived 2-OH-E+ levels were expressed as arbitrary units (A.U) as the difference between PSS vs DHE incubated replicates.

Electron paramagnetic resonance (EPR) was utilised to detect **$O_2^{\bullet-}$ and NO species in HepG2 cells,** and **iron-nitrosylated Hb Species in whole blood** following steatosis induction +/- sodium nitrate (**study I**) and **transferrin, ceroplasmin and metHb** levels of frozen whole blood samples (**Study IV**). EPR data were expressed in arbitrary units. All EPR spectra were obtained utilising a bench top Magnettech MiniScope MS5000 ESR spectrometer (Freiberg Instruments) and expressed as arbitrary units. In **study I,** the spin traps 5,5-Dimethyl-1-Pyrroline-N-Oxide (DMPO) and Fe(II)-diethyldithiocarbamate colloid (DETC) were used to detect O_2^- and NO, respectively.

$O_2^{\bullet-}$ detection: post-48hr treatment, HepG2 cells were washed (PBS, 4°C), centrifuged (1500g x 10 min), suspended in lysis buffer (50 mM Tris, 0.1 mM EDTA, 0.1mM EGTA; pH 7.4) and membrane fractions were isolated (2900g x 10 min). 20ug membrane fraction was added to DETC (10mM), protease inhibitor cocktail (S8830; Sigma, SE), DMPO (50 mM; ALX-430-090, Enzo Life Sciences, SE) and NADPH (1 mM). Instrument settings for $O_2^{\bullet-}$ detection were microwave power: 10 mW; microwave frequency; 100 kHz; amplitude modulation: 0.1 mT; sweep time: 100 secs; sweep width: 11 mT, number of scans: 3; centre field: 337 mT.

NO species detection: Prior to *in situ* lysis, HepG2 cells were incubated (1hr) with $NaNO_3$ +/- colloid solution of $Fe(DETC)_2$ (500 μM). Lysates were pelleted (21000 RPM x 60 secs), resuspended in 50uL PBS and collected in a capillary tube. Instrument settings for NO species detection were microwave power: 10 mW; microwave frequency; 100 kHz; amplitude modulation: 0.6 mT; sweep time: 30 secs; sweep width: 14 mT, number of scans: 3; centre field: 331 mT.

Iron-nitrosylated-Hb species (Hb-NO and DNICs) detection: Venous blood or liver collected from mice +/- HFD +/- nitrate were collected and snap frozen in 1mL syringes. Instrument settings were microwave power: 10mW; microwave frequency; 100kHz; amplitude modulation: 0.6mT; sweep time: 60s; sweep width: 40mT, number of scans: 4; centre field: 330mT. Hb-NO levels in whole blood were determined via the amplitude of the first Hb-NO triplet peak (g-factor: 2.01; AN:1,7 mT). Liver DNIC was quantified by amplitude of peak at g=2.04.

Transferrin (TF), Ceroplasmin (CP) and metHb: Whole blood sampled from PE women at baseline and post-intervention visits from both placebo and treatment arms were immediately snap-frozen in 1mL syringes. Recordings were made at 77K using a Dewar flask (Wilmad, USA). Instrument settings were microwave power: 10 mW; amplitude modulation: 0.8 mT; modulation frequency: 100 kHz; sweep time: 300 secs; number of scans: 1. 175; centre field: 225 mT. Whole blood *TF, CP and metHb* were quantified by the amplitudes of peaks at g=4.2, g=2.05 and g=5.83, respectively. Ceroplasmin to transferrin ratio (CP:TF) was subsequently calculated.

NADPH-mediated formation of O_2^- (**NOX activity)** was determined via a **lucigenin-dependent chemiluminescence** (CL) **assay**, as previously described[190], in HepG2 cells and livers of mice following steatosis induction +/- sodium nitrate (**Study I**). Briefly, supernatants

of tissue lysates were incubated with NADPH (100umol/L) and lucigenin (5umol/L). CL was detected for 3mins by an AutoLumat LB953 Multi-Tube Luminometer (Berthold Technologies, Germany). Cell lysates were incubated with dark-adapted lucigenin (5umol/L, 37^{o}C x 10mins). To start the reaction, NADPH (100 μmol/L) was injected into samples, and CL signal was detected for 3mins. CL were expressed as raw light units (RLU)/min and normalised to protein concentration of samples, as determined by the Bradford Protein assay (Bio-Rad, Sweden).

The **Thiobarbituric acid reactive substances (TBARS)** assay was utilised to measure lipid peroxidation in HUVEC following exposure to PBMC supernatants (**Study V**). Briefly, 100uL of supernatant was incubated for 15 mins with 200uL of ice-cold Trichloroacetic acid (10%; TCA; Sigma, USA). A standard curve was constructed using 1,1,1,3- tetra methoxy propane (TMP; C7H16O4; 133.75 mM; Sigma, USA). Samples and standards were centrifuged (2200g x 15 minutes x 4°C). Next, 200 uL supernatants were incubated with 0.67% thiobarbituric acid (TBA; Sigma, USA) in a water bath (95°C) for 50 mins, then placed on ice for 3 mins. Absorbance of standards and samples was read in a 96-well plate at 532 nm utilising a Spectramax iD3 multi-mode microplate reader (Molecular Devices, USA). Values were obtained via interpolation of the malondialdehyde (MDA) standard curve and expressed as MDA (nmol/ml).

DAF-FM Diacetate (4-Amino-5-Methylamino-2',7'-Difluorofluorescein Diacetate) was utilised to detect NO species in supernatant treated HUVEC (**Study V**), according to manufacturer's instructions. Briefly, HUVEC were seeded in a 96-well plate at a density of 2.5x10^{5} cells/mL and treated with PBMC supernatants from PE vs HP donors for 24hrs in a cell culture incubator (*see above* protocol; 37^{o}C, 5% CO_2). Subsequently, the media was aspirated, 95uL PBS was added to each well and the plate was further incubated for 30 mins. Next, 5uL of DAF-FM™ 200 μM (Sigma-Aldrich, USA) was added to each well, and fluorescence was continually measured at 495/535nm, for 2 hours at 37^{o}C via a Spectramax iD3 multi-mode microplate reader (Molecular Devices, USA). Fluorescence was expressed as arbitrary units as an estimate of NO species.

HO-1 concentrations (ng/mL/10^{7} cells) were measured in HUVEC supernatants (**Study V**) using a commercially available **Human Total HO-1 ELISA kit** (DYC3776-5; R&D systems, USA), according to manufacturer's instructions.

Hb supernatant concentration was quantified via **Drapkin's Reagent** (**Study II**; D5641; Sigma, USA), according to manufacturer's instructions. Based on the conversion of Hb to cyanmethaemoglobin, which then quantified via absorbance (540 nM) using a Spectramax iD3 multi-mode microplate reader (Molecular Devices, USA). A standard curve (0-120 mg/mL) was utilised to interpolate unknown sample absorbance values. Cyanmethaemoglobin values were expressed as mg/mL. In **Study III**, plasma concentrations of Hb were quantified using a commercially available **human Hb ELISA** kit (E88-134; Bethyl Laboratories, TX) according to manufacturer's instructions.

Plasma nitrate and nitrite were measured in **Studies I, III, IV and V** via high-performance liquid chromatography HPLC (ENO-20; EiCom), as previously described[191]. In brief, nitrate is separated via reverse-phase/ion exchange chromatography, followed by inline nitrate reduction to nitrite via reduced copper and cadmium. Finally, reduced nitrite is derivatized by Griess reagent, and levels of diazo compounds are analysed via visible detection at 540nm. In **study I**, 10uL of plasma samples were utilised.

Plasma cGMP was quantified via a commercially available ELISA kit (RPN226; GE Healthcare, VWR, Sweden), according to the manufacturers protocol in **study III** and **IV**. Prior to quantification, samples were treated with 3-isobutyl-1-methylxanthine (10 uM; I7018, Sigma, Merck, Sweden), an inhibitor of cAMP/cGMP phosphodiesterases.

Quantification of **plasma cytokines** (*i.e.,* IL-1β, IL-2, IL-4, IFNγ, IL-12p70, IL-13, IL-10, IL-6, TNFα, IL-8) was conducted via a human pro-inflammatory panel 1 multiplex assay kit (K15049D; MSD, USA) according to the manufacturers protocol, in **study III.** Concentrations of TNFα, IL-10, and IL-1β, in supernatants collected from PE and HP monocyte cultures were quantified via Quantikine ELISA kits (R&D, USA), as per manufacturer's instructions, in **study V**.

Arginase activity in plasma (**study III**) and RBCs (**studies II** and **III**) were quantified via a modified previously described method, based on the conversion of L-Arginine to L-Ornithine and Urea[126,192]. Washed RBCs were lysed in RIPA buffer (N653-100; VWR) containing protease inhibitors (11836170001; Roche). Urea was depleted in diluted (1:6 in Milli-Q H_20) plasma samples via centrifugation (13000g x 30mins x 4°C) in membrane filter columns (Vivaspin 500 VS0102, Sartorius, Germany). Plasma and RBC samples were incubated separately for 2hrs and 1hr, respectively at 37°C with L-Arginine (50 µg sample protein added to 50ul of 500 mM Tris HCL, pH 9.7). Arginase activity was expressed as final urea concentration, quantified by spectrophotometry (Plasma, umol/mL/hr; RBC, nmol/mg protein/min).

Plasma arginase I concentration was quantified in (**Study III**) via a commercial ELISA kit (MBS912500, MyBioSource, USA) as per the manufacturer's protocol.

In **study I**, **neutral lipid accumulation in HepG2 cells and livers** of mice following steatosis induction +/- sodium nitrate was assessed via **Oil Red O staining** (ORO). Post treatment, cells were fixed (4% paraformaldehyde) for 30 mins, washed (PBS x2), exposed to ORO solution (0.2 mg/mL in isopropanol, diluted in $d H_2O$) for 1hr, and washed (PBS x3 for 5 mins). Isopropanol was added to extract the dye from cells, absorbance was measured at 520nm. 6uM cryosections of liver were fixed (1% paraformaldehyde), exposed to propylene glycol (3 mins), incubated with pre-warmed ORO (10 mins) then with propylene glycol (85%, 5 mins), followed by Mayer's Haematoxylin (30 secs). Sections were washed and mounted with glycerine mounting medium and images were acquired and analysed via ImageJ software in a blinded manner. **Liver triglyceride content** was quantified using a **Triglyceride assay Kit** (ab65336; abcam) as per the manufacturer's instructions.

mRNA expression levels of genes of interest were quantified by **RT-PCR** in liver homogenates and human hepatocyte spheroids (**study I**), using Power SYBR green master mix and a TaqMan Universal mix, respectively. RT-PCR was performed in 96-well plates on an ABI 7500 Real-Time PCR System using Power SYBR Green Master mix (Thermo Fisher Scientific). Ct values were obtained for each reaction and were normalized to β-actin using the Delta-Delta Ct method, to indicate changes in target gene expression via fold change output. See study I supplementary information for specific primer sequences.

In study I and **III, protein expression quantification** was conducted by **Western Blot** to detect proteins of interest in HepG2 cells and liver tissue, and RBCs, respectively. HepG2 cells were lysed in lysis buffer (Tris-HCl pH, 10 mmol/L pH 8; NaCl 150 mmol/L; EDTA 5 mmol/L; N-octyl-glucoside 60 mmol/L; 1 % Triton X- 100, protease inhibitor cocktail and phosphatases inhibitors). Liver tissue was homogenised using zirconium oxide beads (0.5 mm) and lysis buffer in a bullet blender. RBCs were lysed with ice cold RIPA buffer with protease inhibitor cocktail and phosphatases inhibitors. Total protein concentration of lysates was quantified using the Bradford protein assay (**study I**) and a bicinchoninic acid protein assay kit (Pierce Biotechnology, Life Technologies, **study III**). Equal amounts of proteins were separated via 4-20% SDS-polyacrylamide gel electrophoresis and transferred onto polyvinylidene difluoride membranes (PDVF) membranes. Enhanced chemiluminescence (ECL) substrate (BioRad, SE) was used to develop blots, band densities were analysed using Image Studio Lite Version 6.0 (LI-COR Biosciences). Data were normalised to Vinculin or GAPDH, for HepG2 and liver tissue, and RBCs, respectively. See study I supplementary information and study III for specific antibodies used.

Statistical Analyses

Unless otherwise indicated below, data are presented as mean ± SEM in all studies. Data were analysed using GraphPad Prism (v6.0, Graphpad Software, UK) and SPSS (IBM, v. 27, USA). Outliers were removed in GraphPad Prism (ROUT Q = 1%). Unless otherwise stated below, parametric variables were subjected to a student's *t*-test for unpaired observations for single comparisons, a *1-way* ANOVA adjusted with Tukey's correction for multiple comparisons with one independent variable, and nonlinear regression analysis was utilised to construct individual vessel concentration-response curves and compared with *2-way* ANOVA with repeated measurements and Tukey *post-hoc* testing. Non-parametric continuous variables were analysed via the Kruskal-Wallis test. Experimental subgroup *n* numbers are stated in figure legends. Statistical significance was defined as $p<0.05$.

Study III & IV

Clinical characteristics of the study groups were compared as follows: parametric variables: chi-squared test (dichotomous variables); two-way ANOVA adjusted with Bonferroni *post-hoc* testing (continuous data, two independent variables); nonparametric variables; Mann-Whitney U test (continuous data).

Study III: Using univariate analyses via a general linear model, the effect of maternal descriptive factors on RBC arginase activity was assessed. Linear correlation analysis was utilised to assess group severity vs arginase activity.

Study IV: Correlations between changes in blood pressure and changes in plasma, urine and saliva nitrate and nitrite were analysed via a Pearson linear regression.

Study V: Non-parametric continuous clinical data was analysed via the Man-Whitney U test.

2.1.9 Ethical Considerations

All animal studies were approved by the regional Institutional Animal Care and Use Committee, Stockholm, Sweden and were performed according to the National Institutes of Health animal protection guidelines (**Study III**: Protocol ID: N139/15), and with the European Union (EU) Directive 2010/63/EU for the conduct of experiments in animals.

Clinical studies were approved by the regional ethics committee, Stockholm, Sweden (**Study III**: Dnr: 2018-1233-32-1, **Study IV**: Dnr: 2020-01596). **Study V** was approved by Botucatu Medical School's ethics committee (protocol ID: 1.622.546 and 3.826.694). All study participants were provided with the study information, including any associated risks, and provided written informed consent prior to inclusion. All procedures were conducted according to the ethical guidelines of the Declaration of Helsinki (1975).

Study IV

The intervention of beetroot juice (70mL, 400mg; James White Drinks, UK) has no known harmful side effects and has been utilised in multiple published clinical studies in non-pregnant[67,68,193–195] and pregnant[186,187] populations with no reports of associated adverse events. Participation in the study was concomitant with standard perinatal care at the women's clinic at Danderyd Hospital. Any serious adverse events which were suspected to be related to the intervention were recorded in the CRF, and the treatment code for that patient was unblinded if deemed necessary for the safety of the patient. The methodological platform is commonplace during the course of perinatal care and carried minimal risk to the patients.

3 RESULTS & DISCUSSION

3.1 STUDY I

AMP-activated protein kinase activation and NADPH oxidase inhibition by inorganic nitrate and nitrite prevent liver steatosis

Study I aimed to investigate the potential therapeutic effect of stimulating the nitrate-nitrite-NO pathway via dietary nitrate on the pathogenesis of NAFLD, a highly common co-morbidity of metabolic syndrome, T2D and obesity[196]. To do this, three separate models of NAFLD were utilised; *in vitro* using HepG2 cells and hepatic 3D spheroids, and an *in vivo* mouse a HFD-induced model.

3.1.1 Beneficial effects of dietary nitrate on aspects of the metabolic syndrome

In accordance with previous publications, supplementation with dietary nitrate prevented systemic metabolic and cardiovascular pathogenesis[84]. Compared to mice fed a HFD + L-NAME (1 g/L in drinking water), those fed with a HFD + L-NAME + dietary nitrate for 7 weeks presented significantly lowered fasting blood glucose (-1.5 mM), prevented impaired glucose clearance (Figure 3A, B) and prevented development of insulin resistance (Figure 3C, D), such that nitrate-treated animals had similar values to controls. Dietary nitrate significantly reduced HFD-induced elevations in MAP, as well as HFD-induced ED (Figure 3E, F). Similar findings were observed in the same groups without L-NAME treatment. These beneficial effects of dietary nitrate were prevented decreases in plasma nitrate and nitrite, as well as Hb-NO in whole blood.

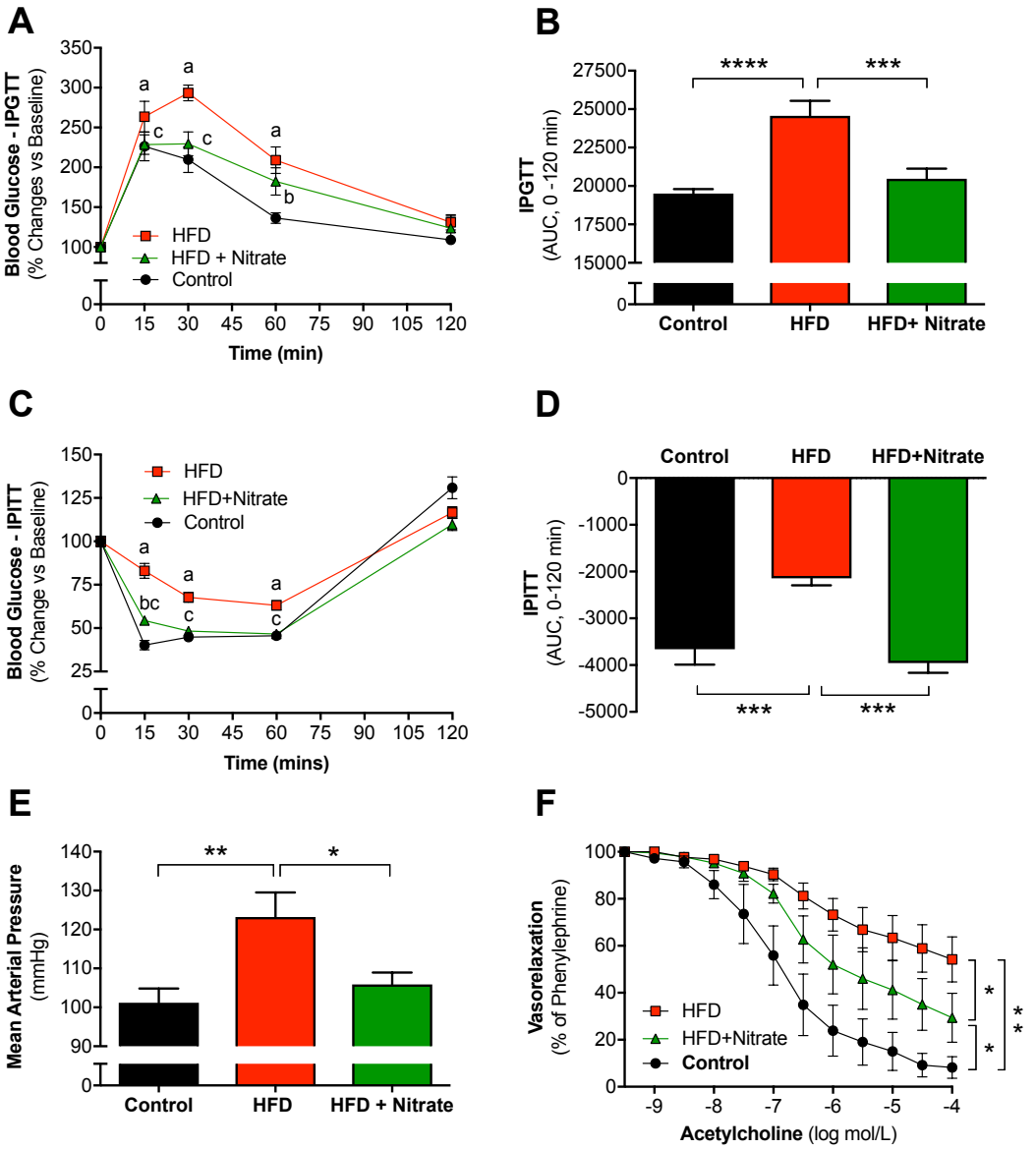

Figure 3. Dietary nitrate improves metabolic and cardiovascular phenotype *in vivo*. Metabolic and cardiovascular parameters of mice fed regular chow (control), a high-fat diet (HFD) or a HFD + nitrate + L-NAME. **(A)** Intraperitoneal blood glucose tolerance test (IPGTT) after 5 weeks of diet. **(B)** IPGTT area under the curve (AUC) **(C)** Intraperitoneal insulin tolerance test (IPITT) after 6 weeks of diet. **(D)** IPITT AUC. **(E)** *In vivo* mean arterial pressure after 6 weeks of diet. **(F)** *Ex vivo* endothelial-dependent vasorelaxation responses after 7 weeks of diet. Conducted on freshly isolated mesenteric arteries following termination. n=6-10 mice per group. Data expressed as mean±SEM. Statistical significance defined as *p<0.05, **p<0.01, ***p<0.001, ****p<0.0001. Letters express a significance level of p<0.05 of (a) Control vs HFD; (b) HFD vs HFD + nitrate groups. Statistical analyses conducted via (A, C, F) a 2-way ANOVA with repeated measures and (B, E, D) a 1-way ANOVA, all with Holm-Sidak *post hoc* testing.

3.1.2 Pathogenesis of liver steatosis is prevented by dietary nitrate

When liver tissue from mice was examined, a HFD + L-NAME diet prevented elevations in liver nitrate and nitrite. Liver nitrate levels were comparable to control levels in the HFD + L-NAME + nitrate treated group, concomitant with the prevention of reduced DNIC levels. These data directly demonstrate that in addition to circulating NO levels, dietary nitrate *per se* prevents HFD-induced reductions in liver NO levels.

To further investigate the impact of dietary nitrate-induced prevention of liver reduced NO levels, we assessed hepatic lipid accumulation in the livers from HFD + L-NAME vs HFD + L-NAME + nitrate treated mice. Nitrate treatment prevented HFD-induced lipid accumulation, such that levels remained comparable to controls. These results were mirrored in our *in vitro* model. Previous studies have linked the beneficial effects of dietary nitrate to reduction of NOX-derived oxidative stress[98,197,198], therefore we next investigated the influence of NOX in our model. Similarly, in liver tissue, the HFD-induced increases in NOX-derived O_2^- were completely prevented by nitrate (Figure 4). Levels of lipid accumulation and NOX activity were positively correlated in liver tissue.

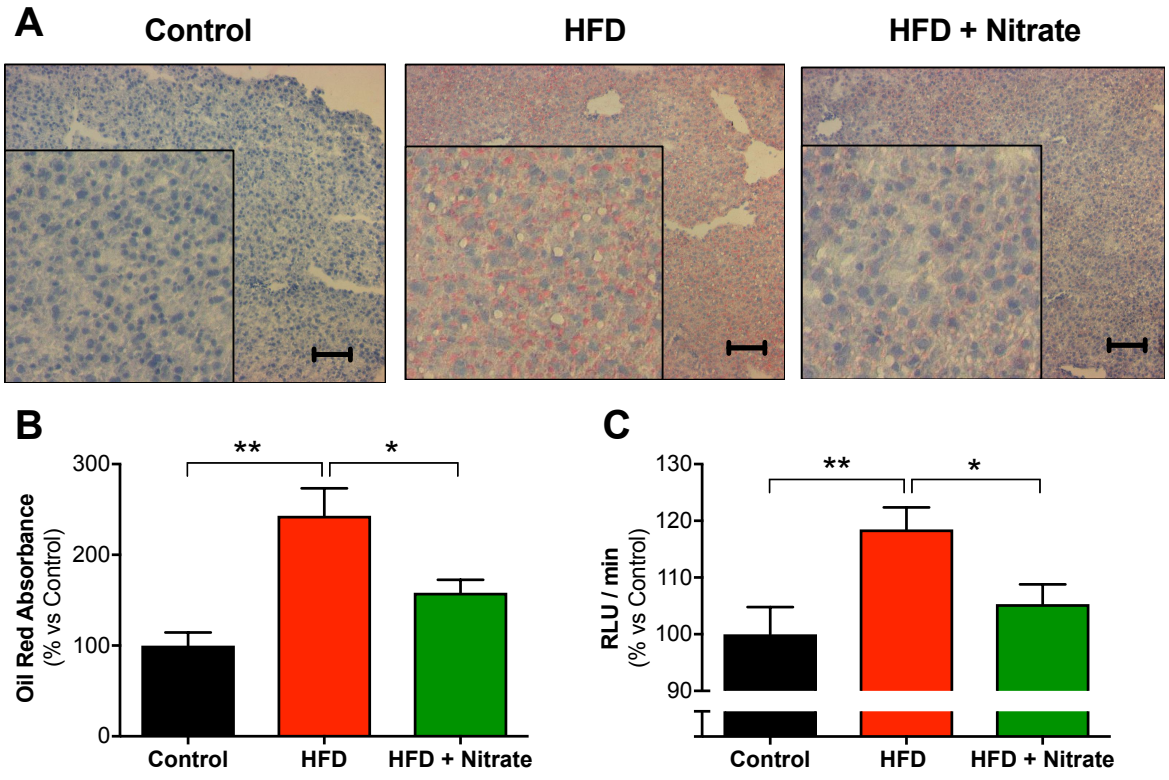

Figure 4. HFD-induced elevated lipid accumulation and NOX activity prevented by dietary nitrate *in vivo*. **(A)** Neutral lipid (red) visualisation in liver sections stained with Oil Red O. Representative images from each group. Nuclei counterstained with Mayer's hematoxylin (blue). Scale bars; 1μm, Insets 4x magnification. **(B)** Quantification of Oil Red O absorbance (% vs control) **(C)** NADPH oxidase activity (RLU/min). *n*=5-9 mice per group. Data expressed as mean±SEM. Statistical significance defined as **p*<0.05, ***p*<0.01. Statistical analyses conducted via Kruskal-Wallis Test with Dunn's *post hoc* testing.

Similarly, 48hrs incubation of HepG2 cells with a '*steatosis cocktail*' (see methods section) significantly increased NOX-derived O_2^- generation and lipid accumulation, which was prevented by nitrite treatment (Figure 5B, C, D, E). Similarly, to our *in vitro* observations following nitrate treatment, the steatosis-induced elevations in lipid accumulation and NOX-derived O_2^- generation was also prevented by incubation with the O_2^- scavenger; TEMPOL (Figure 5D, E) and a NOX2/4 inhibitor in a dose-dependent manner (Figure 5F, G). Thus, highlighting an association between elevated oxidative stress via NOX-derived O_2^- and steatosis pathogenesis. This was further supported by EPR evidence whereby cellular steatosis was associated with an increase in DMPO-OH signal, which nitrite, a NOX2/4 inhibitor, and SOD treatment all separately significantly reduced (Figure 6B). Together, these findings support that the beneficial hepatic effects of nitrate are mediated via reducing NOX-derived O_2^- generation.

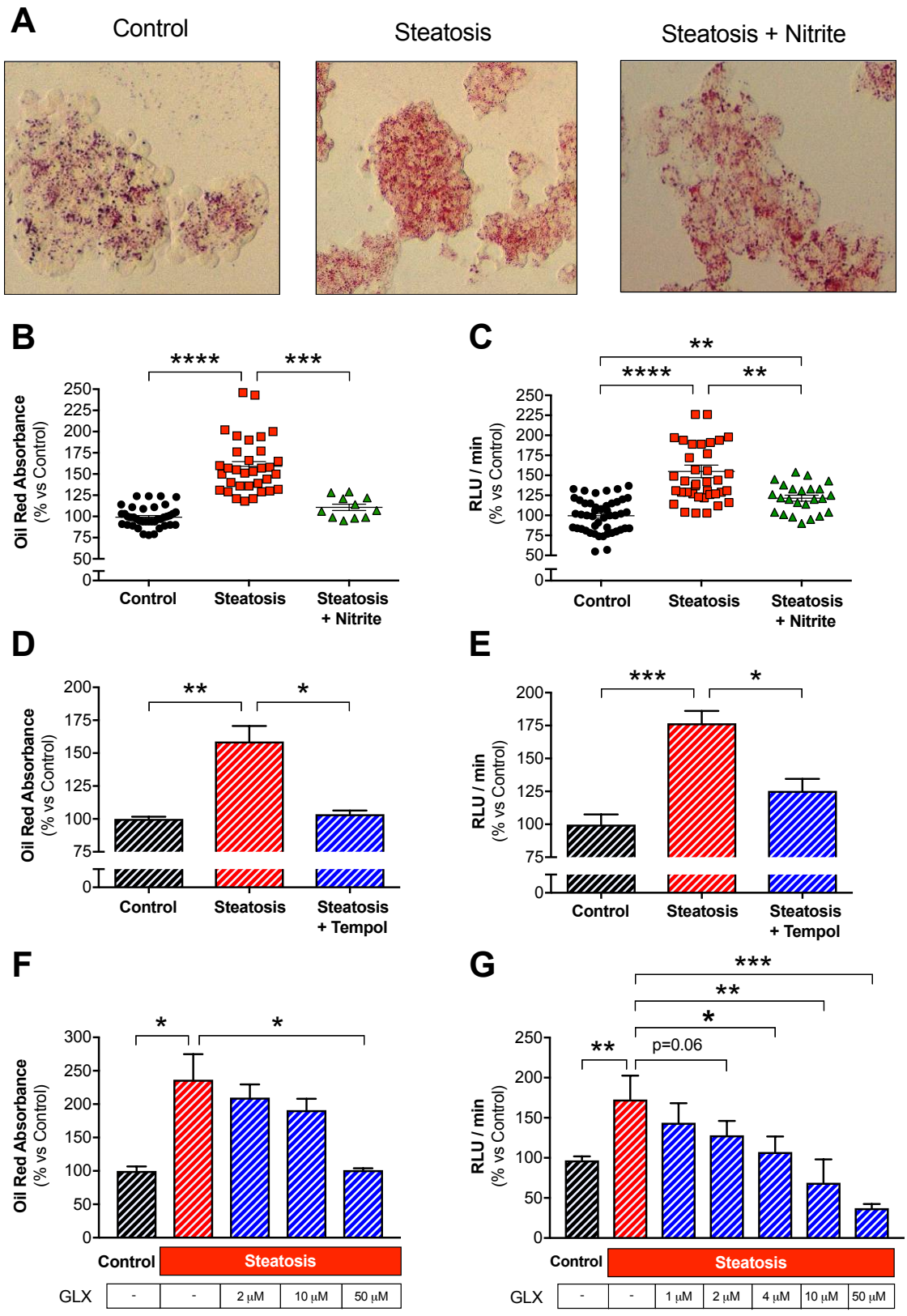

Figure 5. Steatosis media-induced elevated lipid accumulation and NOX activity prevented by dietary nitrate *in vitro*. HepG2 cells treated with control, steatosis, and steatosis + nitrate media for 24hrs. **(A)** Representative images of HepG2 neutral lipid accumulation via Oil red O staining (40x Magnification). **(B)** Quantified HepG2 Oil Red O absorbance (% vs controls) **(C)** NADPH oxidase activity (RLU/min), **(D, E)** +/- simultaneous 24hr TEMPOL treatment **(F, G)** simultaneous 24hr treatment with increasing concentrations of the NOX2/4 inhibitor, GLX481304. Per group; (A) n=6, (B) n=11-17, (C) n=26-50, (D, E) n=6-8, (F, G) n=4-16. Data expressed as mean±SEM. Statistical significance defined as *p<0.05, **p<0.01, ***p<0.001, ****p<0.0001. Statistical analyses conducted via Kruskal-Wallis Test with Dunn's *post hoc* testing.

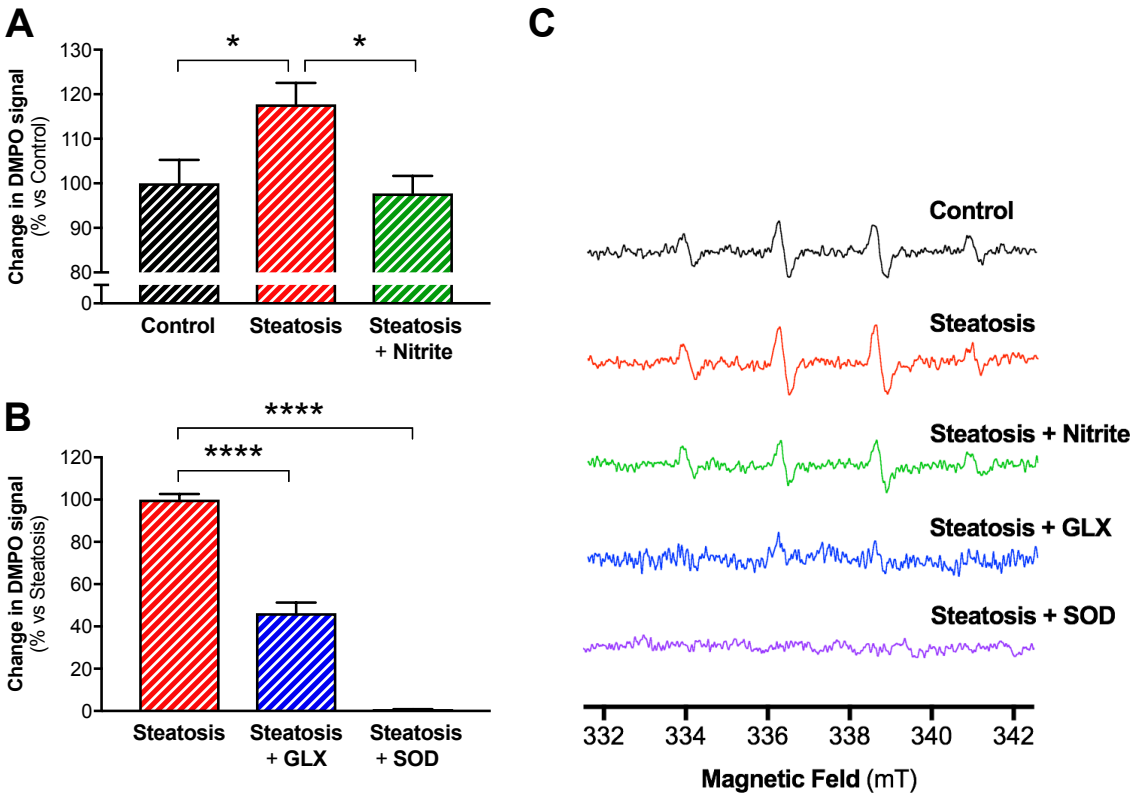

Figure 6. Steatosis media-induced increases in O_2^- production in HepG2 cells is prevented by nitrite. HepG2 cells treated with control, steatosis, and steatosis + nitrate media for 48hrs. Quantification of DMPO signal in the membrane fraction of HepG2 cells treated with **(A)** control, steatosis, and steatosis + nitrate media **(B)** HepG2 cells simultaneously treated with steatosis media and NOX2/4 inhibitor, GLX481304 or SOD. **(C)** Representative EPR spectra of all groups. Per group; n=4-11. Data expressed as mean±SEM. Statistical significance defined as *p<0.05, **p<0.01, ***p<0.001, ****p<0.0001. Statistical analyses conducted via Kruskal-Wallis Test with Dunn's *post hoc* testing.

Lipid accumulation is prevented by AMPK, a central regulator of lipid and glucose metabolism. Under conditions of overnutrition, its activity is supressed[91,92]. In our *in vivo* model, the p-AMPK/AMPK protein ratio, thus AMPK activation, was decreased in the livers of mice fed a HFD+L-NAME. Whereas those treated with nitrate exhibited levels comparable to controls, suggesting a nitrate-mediated preservation of hepatic AMPK signalling (Figure 7A). Indeed, protein levels of downstream targets of AMPK; SREBP1c, ACADM and p-ACC were all similarly observed to be protected by nitrate treatment (Figure 7B, C, D, respectively). These findings were mirrored in our *in vitro* model, albeit to a less potent degree following nitrite treatment. Further, *in vitro* treatment with an inhibitor of AMPK (compound C), prevented the beneficial effects of nitrite on preventing steatosis-induced elevations in NOX activity. This suggests that the beneficial metabolic effects of nitrate are mediated via modulation of AMPK signalling and in turn, preventing the induction of lipogenesis and reducing hepatic β-oxidation.

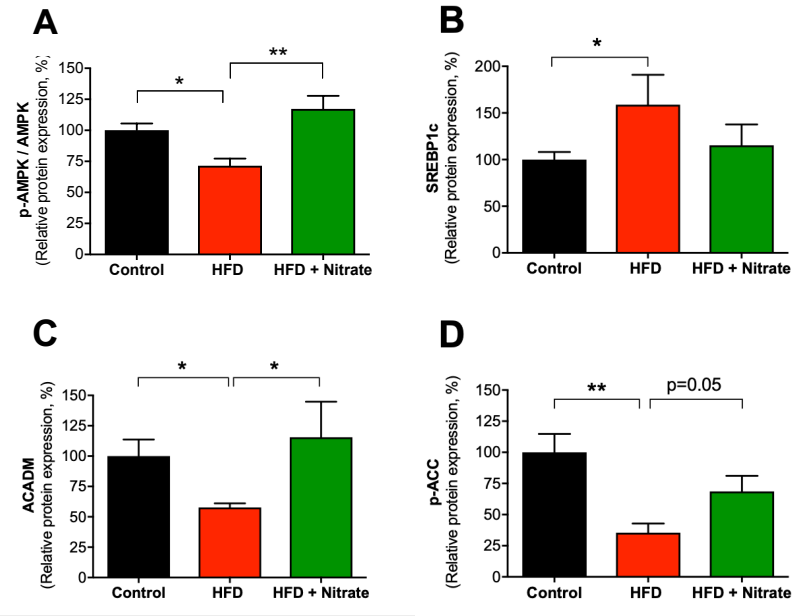

Figure 7. Effects of nitrate are mediated via altered hepatic metabolic regulatory protein expression *in vivo*. After 7 weeks of diet, liver protein levels of **(A)** p-AMPK/AMPK, **(B)** SREBP1c, **(C)** ACADM, **(D)** p-ACC. Measured by western blot. Per group, (A) *n*=9-10, (B) *n=7-8*, (C) *n*=6-8, (D) *n*=8-10. Data expressed as mean±SEM. Statistical significance defined as **p*<0.05, ***p*<0.01. Statistical analyses conducted via Kruskal-Wallis Test with Dunn's *post hoc* testing.

To further investigate the mechanistic role of nitrite-derived NO, *in vitro* lipid accumulation (Figure 8A) and NOX activity (Figure 8B) were measured after induction of steatosis +/- the following compounds: nitrite; NO donor, DetaNONOate; a cGMP analogue, 8-CPT; XOR-inhibitor, Febuxostat; and sGC inhibitor, ODQ. The key findings from these experiments were that the salutatory effects of nitrite were mimicked by DetaNONOate, and the cGMP analogue, but prevented by sGC inhibition.

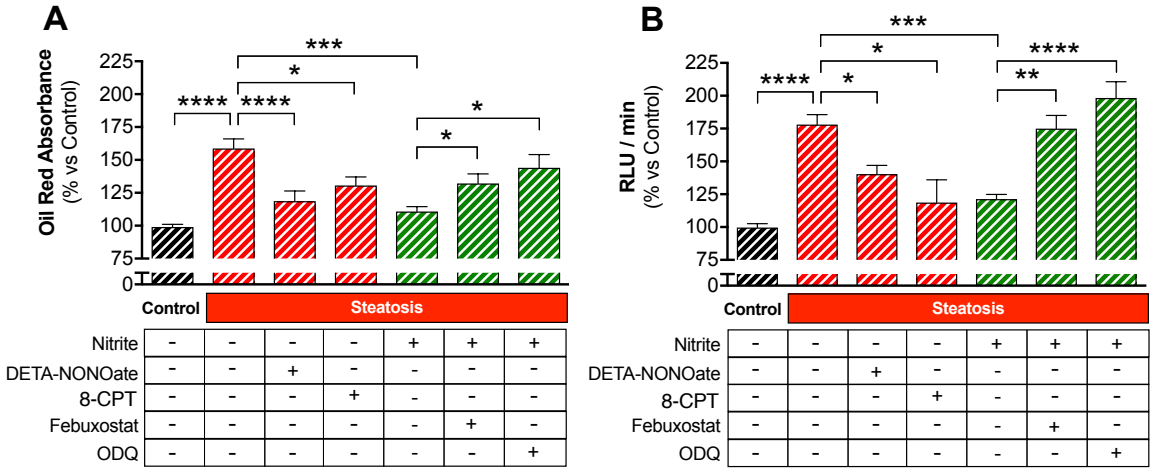

Figure 8. Mechanisms underlying nitrate-mediated protection against steatosis *in vitro*. HepG2 cells treated with control, steatosis, and steatosis + nitrate media for 24hrs +/- DetaNONOate, 8-CPT, Febuxostat or ODQ. **(A)** Quantified HepG2 Oil Red O absorbance (% vs controls) **(B)** NADPH oxidase activity (RLU/min). Per group, (A) *n*=5-32, (B) *n*=5-60. Data expressed as mean±SEM. Statistical significance defined as **p*<0.05, ***p*<0.01, ****p*<0.001, *****p*<0.0001. Statistical analyses conducted via Kruskal-Wallis Test with Dunn's *post hoc* testing.

A key enzymatic mediator of nitrite bioactivation is xanthine oxidoreductase (XOR)[64], due to its nitrite reductase activity. In combination with nitrite treatment, XOR partially blocked the steatosis-induced elevation in lipid accumulation and NOX activity (Figure 8). Similarly, using the EPR spin trap probe for NO species; Fe-DETC, the nitrite-derived NO signal was reduced when HepG2 cells were concomitantly treated with XOR. Together these findings suggest that the beneficial effects of nitrite on liver steatosis is mediated via nitrite-derived NO and cGMP/sGC-dependent signalling. In addition, XOR plays a role in the bioconversion of nitrate-nitrite-NO, however other NiRs are likely contributing in this HepG2 *in vitro* model.

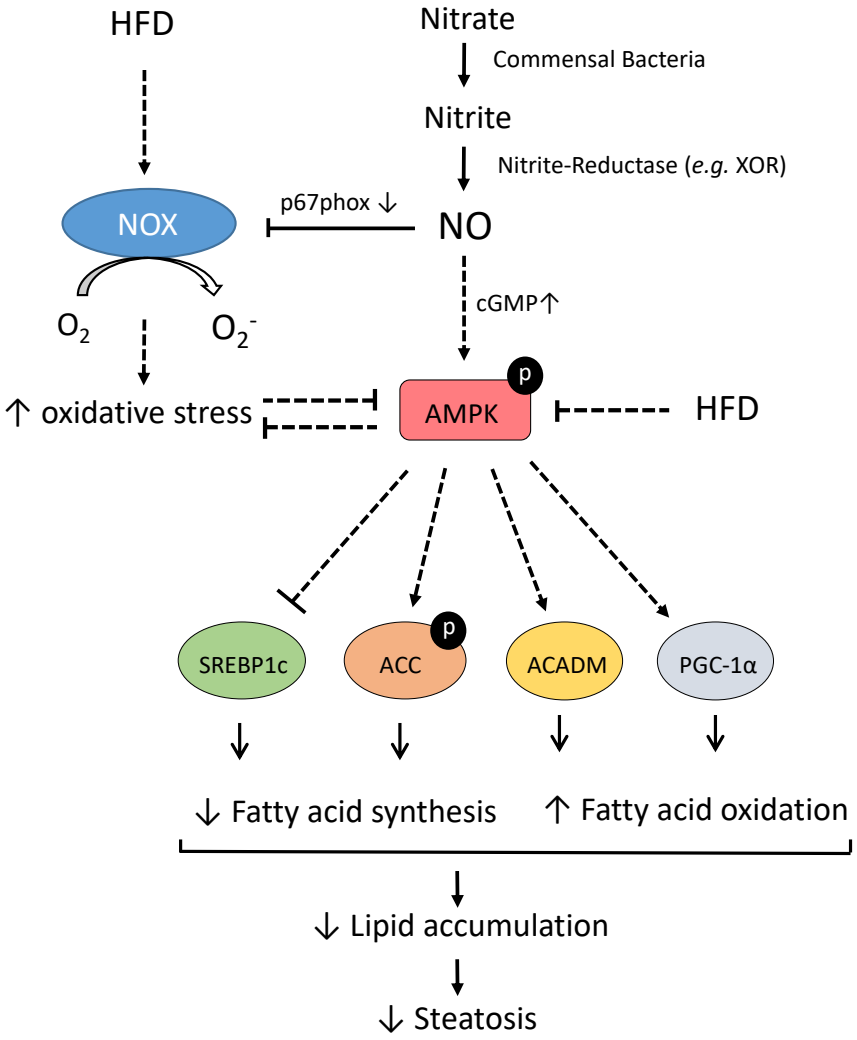

Figure 9. Proposed mechanisms by which nitrate mediates its beneficial metabolic effects in liver.

In summary, the findings of study I highlight a novel therapeutic role of dietary nitrate in liver steatosis, which exerts its effects via modulating AMPK signalling, resulting in the maintenance of downstream metabolic homeostasis, and via reducing NOX-derived oxidative stress (Figure 9). Of note, increased ROS has been demonstrated to directly mediate reduction of AMPK activation[199], suggesting that these beneficial effects of nitrate on AMPK signalling are also indirectly mediated via the reduction in NOX activity. Importantly, it is the nitrate derived-NO bioactivity which directly mediates these effects, independently of NOS-derived NO. Further clinical trials are warranted to determine whether this promising, dietary intervention could be of therapeutic value to combat the highly prevalent NAFLD.

3.2 STUDY II

Red Blood Cells from Endothelial Nitric Oxide Synthase-Deficient Mice Induce Vascular Dysfunction Involving Oxidative Stress and Endothelial Arginase

In recent years, the RBC has emerged as a key player in vascular homeostasis, via interaction(s) with the vascular endothelium[114]. The presence and catalytic activity of an RBC eNOS in the production of RBC eNOS-derived NO bioactivity has also been observed[122]. As endothelial eNOS has been widely established as dysfunctional in cardiovascular and metabolic disease states, which are characterised by endothelial dysfunction, study II aimed to dissect whether RBC eNOS *per se* is directly involved in mediating the RBC-endothelial interactions which maintain vascular homeostasis. To do this, we designed an experimental protocol (Figure 10) utilising an *ex vivo* approach to specifically investigate the impact of RBC eNOS on erythrocrine function and vascular homeostasis.

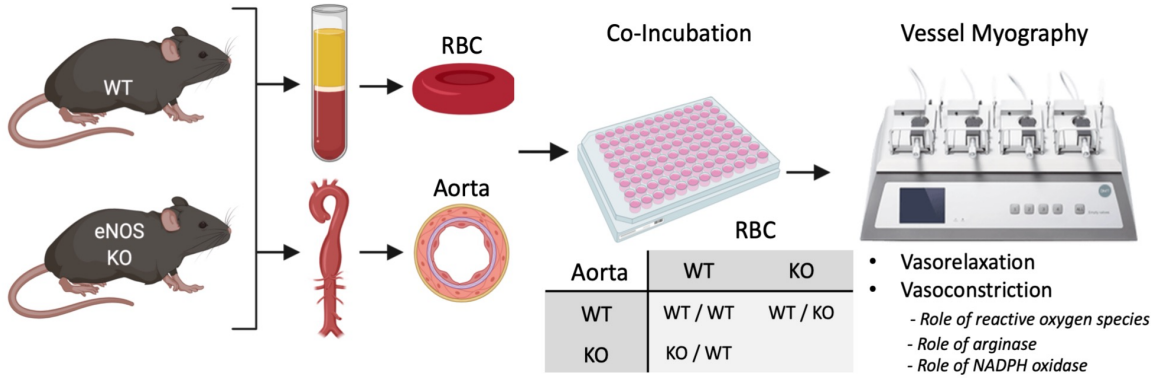

Figure 10. Schematic overview of experimental protocol. Whole blood and thoracic aortae were isolated from WT and global eNOS KO mice. RBCs were separated from other blood components and washed. Aortas were cute into rings (~2 mm) in PSS. Co-incubations were prepared in the indicated aorta-RBC combinations, with 10% haematocrit in DMEM media, and incubated overnight (18hrs) in a tissue culture incubator (37°C, 5% CO_2). Subsequently, aortic rings were thoroughly washed with fresh PSS and mounted onto the pins of a wire myograph. Vascular reactivity (vasodilation and contraction) was assessed. Mechanistic studies included simultaneous treatment with TEMPOL, nor-NOHA and NOX inhibitors to assess the role of reactive oxygen species (ROS), arginase and NADPH oxidase (NOX) activity, respectively.

3.2.1 RBCs from eNOS KO mice induced endothelial dysfunction

Exposure of a healthy WT mouse aorta to RBCs isolated from an eNOS KO mice (18hrs) significantly reduced vasorelaxation responses to endothelial-dependent vasodilator ACh, compared to those incubated with RBCs from WT mice. However, in the same vessels, endothelium-independent vasodilatory responses to SNP were not affected by RBCs from eNOS KO mice (Figure 11). This dysfunctional phenotype was independent of mouse gender or strain. These findings demonstrated the presence of a functional interaction between RBC eNOS *per se* and the endothelium, which was maintained following washing of RBCs from vessels.

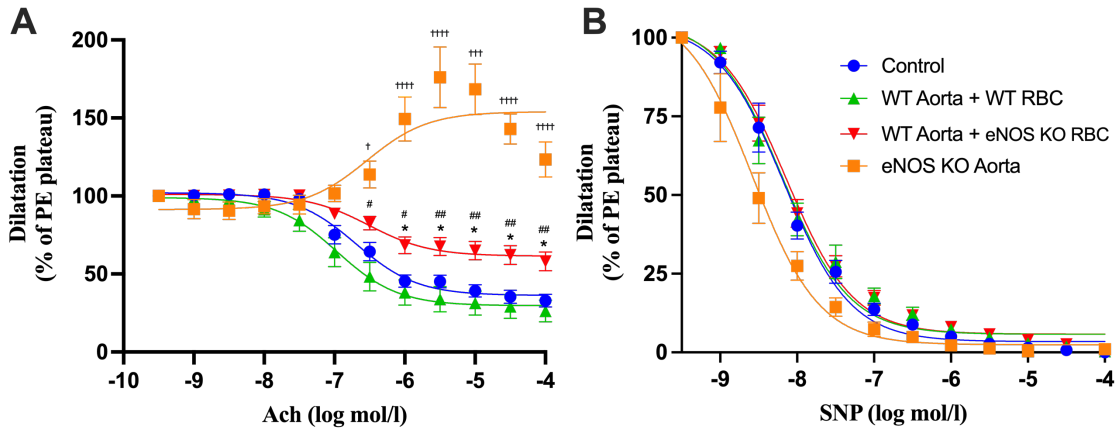

Figure 11. RBCs from eNOS KO mice induce endothelial dysfunction. (A) Endothelial-dependent vasorelaxation responses to acetylcholine (ACh) and **(B)** endothelial-independent vasorelaxation responses to nitroprusside (SNP) of aortic rings following 18hr incubation with Control, RBCs from WT mice (WT RBC; 10%) or RBCs a global eNOS KO mouse (eNOS KO RBC; 10%). WT aorta (Control) and eNOS KO aorta were incubated with DMEM alone. Data expressed as mean ± SEM; Control, n=7; WT aorta + WT RBC, n=17; WT aorta + eNOS KO RBC, n=18; eNOS KO aorta; n=10. Data analysed via ordinary 2-way ANOVA with multiple comparisons and Tukey's *post hoc* test. Statistical significance defined as *p<0.05, **p<0.01; ***p<0.005; ****p<0.001; Comparisons of WT aorta + eNOS KO RBC *vs Control; # vs WT aorta + WT RBC; † vs eNOS KO aorta.

3.2.2 Elevated oxidative stress and reduced NO bioavailability mechanistically involved in eNOS KO RBC-induced ED

In cardiometabolic disease, erythropathy has been associated with increased ROS formation, so we next investigated whether a lack of RBC eNOS induced an elevation of oxidative stress in the vascular microenvironment. When TEMPOL was included in overnight co-incubations of WT aorta and eNOS RBCs, the endothelial function was protected, whereby ACh-induced vasorelaxation was comparable to controls (Figure 12A). Following co-incubations and washing away of RBCs, addition of TEMPOL acutely into the myography chamber inferred protection to the endothelium (Figure 12B). Endothelial-dependent responses following WT RBC co-incubation and endothelial-independent responses remained unchanged following any TEMPOL treatments (*see full manuscript*). Similarly, following co-incubation with eNOS KO RBCs, *in situ* quantification of O_2^- utilising DHE demonstrated significantly increased O_2^- generation vs controls and WT aortas exposed to WT RBCs. Interestingly, the O_2^- levels in aortas exposed to eNOS KO RBCs were comparable to eNOS KO aorta (Figure 13).

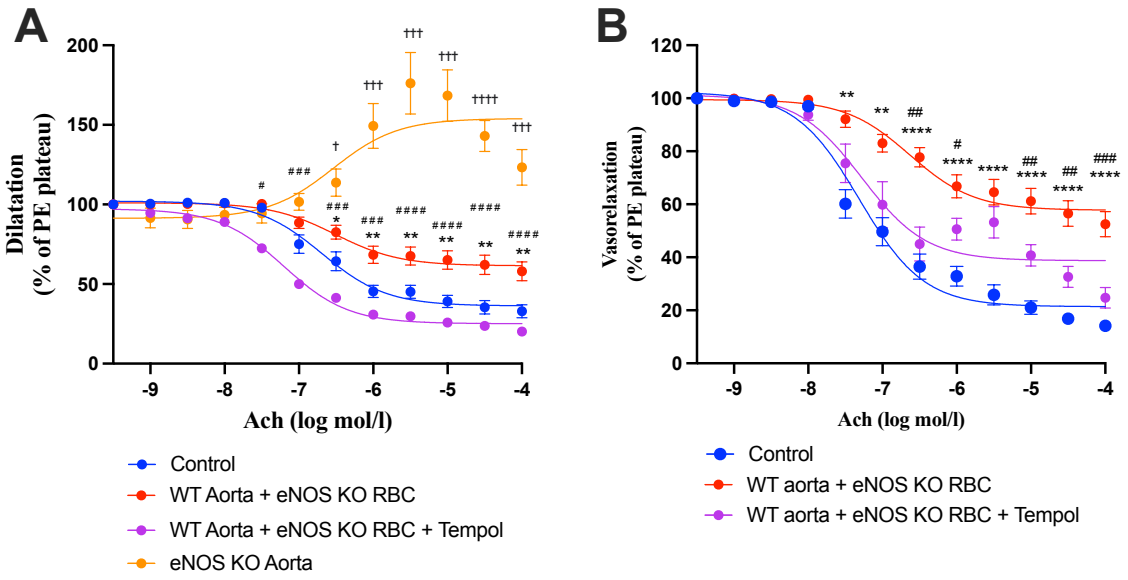

Figure 12. Functional role of vascular oxidative stress in eNOS KO RBC-induced endothelial dysfunction. Endothelial-dependent vasorelaxation response curve to acetylcholine (ACh) of WT mouse aortic rings following overnight incubation with Control, RBC from an eNOS KO mouse (eNOS KO RBC; 10%) **(A)** simultaneously +/- TEMPOL (1 mM) and **(B)** only with TEMPOL (300uM) added acutely into myograph chamber. Control denotes WT aorta without RBCs. Control incubation denotes incubation with DMEM media without RBC. Data expressed as mean ± SEM; *n*=6-8 per group; analysed via ordinary 2-way ANOVA with multiple comparisons and Dunnett's *post hoc* test. Statistical significance defined as **p<0.05, **p<0.01; ***p<0.005; ****p<0.001; Comparisons of WT aorta + eNOS KO RBC *vs Control; # vs WT aorta + eNOS KO RBC + TEMPOL; † vs eNOS KO aorta.

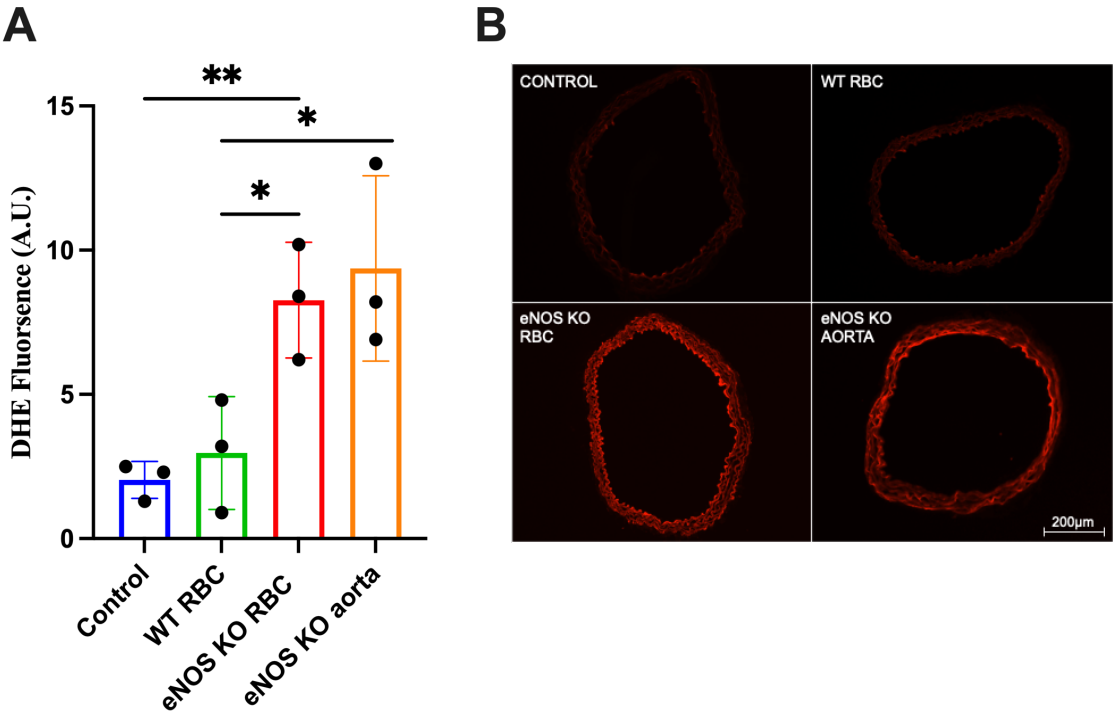

Figure 13. eNOS KO RBCs induce elevated vascular O_2^- production. (A) DHE fluorescence signal (A.U.) of WT mouse aortic rings after overnight incubation with RBC from a WT or an eNOS KO mouse. Control denotes WT aorta without RBCs. **(B)** Representative images of same aortic ring sections incubated in the presence DHE (x10 magnification; scale bar, 200µm). Red fluorescence produced upon $O2^{\bullet-}$-induced DHE oxidation to 2-hydroxyethidium. Data expressed as mean ± SEM; n=3 per group. Statistical significance defined as *p<0.05; **p<0.01 between indicated groups.

In the endothelium, NOX enzymes are important sources of ROS which are upregulated in cardiometabolic pathologies. We next assessed NOX as a potential source of this elevated ROS in our model via including specific NOX inhibitors (NOX2/4 and NOX4) in the WT aorta + RBC co-incubations. The induction of ED was prevented following simultaneous co-incubation with the NOX2/4 and NOX4 specific inhibitors (Figure 14). The NOX inhibitors did not alter endothelial function when combined with WT RBCs, nor endothelial-independent responses in any experimental groups (*see full manuscript*).

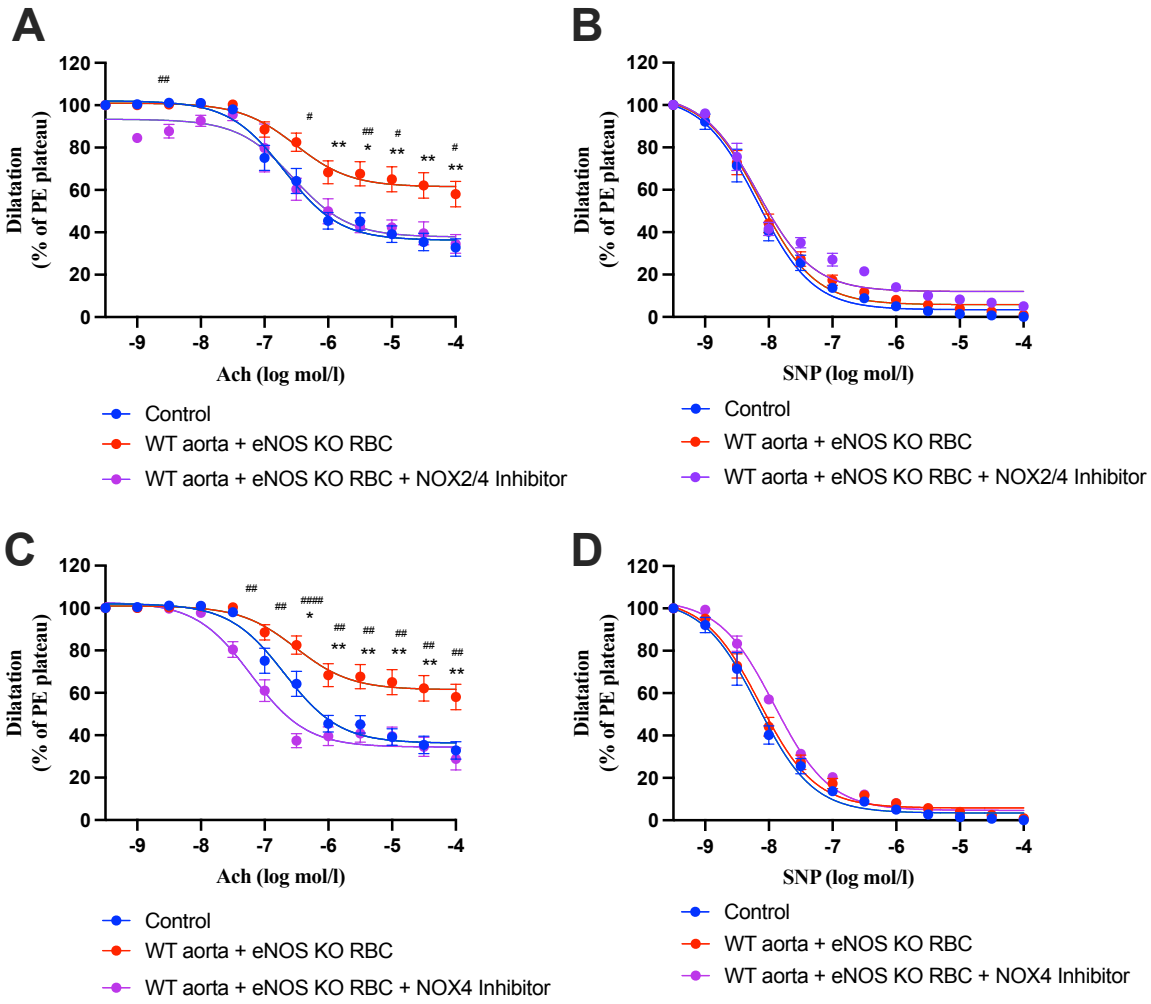

Figure 14. Functional role of dysregulated elevated ROS in eNOS KO RBC-induced endothelial dysfunction. (A, C) Endothelial-dependent vasorelaxation (% of Phe plateau; PE) response curve to acetylcholine (Ach; log mol/L) and **(B, D)** endothelial-independent vasorelaxation (% of Phe plateau; PE) response curve to nitroprusside (SNP) of WT mouse aortic rings following overnight incubation with Control, RBC from an **(A)** eNOS KO mouse (eNOS KO RBC; 10%) or **(B)** WT mouse +/- NOX 2&4 inhibitor (3uM) or **(C)** an eNOS KO mouse (eNOS KO RBC; 10%) or **(D)** WT mouse +/- NOX 4 inhibitor (30uM). Control denotes WT aorta without RBCs. Data expressed as mean ± SEM; n=10-15 per group; analysed via ordinary 2-way ANOVA with multiple comparisons and Dunnett's *post hoc* test. Statistical significance defined as *p<0.05, **p<0.01; Comparisons of WT aorta + eNOS KO RBC *vs Control; # vs WT aorta + eNOS KO RBC + Treatment.

NO is a central mediator of endothelial function, the bioavailability of which can be reduced by ROS scavenging. Following our observations of elevated ROS in our model, we next utilised DetaNONOate to investigate whether reduced NO bioavailability was contributing to the observed endothelial dysfunction. In separate experiments, co-incubations including

DetaNONOate prevented the eNOS KO RBC-induced endothelial dysfunction, such that ACh-induced vasodilation was comparable to controls (Figure 15). Endothelial-independent responses remained unchanged in all experimental groups.

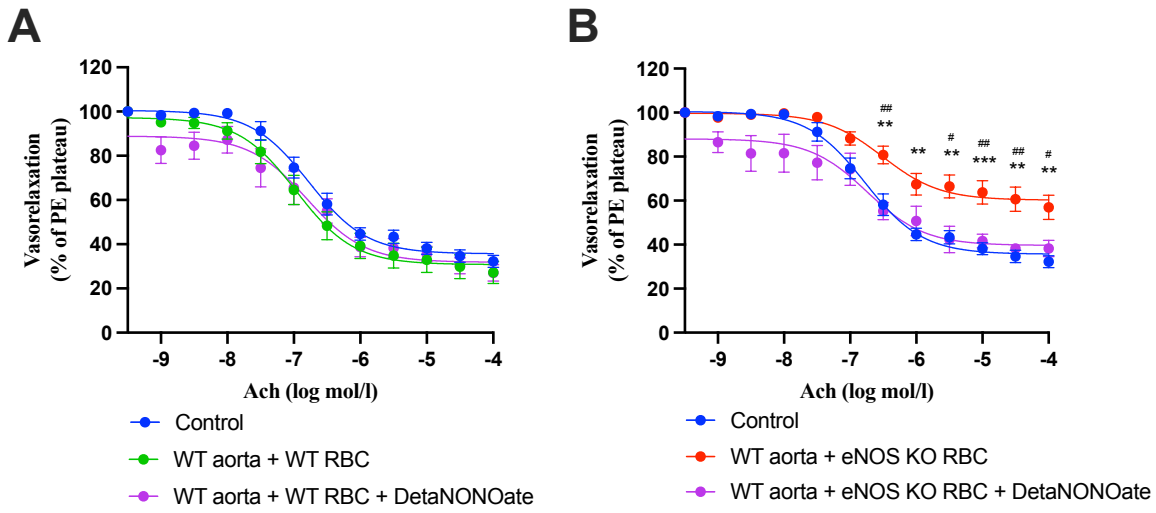

Figure 15. Functional role of dysregulated NO homeostasis in eNOS KO RBC-induced endothelial dysfunction. Endothelial-dependent vasorelaxation response curve to acetylcholine (ACh) of WT mouse aortic rings following overnight incubation with Control, **(A)** RBC from a WT mouse (WT RBC; 10%) and **(B)** RBC from an eNOS KO mouse (eNOS KO RBC; 10%) +/- DetaNONOate (30uM). Control denotes WT aorta without RBCs. Data expressed as mean ± SEM; n=6-7 per group; analysed via ordinary 2-way ANOVA with multiple comparisons and Dunnett's *post hoc* test. Statistical significance defined as *p<0.05, **p<0.01; ***p<0.005; Comparisons of WT aorta + eNOS KO RBC *vs Control; # vs WT aorta + eNOS KO RBC + DetaNONOate.

Together these findings highlight that oxidative stress, in part derived from NOX4, is a mediator of the eNOS KO RBC-induced endothelial dysfunction, which results in induction and maintenance of endothelial oxidative stress and reduced NO bioavailability, even when RBCs are removed. Exposure of the endothelium to RBCs without eNOS induces the equivalent oxidative burden on the endothelium to a lack of endothelial eNOS. This suggests that in addition to endothelial eNOS, RBC eNOS plays a role in the mediation of endothelial dysfunction.

3.2.3 eNOS KO RBCs mediate ED via vascular arginase 1

NOS enzymes compete with arginase for the common substrate L-Arginine in both the endothelium and RBCs. Changes to NOS and arginase activity can result in NO bioavailability and oxidative stress becoming unbalanced, and the propagation of a vicious oxidative cycle. Further, arginase activity can be upregulated via oxidative stress, and in T2Ds, $ONOO^-$ induced elevations in RBC arginase activity has been associated with mediating endothelial dysfunction[131–133]. Therefore, we next investigated whether a lack of RBC eNOS impacted function of arginase I in our model. To do this, we first utilised a pharmacological inhibitor of arginase; Nor-NOHA, in the co-incubation preparations. We observed complete prevention of eNOS KO RBC induced-ED in vessels concomitantly treated with Nor-NOHA, but it did not impact vessels incubated with WT RBCs or the endothelial-independent responses of any experimental groups (Figure 16A, B). Next, we co-incubated WT or eNOS KO RBCs with

aorta from endothelial-specific arginase 1 KO mice. Aorta lacking endothelial arginase I were protected from eNOS KO RBC-induced endothelial dysfunction, with comparable endothelial dependent and independent responses across all experimental groups (Figure 16C, D).

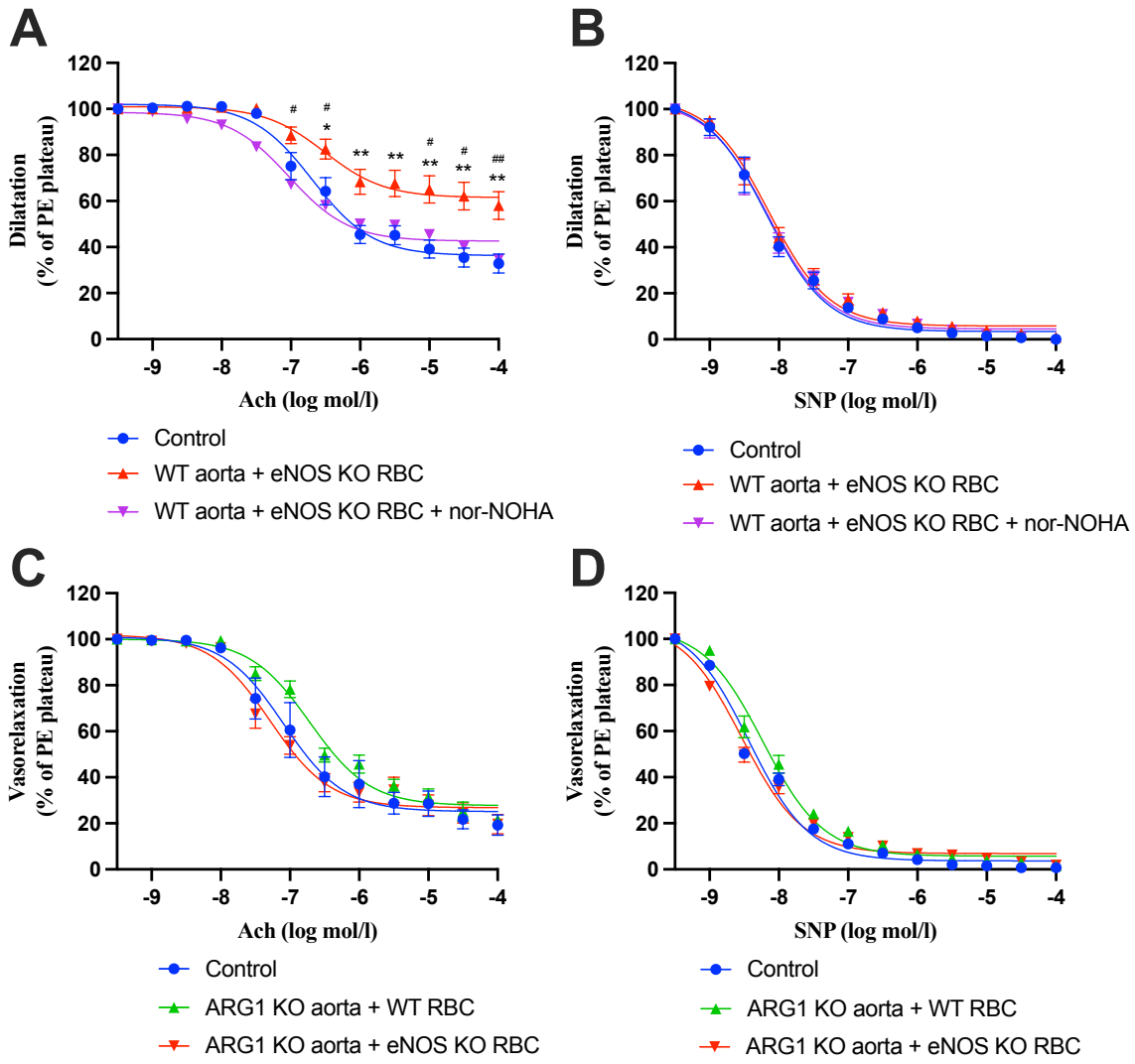

Figure 16. Functional role of dysregulated Arginase in eNOS KO RBC-induced endothelial dysfunction. (A, C) Endothelial-dependent vasorelaxation response curve to acetylcholine (ACh) and **(B, D)** endothelial-independent vasorelaxation response curve to nitroprusside (SNP) of mouse aortic rings. **(A, B)** WT mouse aortic rings following overnight incubation with Control, RBC from an eNOS KO mouse +/- Nor-NOHA (10 µM). **(C, D)** Endothelial-specific Arginase 1 KO mouse aortic rings following overnight incubation with Control, RBC from a WT mouse (WT RBC; 10%) or RBC from an eNOS KO mouse (KO RBC; 10%). Control denotes WT aorta without RBCs. Data expressed as mean ± SEM; n=9-11 per group; analysed via ordinary 2-way ANOVA with multiple comparisons and Dunnett's *post hoc* test. Statistical significance defined as *p<0.05, **p<0.01; Comparisons of aorta + eNOS KO RBC *vs Control; # vs eNOS KO RBC + Nor-NOHA.

To determine whether RBC arginase was involved in this deleterious interaction, we measured RBC arginase activity. We did not observe a difference in arginase activity between RBCs isolated from WT vs eNOS KO mice, suggesting that a lack of RBC eNOS *per se* does not upregulate arginase activity (Figure 17). Together, these data suggest that the ED induced following exposure to eNOS KO RBCs, is primarily mediated via endothelial arginase.

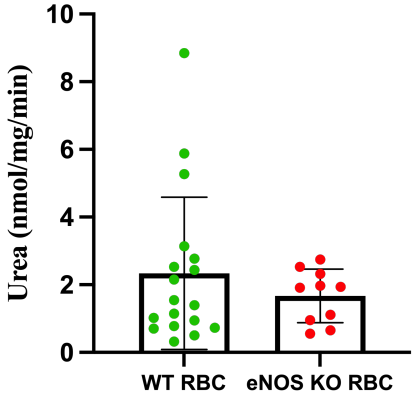

Figure 17. Comparable arginase activity in membrane fractions of red RBCs from wild-type (WT) and eNOS KO mice. Data expressed as mean±SEM; WT (n=18), eNOS KO (n=10). Analysed with Student's t test for unpaired observations. Statistical significance defined as $p<0.05$.

3.2.4 eNOS KO RBC-induced ED not mediated via elevated haemolysis

Cell-free heme is a product of haemolysis which scavenges NO at a rate ~1000-fold faster vs intracellular heme, thus highly influences vascular tone[200]. Further, its metabolites are known initiators of oxidative, inflammatory, apoptotic, and cytotoxic signalling. Once released, cell-free heme is largely scavenged via plasma proteins (hemopexin and haptoglobin)[201], a buffer system not present in our model. This led us to investigate whether the observed deleterious effects on the endothelium in our model were a result of RBCs from eNOS KO mice undergoing haemolysis to a greater degree vs WT RBCs.

To do this, we first investigated the degree of haemolysis required to induce an equivalent ED in our model, and whether this differed between WT vs eNOS KO RBCs. RBCs were lysed to different concentrations (%). Lysed RBC samples were co-incubated with WT aortic rings, and subsequently vascular function was assessed. Following co-incubation, supernatants were collected, and Hb (mg/ml, cyanmethaeoglobin) was quantified. For both WT and eNOS KO lysates, induction of ED required 1.5% haemolysed RBCs (Figure 18A, B), equivalent to ~2700mg/ml cyanmethaemoglobin (Figure 18C). Co-incubation with all other lysate concentrations (%) resulted in comparable endothelial-dependent vasodilation responses vs control (0%). Next, the level of haemolysis in our model was quantified. Following co-incubation with WT aorta, we observed a comparable level of haemolysis, ~500mg/ml cyanmethaemoglobin, for both preparations with WT RBCs and eNOS KO RBCs (Figure 18D). Together these data do not support a role for elevated haemolysis, and the associated downstream deleterious signalling, in mediation of eNOS KO-induced endothelial dysfunction.

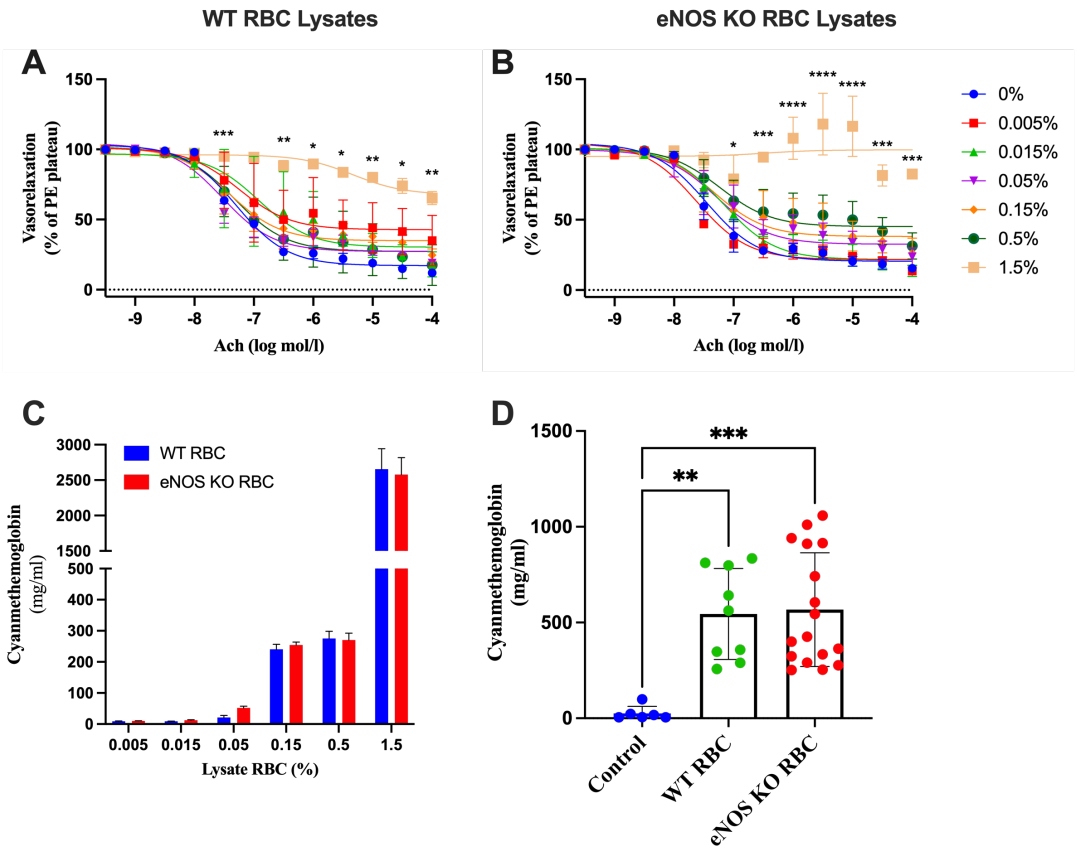

Figure 18. eNOS KO RBCs unlikely to induce ED via elevated haemolysis. Endothelial-dependent vasorelaxation in response to acetylcholine (ACh) of WT aortic rings following overnight co-incubation with lysed RBCs from a **(A)** WT mouse and **(B)** eNOS KO mouses, at increasing concentrations (%). 0% haematocrit denotes incubation with DMEM media without RBC. **(C)** Cyanmethaemoglobin (mg/ml) concentrations of supernatants following co-incubation of WT aorta and RBC **(D)** Cyanmethaemoglobin (mg/ml) concentrations of supernatants collected post-coincubation of WT aortae and Control, RBC from WT mouse (10%) or eNOS KO mouse (10%). Data expressed as mean ± SEM; (A, B, C) N=3; (D) Control, n=6; WT RBC, n=9; eNOS KO RBC, n=17. Statistical significance defined as *p<0.05, **p<0.01; ****p<0.001, (A, B) *vs 0% RBC lysates.

In summary, the findings of study II provide further support for a role of erythrocrine signalling in the regulation of vascular function via its interactions with the endothelium. Importantly, RBC eNOS *per se* has the capacity to influence endothelial homeostasis, highlighting the importance of RBC eNOS-derived NO bioactivity. A lack of RBC eNOS stimulates a deleterious crosstalk with the endothelium via elevation of arginase and NOX-dependent oxidative stress, and reduction of bioavailable NO in the vascular environment, which is maintained after RBCs are removed. Clinically, a lack of RBC-derived NO bioactivity has been demonstrated in T2D[131–133] and COVID[202] patients, diseases which have clear associations with endothelial dysfunction. Further studies are warranted to further dissect the mechanisms underlying regulation of RBC-endothelial crosstalk and elucidate the role of RBC function in the mediation of cardiovascular and metabolic pathogenesis. In future, targeting of erythrocrine function for therapeutic exploitation to improve endothelial function may be a promising novel approach to CMD.

3.3 STUDY III

Red blood cells from patients with preeclampsia induce endothelial dysfunction

The clinical manifestations of PE are characterised by systemic ED as a result of mechanisms including elevated oxidative stress and reduced NO bioavailability. Consensus regarding the definitive link between the placental (stage I) and maternal systemic (stage II) dysfunction in PE has yet to be reached. In *study II* we provided further support for the presence of a functional interaction between RBCs and the endothelium, in maintaining vascular homeostasis via balance of redox status and NO bioavailability in the vascular microenvironment. This important interaction has similarly been observed in T2D, COVID-19, regulation of cardiac function and hypertension[125,126,131–133,202]. Given these observations, in *study III*, we aimed to investigate the functional interaction between RBCs from preeclamptic (PE) vs health pregnant (HP) women, and the endothelium.

3.3.1 Clinical characteristics of study population at delivery

The clinical characteristics of the study population at delivery, stratified by PE severity, are presented in Table 2. Overall, 58 HP and 64 PE women participated in the study, with 38 being classified with sPE. Across all study groups, no significant differences were observed between maternal age, BMI, parity, or incidence of smoking. Whereas, gestational age, newborn weight, proportion of small for gestational age (SGA) offspring and premature births, and incidence of caesarean section were significantly different between all groups.

Table 2. Clinical characteristics of study population at delivery

	HP (n=58)	**PE** (n=26)	**sPE** (n=38)	***P* Value** #
Maternal Age				
Mean *(SD)*	31 (4.9)	34 (6.8)	33 (8.0)	ns
Gestational age *(wk)*				
Mean *(SD)*	39 (2.34)	28 (5.51)**	26 (5.86)***	<0.0001
Body Mass Index *(kg/m²)*				
Mean *(SD)*	25.7 (3.96)	27.5 (5.7)	25.9 (5.86)	ns
Nulliparous, *n (%)*	33 (56.9)	17 (65.4)	23 (60.5)	ns
Caesarean Section, *n (%)*	22 (38.5)	15 (57.7)*	32 (84.2)	<0.0001
Newborn Weight, *(g)*				
Mean *(SD)*	3445 (593)	2719 (813)****	2026 (689)****	<0.0001
SGA, *n (%)*	2 (3.5)	10 (38.5)*	19 (50)	<0.0001
Prematurity, *n (%)*	9 (15.5)	12 (48.0)*	33 (86.8)	<0.0001
Smokers, *n (%)*	3 (5.17)	1 (3.85)	0 (0)	ns

HP, healthy pregnant; PE, preeclampsia; sPE, severe PE; SGA, small for gestational age; n, number of female participants; wk, week; IQR, interquartile range; SD, standard deviation. Parametric variables: Chi-squared test (dichotomous variables); 1-way ANOVA (continuous data); Nonparametric variables; Kruskal-Wallis test (continuous data). Statistical significance defined as *p<0.05; ** p<0.01; ***p<0.0001 vs HP group, and # between all three groups.

3.3.2 Altered NO homeostasis and signalling in preeclamptic women

Differing findings regarding the status of circulating bioavailable NO in preeclamptic patients have been reported. In this cohort of patients, we observed a decrease in circulating nitrite in PE vs HP women, but not nitrate. However, when nitrate and nitrite were quantified in umbilical cord plasma from the offspring of PE vs HP immediately post-delivery, no differences were observed. Further, only maternal plasma cGMP levels were reduced in PE vs HP women, not their offspring (Figure 19). These findings suggest that in the studied cohort, maternal circulating NO homeostasis and signalling is perturbed in PE, but not HP women. However, this was not conferred to the fetoplacental circulation.

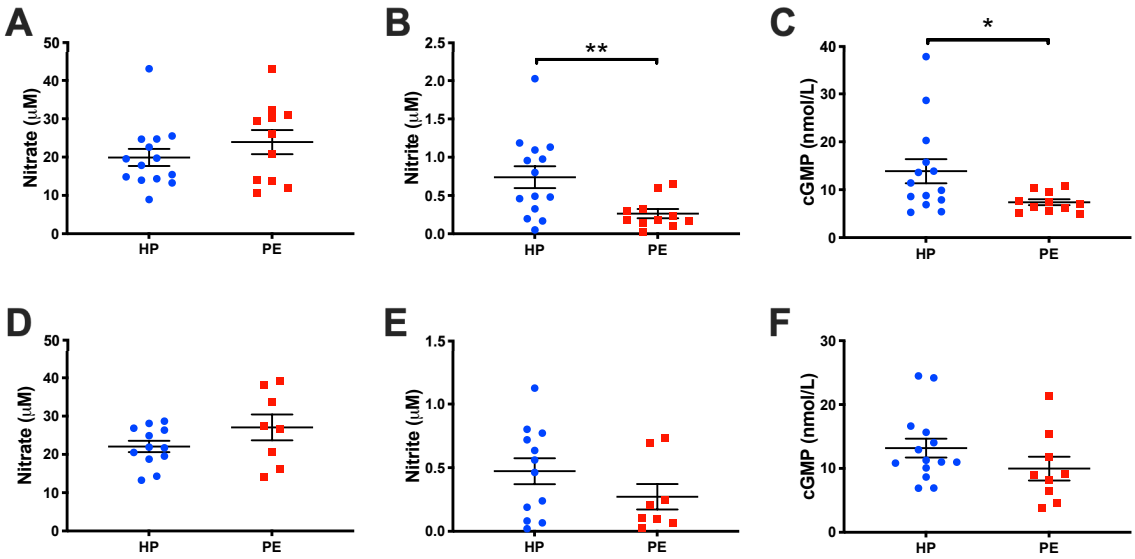

Figure 19. NO homeostasis altered in pre-eclamptic women. Plasma isolated from **(A, B, C)** venous maternal blood and **(D, E, F)** umbilical cord blood, immediately post-delivery. Quantification of plasma concentrations of **(A)** nitrate, **(B)** nitrite and **(C)** cGMP in healthy pregnant (HP; *n*=14) vs pre-eclamptic (PE; *n*=11) mothers. Plasma concentrations of **(D)** nitrate, **(E)** nitrite (HP; *n*=12 and PE; *n*=8) and **(F)** cGMP (HP; *n*=14 and PE; *n*=9) in the offspring from the same healthy pregnant (HP) and pre-eclamptic (PE) mothers. Data expressed as mean ± SEM; analysed with a student's *t*-test for unpaired observations. Statistical significance defined as *p<0.05; **p<0.01.

3.3.3 RBCs, but not plasma, from patients with PE induce endothelial dysfunction

Following our observations of altered circulating NO homeostasis and signalling in PE women, we became interested in whether specific blood components could mediate any functional changes to the endothelium. Using the same *ex vivo* approach as *study II*, we investigated the impact of plasma vs RBC from preeclamptic women on endothelial function. Following co-incubation of WT aorta and plasma (5%) from PE or HP women, endothelial-dependent and -independent vasorelaxation were comparable across all groups (Figure 20C, D). However, when RBCs from PE women were co-incubated with WT aorta, we observed significant reduction of endothelial-dependent vasorelaxation vs HP RBC co-incubated vessels and controls. Endothelial-independent responses remained comparable across groups (Figure 20A, B).

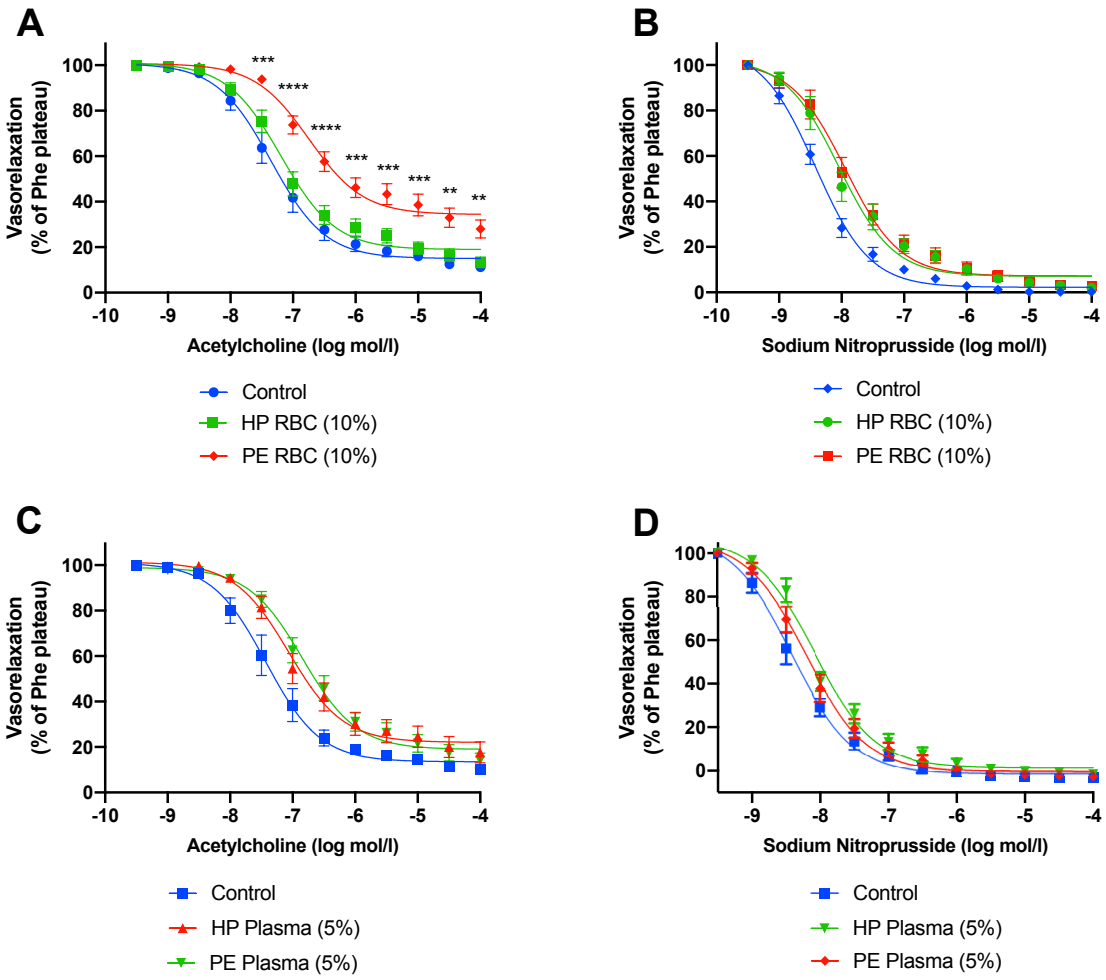

Figure 20: ED induced following exposure to RBCs from PE women. (A, C) Endothelial-dependent vasorelaxation response curve to acetylcholine (ACh), **(B, D)** endothelial-independent vasorelaxation response curve to nitroprusside (SNP) of mouse aortic rings following overnight incubation with Control, **(A, B)** RBCs or **(C, D)** plasma isolated from healthy pregnant (HP) or preeclamptic (PE) mothers. Control incubation denotes incubation with DMEM media without RBC. Data expressed as mean ± SEM; (A, B) n=4; (C, D) n=5; analysed via 2-way ANOVA with repeated measurements and Tukey *post hoc* test. Statistical significance defined as *p<0.05; comparisons between HP vs PE RBC (10%) co-incubated aortic rings.

3.3.4 PE RBCs mediate ED via arginase, ROS and compromised NO bioavailability

These novel findings were reminiscent of previous observations by Yang *et al*[126], whereby the cardioprotective effects of arginase inhibition in an *ex vivo* model of myocardial ischemia-reperfusion were only observed when perfused in the presence of RBCs, but not with buffer alone or plasma. Following a similar line of enquiry, we next investigated the role of arginase, oxidative stress, and NO bioavailability in the observed PE RBC-induced endothelial dysfunction. To do this, in separate experiments, we included an arginase inhibitor (Nor-NOHA), sodium nitrite, or a O_2^- scavenger (TEMPOL) with the overnight WT aorta + RBC co-incubations. When these treatments were separately incubated with WT aorta + RBCs from HP women, endothelial dependent vasorelaxation remained comparable to controls across all experimental groups (Figure 21A, C, E). Whereas, when the same treatments were separately included in WT aorta + RBC from PE women co-incubations, the PE RBC-induced ED we previously observed was ameliorated for each treatment, such that endothelial-dependent

vasorelaxation was comparable with controls (Figure B, D, F). Endothelial-independent vasorelaxation responses were not impacted in all treatment groups. These data suggest that the detrimental functional endothelial effects observed following exposure to RBCs from PE women is mediated via elevated arginase activity, ROS generation and subsequent reduction in NO bioavailability.

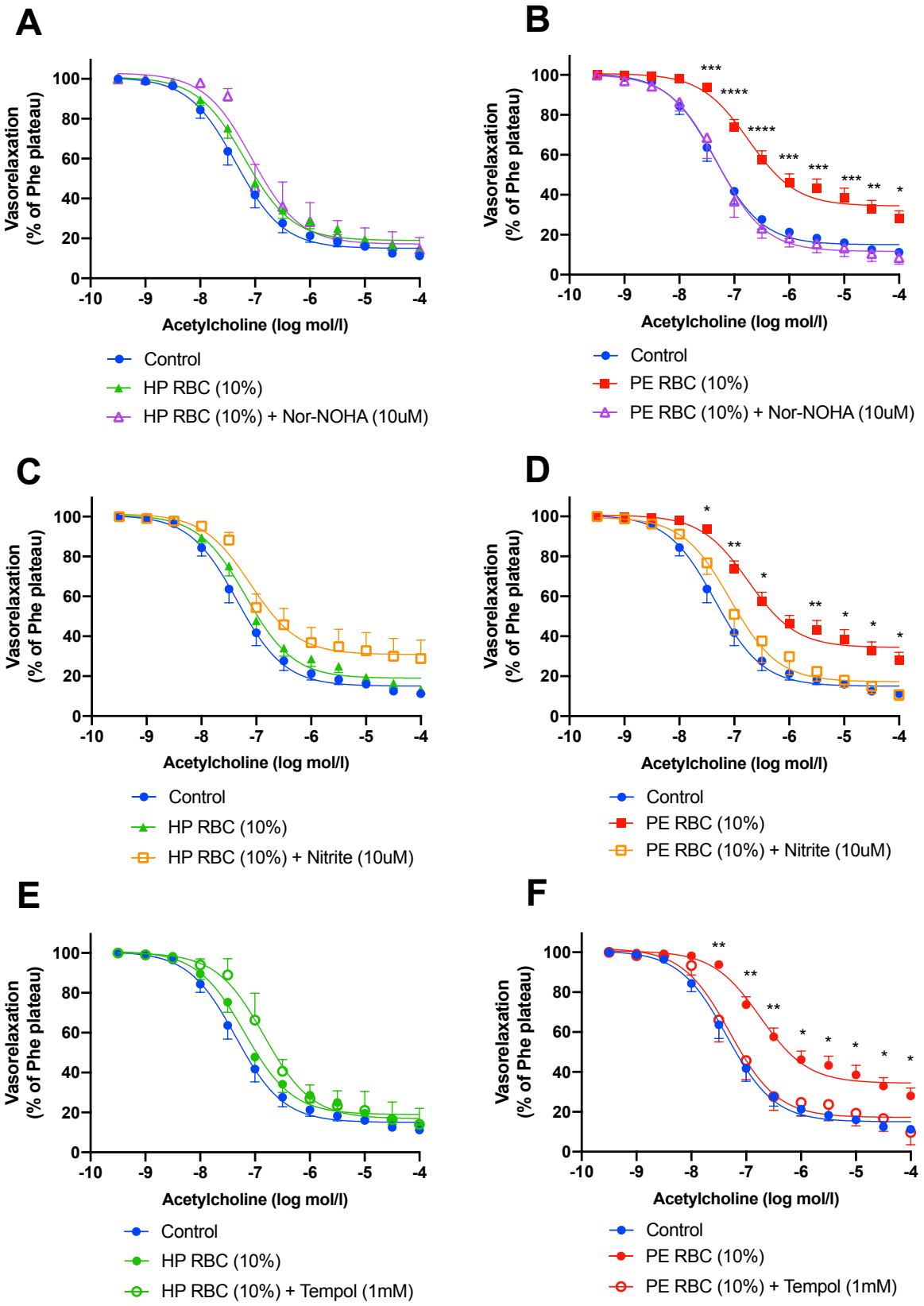

Figure 21: Altered NO homeostasis and elevated ROS play a role in mediating PE RBC-induced endothelial dysfunction. Endothelial-dependent vasorelaxation response curve to acetylcholine (ACh) of murine aortic rings following overnight incubation with Control **(A)** HP RBC or **(B)** PE RBC +/- Nor-NOHA (10 μM); **(C)** HP RBC or **(D)** PE RBC +/- Nitrite (10 μM); **(E)** HP RBC **(F)** PE RBC +/- TEMPOL (1 mM). Control incubation denotes incubation with DMEM media without RBC. Data expressed as mean ± SEM; analysed via a 2-way ANOVA with repeated measurements and Tukey *post hoc* testing.; (A, B) n=4; (C, D) n=5. (E, F) n=3. Statistical significance defined as *p<0.05; **p<0.01 between PE RBC and (B) PE + Nor-NOHA (10 μM), (D) PE RBC + Nitrite (10 μM), and (F) PE RBC + TEMPOL (1 mM).

3.3.5 Elevated arginase activity and expression in PE RBCs influenced by PE severity

Next, we aimed to determine whether RBC arginase activity and expression was dysfunctional in PE. Samples from the same cohort of patients as the myography studies demonstrated increased arginase activity in PE vs HP RBCs, which was concomitant to elevated arginase expression (Figure 22). Further, following adjustment for maternal descriptive factors (PE severity, BMI, parity, age, and smoking), PE severity (HP vs PE vs sPE) was the dominant factor associated with RBC arginase activity and expression. When stratified via PE severity, both arginase activity and expression increased with increasing PE severity. Plasma arginase activity and expression was comparable between all experimental groups. Thus, highlighting an association between RBC arginase and blood pressure in PE (*see study III supplement*). Together, these findings support a role of altered RBC arginase expression and function in PE, independent of maternal descriptive factors.

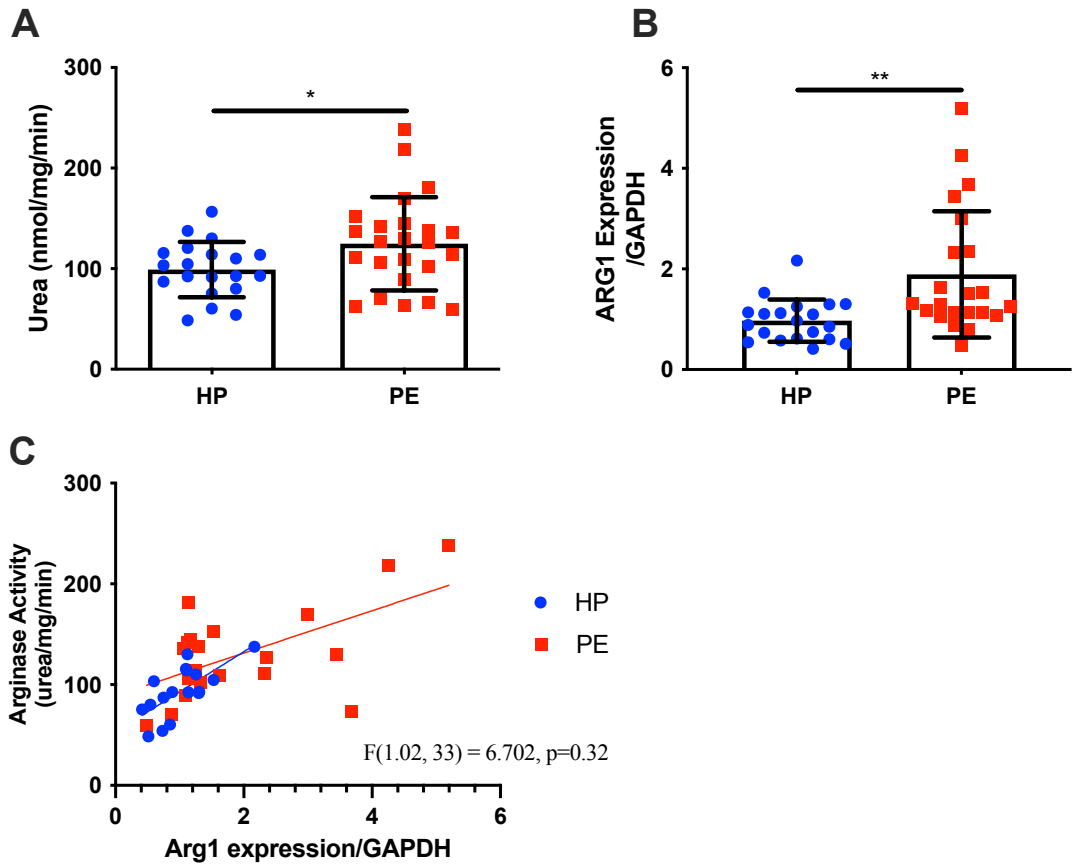

Figure 22: RBC arginase activity and expression increased in PE. (A) Arginase activity and **(B)** Arginase 1 expression in RBC from healthy (HP) and pre-eclamptic (PE) mothers. **(C)** Correlation analyses comparing arginase activity and expression between groups. Data expressed as mean ± SEM; (A) HP, n=21, PE, n=24 (B) HP, n=20, PE, n=22; analysis conducted with (A, B) a student's *t*-test for unpaired observations and (C) linear correlation analysis. Statistical significance defined as *p<0.05, **p<0.01.

3.4 Haemolysis unlikely to mediate PE RBC-induced endothelial dysfunction

Utilising a similar approach as *study II*, we investigated whether elevated haemolysis of RBCs could account for the observed endothelial dysfunction. The concentrations of lysed RBCs

which induced ED were 0.5 and 1.5% vs 0% lysed RBCs. When compared to previously reported levels of haemolysis in PE[170] (0.005%), the concentration of lysed RBCs was not sufficient to induce ED in our model (Figure 23). Additionally, we observed no differences in haemolysis, as measured via plasma Hb, between HP and PE samples. Next, we utilised transwell inserts in our co-incubation preparations, such that direct contact between RBCs and aortae was prevented, but cell-free Hb could pass through the pores of the membrane (0.4 µm). When direct contact between PE RBCs and aortae was prevented, endothelial function was comparable to HP RBC-incubated vessels and controls (Figure 24A). Together, these data suggest that haemolysis is comparable in HP and PE women and that cell free heme and its downstream mediators are unlikely to mediate the observed PE RBC-induced endothelial dysfunction.

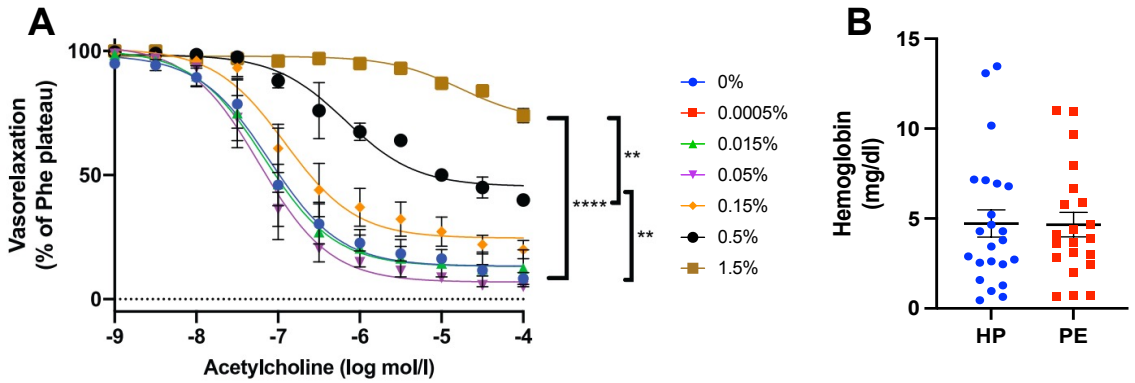

Figure 23: Products of haemolysis unlikely mediators of PE RBC-induced endothelial dysfunction. (A) Endothelial-dependent vasorelaxation (% of Phe plateau) response curve to acetylcholine (ACh), following overnight incubation with increasing concentrations of healthy non-pregnant lysed RBCs (0, 0.015, 0.05, 0.15, 0.5, 1.5%) diluted in DMEM. **(B)** Levels of Hb (g%) in plasma from healthy pregnant (HP) and pre-eclamptic (PE) mothers. Data expressed as mean ± SEM; (A) n=3; (B) HP; n=23, PE; n=21. Analysed via (A) 2-way ANOVA with repeated measurements and Tukey *post hoc* testing, (B) Student's *t*-test for unpaired observations. Statistical significance defined as **p*<0.05; ***p*<0.01.

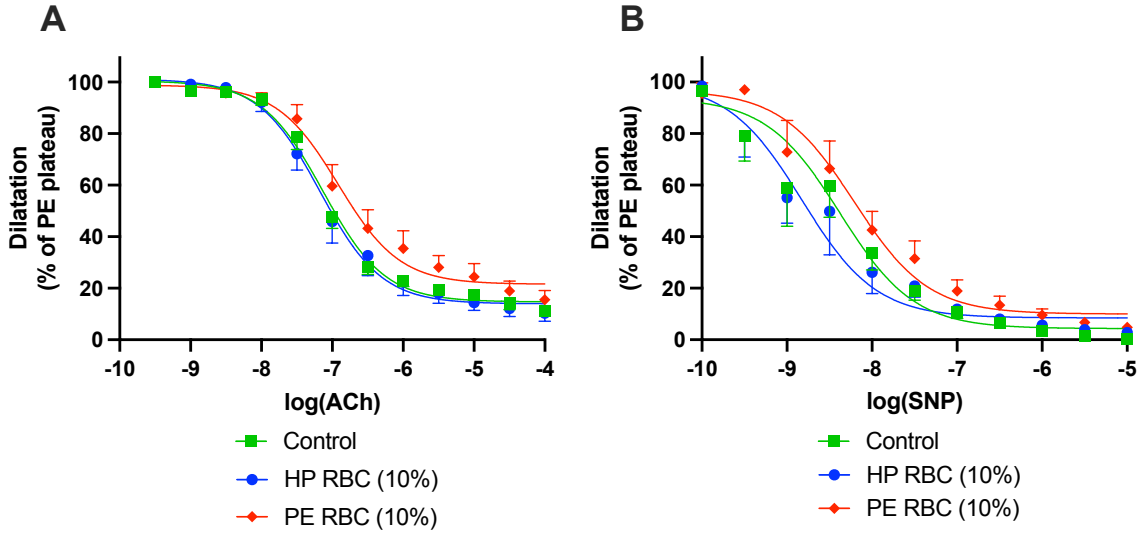

Figure 24: Contact between vessels and RBCs required for induction of endothelial dysfunction. (A) Endothelial-dependent vasorelaxation response curve to acetylcholine (ACh) and **(B)** endothelial-independent vascular responses to sodium nitroprusside of mouse aortic rings following overnight incubation, with transwell (pore size, 0.4 µm) permeable inserts, and RBCs from healthy pregnant (HP) or preeclamptic (PE) in DMEM media. Data expressed as mean ± SEM; n=3; analysed via a two-way ANOVA with repeated measurements and Tukey post-hoc testing. Statistical significance defined as **p*<0.05.

In summary, the findings of *study III* bring to light the RBC as a novel mediator of ED in PE, in part via arginase-dependent and oxidative stress-dependent mechanisms. These mechanistic insights may pave the way for the future development of pharmacological drug targets focused on PE RBCs. In addition, based on the observed significant linear correlation of RBC arginase activity and PE severity, further research is warranted investigating the role of RBC arginase activity in propagating the clinical maternal manifestations in PE *in vivo*.

3.4 STUDY IV

Effects of dietary nitrate supplementation on blood pressure and gestational outcomes in preeclamptic women: a double-blind, randomised-controlled pilot study (NITBEETPE)

As highlighted in section 1.6.4. clinical trials investigating novel therapeutic options to boost NO in PE have been unpromising. Together with previously evidenced dysregulated NO homeostasis and hypoxic utero-placental circulation, in *study IV* we aimed to investigate the potential salutatory cardiovascular effects of dietary nitrate supplementation in preeclamptic women. *Study IV* was a small pilot trial to investigate study protocol feasibility and inform the design of a larger RCT.

3.4.1 Clinical characteristics of study population & feasibility

The clinical characteristics of the study population for *study IV* is shown in Table 3. Overall, 22 women with PE completed the full study protocol, with 5 HP women recruited as baseline experimental controls. All clinical characteristics of placebo vs intervention groups were comparable. Whereas, gestational age at baseline (Day 0) was significantly different between HP vs placebo and treatment groups.

In total, 45 women were identified as eligible, 86.7% of which agreed to participate. Of the 39 women allocated to a study arm, only 22 completed the full protocol (56.4%). In patients who completed the full protocol, self-reported intake aligned with plasma, saliva and urinary nitrate and nitrite levels (Figure 26). The majority of dropouts were a result of non-study related clinical intervention mid-protocol, including delivery before follow-up and rediagnosis to gestational hypertension. This highlights the challenges of conducting clinical trials in preeclamptic populations specifically, including diagnostic difficulty and the dynamic, often unpredictable nature of PE pathogenesis.

Table 3. Clinical characteristics of study population.				
	HP (*n*=5)	**Placebo** (*n*=12)	**Treatment** (*n*=10)	***P* Value**[#]
Maternal Age, *mean (SD)*	33 ± 3	32 ± 5	34 ± 5	0.6492
Severe PE, *n (%)*	0 (0)	6 (50)	2 (20)	0.12
Gestational age, *(wk)*				
Baseline	39 ± 2	33 ± 3**	34 ± 3*	0.0059[#]
Delivery	40 ± 2	37 ± 2	37 ± 3	0.0739
Body Mass Index, *(kg/m²) Mean (SD)*	21.0 ± 2.4	27.4 ± 7.7	30.2 ± 5.6	0.0724
History of PE, *n (%)*	0 (0)	1 (8.3)	2 (20)	0.481
Nulliparous, *n (%)*	3 (60)	10 (83.3)	8 (80)	0.165
Caesarean Section, *n (%)*	3 (60)	7 (63.6)	5 (50)	0.632
Newborn Weight, (g) *Mean (SD)*	3649 ± 745	2621 ± 781	2910 ± 505	0.085
SGA, *n (%)*	0 (0)	3 (27.3)	0 (0)	0.143
Prematurity, *n (%)*	0 (0)	4 (33.3)	4 (40)	0.345
Smokers, *n (%)*	1 (20)	0 (0)	0 (0)	0.111
Medication days during juice intake, *n (%)*				
Trandate		10 (83.3)	8 (80.0)	0.84
Adalate		5 (41.7)	5 (50.0)	0.69
Amlodipine		2 (16.7)	4 (40.0)	0.22
Apresolin		1 (8.3)	1 (10.0)	0.89
Medication changed over juice intake days, *n (%)*		5 (41.7)	4 (40)	0.94

HP, healthy pregnant; BMI, body mass index; SGA; small for gestational age; *n*, number of participants; wk, week; CI, 95% confidence intervals; SD, standard deviation. Parametric variables: Chi-squared test (dichotomous variables); 1-way ANOVA with repeated measures and Tukey *post-hoc* testing (continuous data); Nonparametric variables; Kruskal-Wallis test (continuous data). Statistical significance defined as *p<0.05; ** p<0.01; vs HP, and # between all groups in row.

3.4.2 Blood Pressure

Office BP was not significantly changed following 7-day supplementation of dietary nitrate in PE women, compared to placebo (Figure 25), although a trend towards an increase in DBP (p=0.057) was observed. These findings align with the previous report investigating dietary nitrate supplementation in borderline hypertensive women[187]. However, it is important to note that both *study IV* and Ormesher *et al*[187] observed significantly greater variability in blood pressure measurements (~8-18 mmHg) compared with estimated variability utilised in power calculations (~7 mmHg), the latter having been based on previous dietary nitrate supplementation studies in non-pregnant, mostly male populations. These data will inform a larger RCT, considering gender and pregnancy in estimation of effect size within this specific population.

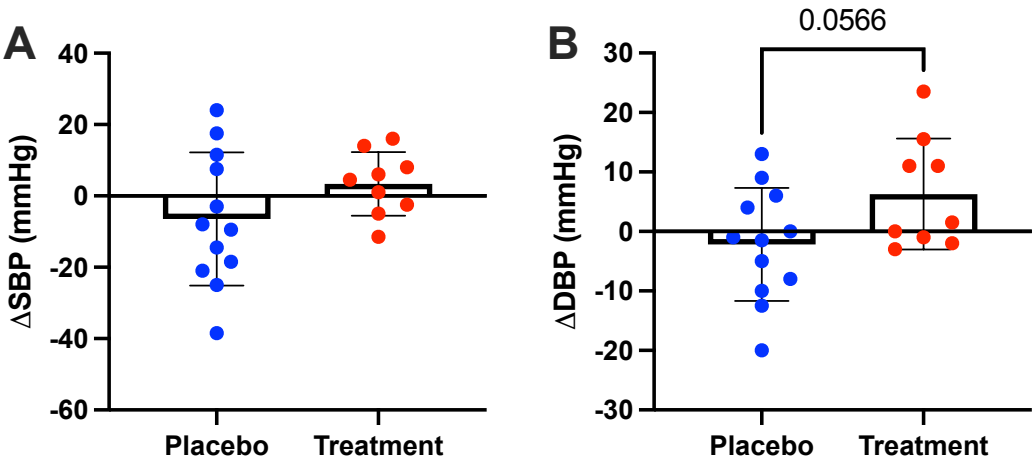

Figure 25. Comparable office blood pressure measurements in placebo vs treatment arms. Change in office **(A)** SBP and **(B)** DBP from baseline (mmHg). SBP; systolic blood pressure, DBP; diastolic blood pressure. Data are presented as mean±SD. *n*=9-12. Statistical significance defined as *$p<0.05$.

3.4.3 Circulating NOx homeostasis

Despite no changes in blood pressure, plasma and salivary nitrate and nitrite both increased from baseline to post-intervention in treatment vs placebo arms (Figure 26A-D). Only urinary nitrate was increased post intervention in treatment vs placebo arms (Figure 26E). Plasma cGMP remained unchanged between groups at baseline and post-intervention visits (Figure 26F).

To assess any potential impact of inter-patient variability between plasma nitrate and nitrite levels vs blood pressure responses, we conducted correlation analyses of changes in SBP and DBP vs plasma nitrate and nitrite measurements (Table 4), however no significant associations were observed. These findings were similarly observed in saliva and urinary nitrate and nitrite when compared with changes in SBP and DBP. However, we did observe a trend (p=0.08) towards a negative linear correlation between SBP and salivary nitrate in the treatment group, suggesting a potential dependence of blood pressure responses on individual enterosalivary capacity.

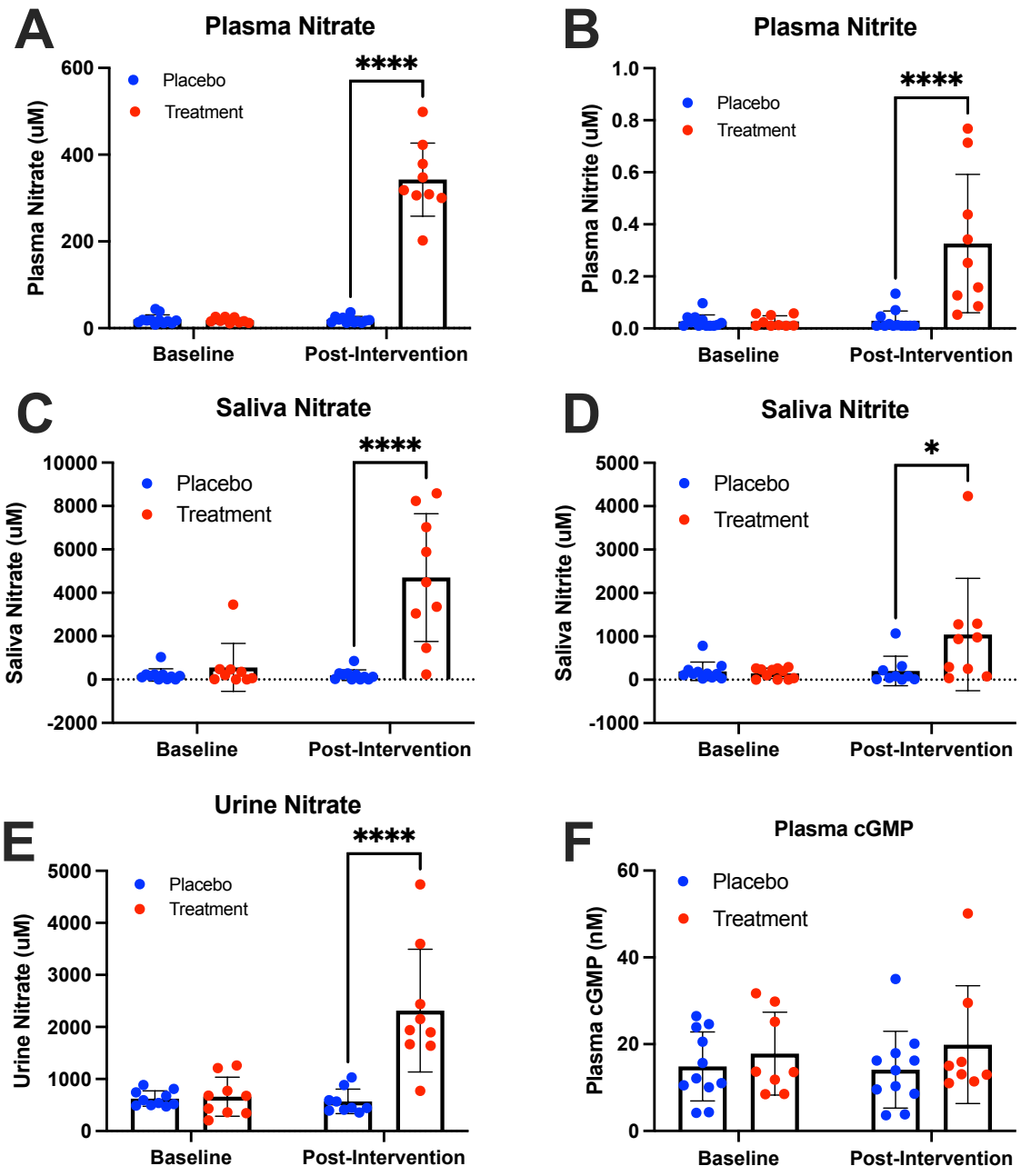

Figure 26. Dietary nitrate supplementation alters NOx concentrations in plasma, saliva, and urine but not plasma cGMP (A, B, F) Plasma, **(C, D)** Saliva, **(E)** Urine concentrations of **(A, C, E)** nitrate (uM), and **(B, D)** nitrite (uM) and **(F)** cGMP in placebo and treatment groups at baseline and post-intervention. Data are presented as mean±SD. *n*=9-12. Analysed with 2-way ANOVA with Bonferroni *post-hoc* testing. Statistical significance defined as *p<0.05; ** p<0.01; ***p<0.0001; ****p<0.00001, comparisons between indicated groups.

Table 4. Changes in Plasma, Salivary and Urine NOx levels are not associated with changes (Δ) in blood pressure.				
	Placebo		**Treatment**	
	ΔSBP (mmHg)	**ΔDBP** (mmHg)	**ΔSBP** (mmHg)	**ΔDBP** (mmHg)
ΔPlasma NO_2^-	0.132 (0.25)	0.035(0.56)	0.07 (0.47)	0.0002 (0.97)
ΔPlasma NO_3^-	0.057 (0.46)	0.014 (0.71)	0.022 (0.26)	0.018 (0.26)
ΔSaliva NO_2^-	0.095 (0.421)	0.017 (0.70)	0.421 (0.08)	0.109 (0.39)
ΔSaliva NO_3^-	0.036 (0.57)	0.15 (0.24)	0.13 (0.34)	0.0006 (0.95)
ΔUrine NO_2^-	0.079 (0.43)	0.018 (0.71)	0.074 (0.44)	0.012 (0.76)
ΔUrine NO_3^-	0.067 (0.80)	0.045 (0.58)	0.009 (0.80)	0.033 (0.61)
Linear correlation analyses comparing plasma, salivary and urine nitrate, and nitrite vs changes in systolic (SBP) and diastolic (DBP) blood pressure. NO_2^-; Nitrite, NO_3^-; Nitrate. Data presented as; R^2 (*P* value). Data analysed via Pearson linear regression. *n*=9-12 per group.				

3.4.4 Nitrate-independent improvement of ED induced by RBCs from patients with PE

In *study III* we highlighted RBCs as a novel mediator of ED in PE. Additionally, in the same study, stimulating the nitrate-nitrite-NO pathway via concomitant treatment with nitrite, ameliorated the PE RBC-induced endothelial dysfunction. Considering these findings, we first aimed to further support our previous *ex vivo* findings regarding RBC-endothelial interaction(s), and we were curious as to whether *in vivo* dietary nitrate supplementation would similarly confer beneficial endothelial effects to erythrocrine function. To do this, we utilised the *ex vivo* approach from *study II and III* with washed RBCs from HP and PE women (placebo and intervention groups).

Similarly to *study III*, we observed significant *ex vivo* ED in healthy murine aorta following overnight incubation with RBCs isolated from PE vs HP women at baseline (Figure 27A). The degree to which PE RBCs-induced ED at baseline was comparable between placebo and treatment arms (Figure 27C). Baseline endothelial-independent responses were comparable between all groups. In contrast, RBCs isolated from post-intervention samples did not induce an ED for both placebo and treatment groups, as demonstrated by comparable ACh-induced vasorelaxation responses (Figure 27C, D). Post-intervention RBCs had no impact on endothelial-independent responses. These findings suggest beneficial nitrate-independent effects on erythrocrine function and interaction with the endothelium.

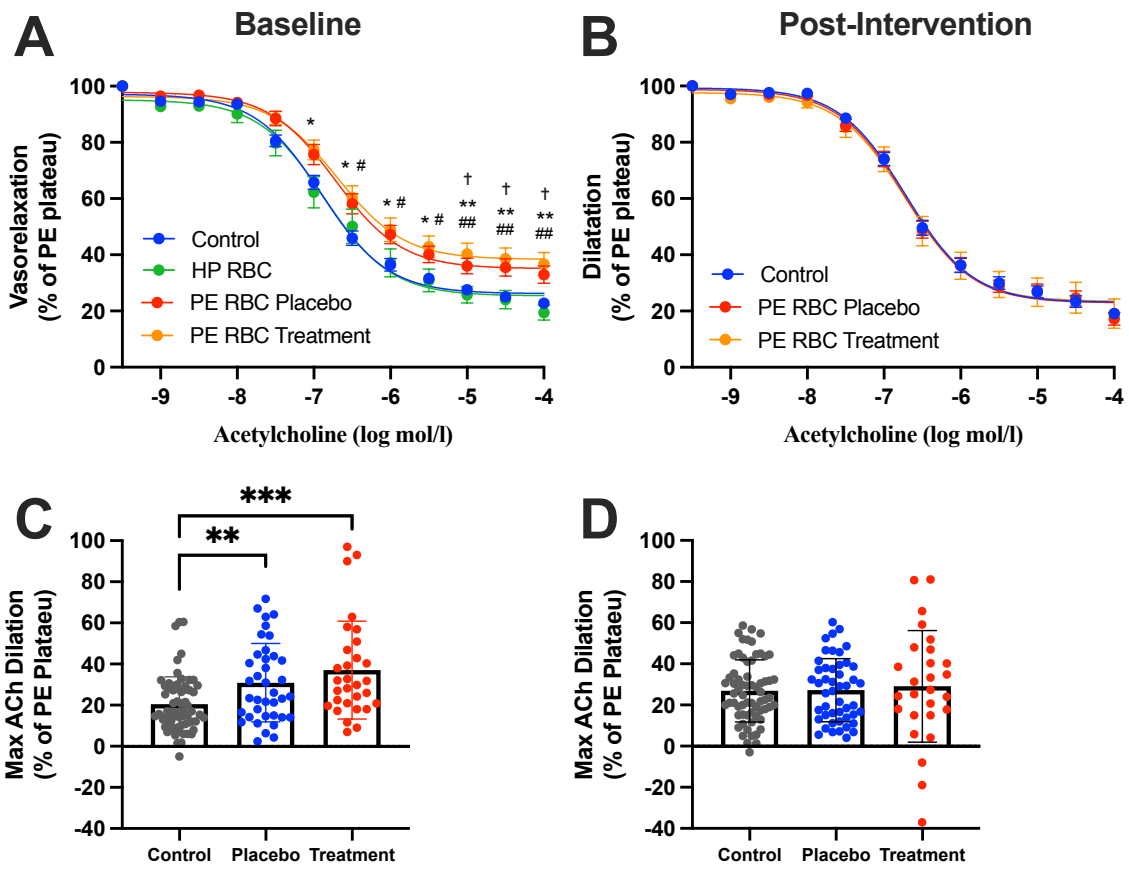

Figure 27: Both placebo and dietary nitrate supplementation prevent PE RBC-induced ED (A, B) Endothelial-dependent vasorelaxation response curve to acetylcholine (ACh) of mouse aortic rings following overnight incubation with **(A)** Control, RBCs from healthy pregnant (HP) or preeclamptic (PE) mothers, stratified by group at baseline. **(B)** Control, RBCs preeclamptic (PE) mothers who received placebo or dietary nitrate (treatment) supplementation post-intervention. Control incubation denotes incubation without RBC. Maximum ACh (100 mmol/L) induced vasodilation at **(C)** baseline and **(D)** post-intervention. Data expressed as **(A, B)** mean ± SEM, **(C, D)** mean ± SD. Experimental replicates, control, n=67; HP, n=15, Placebo, n=38; Treatment, n=30. Biological replicates, HP, n=5, Placebo, n=9; Treatment, n=8. Analysed via **(A, B)** 2-way ANOVA with repeated measurements and Tukey's *post hoc* testing, **(C, D)** one-way ANOVA with Tukey's *post hoc* test. Statistical significance defined as *p<0.05; ** p<0.01; ***p<0.0001. comparisons between **(A, B)** *PE RBC Treatment vs Control, #PE RBC Placebo vs Control, †PE RBC Treatment and PE RBC Placebo vs HP RBC, **(C, D)** indicated groups.

3.4.5 Circulating markers oxidative stress comparable between arms

To determine whether dietary nitrate supplementation reduced the systemic oxidative stress associated with PE, we measured systemic mediators of oxidative damage and inflammation; TF, CP and metHb in whole blood via EPR. No significant differences were observed in placebo vs treatment arms both at baseline and post-intervention (Figure 28). Although, CP:TF indicated a potential nitrate-dependent systemic antioxidant effect post-intervention, demonstrated by a trend towards decreased CP:TF. These findings suggest potential nitrate-dependent systemic antioxidant effects.

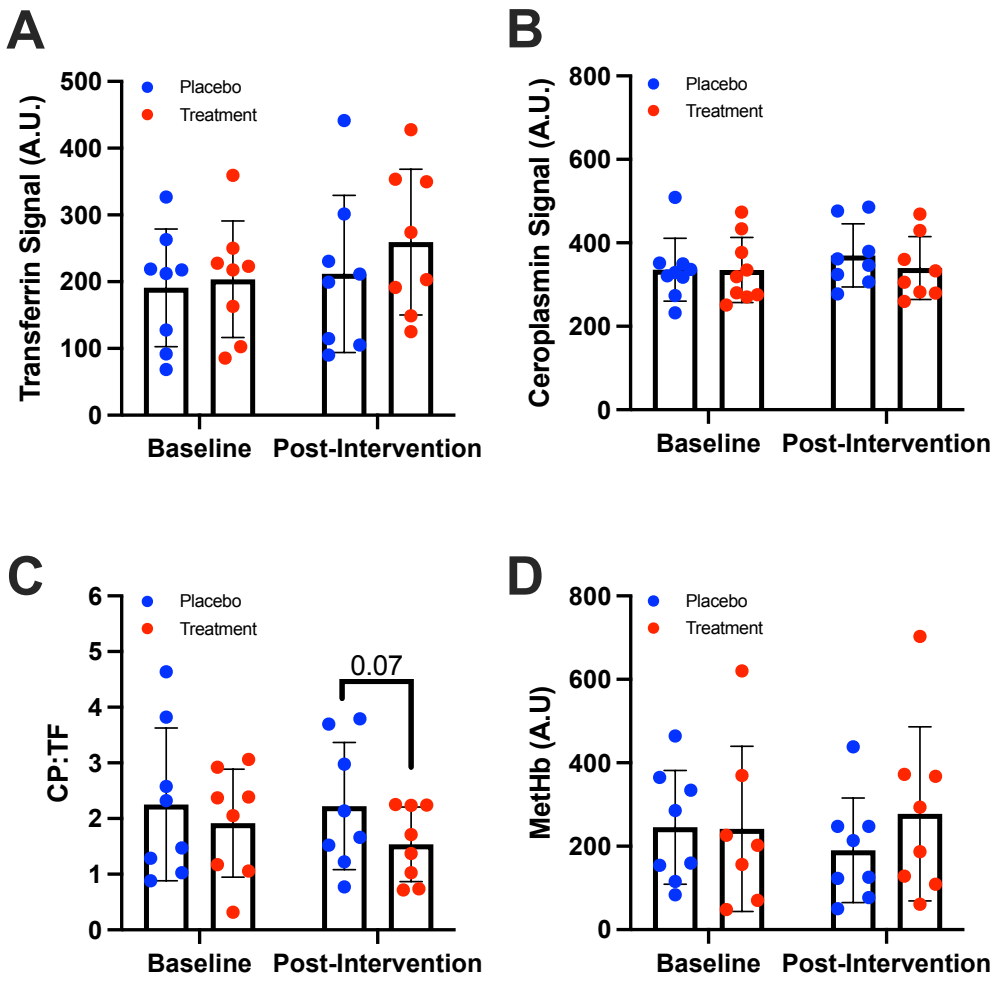

Figure 28: EPR quantification of Transferrin, Ceroplasmin and metHb signal in whole blood. Blood samples from placebo and treatment PE women were collected at baseline and post-intervention visits, and subsequently quantified for **(A)** Transferrin (TF), **(B)** Ceroplasmin (CP) and **(D)** methaemoglobin (MetHb). **(C)** Displays the calculated ratio between CP and TF. Data analysed via 2-way ANOVA with Bonferroni *post-hoc* testing. n=8 per group. Statistical significance defined as *p<0.05.

In summary, the experimental findings from *study IV* provided further evidence of a role of the RBC as a mediator of the ED observed in PE. Further, in our model, this dysregulated erythrocrine function in PE can be targeted via *in vivo* beetroot juice consumption, in a nitrate-independent manner. Evidence continues to mount which supports the importance of a homeostatic crosstalk between RBCs and the endothelium, which may provide a crucial therapeutic target(s) between stages I and II of PE pathogenesis. Further research is warranted to elucidate the alternative candidates within beetroot juice which may hold therapeutic promise, and to further dissect PE erythrocrine function, their interaction(s) with the endothelium and the dynamics of this phenotype over gestation.

This pilot study crucially highlighted the aspects of clinical methodology which need to be addressed during the planning of a larger scale RCT. The beetroot juice shots were well accepted and not associated with any adverse events. Although a challenge in robust clinical preeclamptic research, the recruitment and retention of patients must be considered when synthesising recruitment strategies and goals, including consideration of further support and

visibility of the clinical research team and estimated completion time, to prevent unrepresentative sample sizes and any negative impact on external validity of a larger study. Before any firm conclusions are drawn regarding nitrate dependent or independent effects of beetroot juice supplementation on blood pressure, sufficiently powered studies are required. This is especially important due to the heterogenous, multifactorial nature of PE.

Over the last 20 years, ED has emerged as a key player in PE pathogenesis which unifies the heterogeneity of PE, with some arguing that it is more important vs hypertension associated with PE[203]. To compliment the experimental findings of *study IV*, further non-invasive investigation of endothelial function *in vivo* in preeclamptic patients will be conducted to assess the therapeutic impact of dietary nitrate supplementation and the relative contribution of RBCs *in vivo*.

3.5 STUDY V

Monocytes from preeclamptic women previously treated with Silibinin attenuate oxidative stress in human endothelial cells

Elevated oxidative stress and inflammation are widely accepted as pathogenic mechanisms in PE by which placental dysfunction radiates its effects systemically. This is associated with saturation of both placental and systemic antioxidant capacities. PE is associated with activation and an altered functional phenotype of monocytes. This results in increased monocyte secretion of ROS and elevated cytokine secretion, which both contribute to endothelial dysfunction[204,205]. In *study V*, we aimed to investigate whether monocyte-derived factors which drive systemic oxidative stress and inflammation, could mediate the systemic ED observed in PE. In addition, the therapeutic value of treatment with Silibinin (Sb) on monocyte activation. To do this, we co-incubated supernatants collected from PBMCs isolated from PE and HP women, with HUVEC *in vitro*.

3.5.1 Clinical characteristics of study population

Analyses of the clinical characteristics is presented in Table 5. There were no differences in maternal age and gestational age at diagnosis between groups. As expected, both systolic and diastolic blood pressures, as well as proteinuria concentration, were significantly greater in PE vs HP women.

Table 5. Clinical characteristics of study population at diagnosis

	HP (n=10)	**PE** (n=10)
Maternal Age *(years)*	27 (19-39)	29 (18-40)
Gestational age *(wk)*	36 (29-40)	34 (28-39)
Systolic Blood Pressure *(mmHg)*	110 (80-120)	160 (140-210)*
Diastolic Blood Pressure *(mmHg)*	65 (63-70)	110 (90-125)*
Proteinuria *(mg/24h)*	<300	960 (320-1880)*

Data presented as median (range). Healthy (HP) vs preeclamptic (PE) women. Analysed via Mann Whitney-U test; Statistical significance defined as $p<0.05$; *vs HP

3.5.2 Silibinin treatment significantly reduces pro-inflammatory cytokine secretion from PE-isolated monocytes

In accordance with previous reports, pro-inflammatory cytokine secretion (IL-β and TNFα) from monocytes isolated from PE women (PE-PBMCs) was significantly greater than those isolated from HP women (HP-PBMCs). Whereas the anti-inflammatory cytokine; IL-10 was significantly decreased in PE-PBMCs vs HP-PBMCs (Table 6). Sb is the active component of the polyphenolic flavonoid; Silymarin, which has been used as an anti-inflammatory agent for >2,000 years[206]. More recently, *in vitro* Sb treatment reduced mRNA and protein levels of pro-inflammatory cytokines (IL-1β, IL-18 and TNF-α) in PE-PBMCs vs non-treated controls, via suppression of NF-κB activation and signalling[207]. In accordance with this, when cultured in the presence of Silibinin, levels of secreted IL-β and TNFα were significantly reduced, and IL-10 was significantly increased in PE-PBMCs vs non-treated PE-PBMCs (Table 6).

Table 6. PBMC supernatant cytokine concentrations +/- Silibinin treatment

Cytokines	HP		PE	
	Sb-	Sb+	Sb-	Sb+
IL-1 β *(pg/mL)*	87.19 ± 19.22	81.25 ± 16.98	590.71 ± 97.65#	200.04 ± 55.86*
TNF-α *(pg/mL)*	26.82 ± 6.28	29.80 ± 6.76	314.68 ± 55.24#	173.86 ± 30.27*
IL-10 *(pg/mL)*	181.46 ± 22.60	167.63 ± 20.23	88.09 ± 4.47#	93.16 ± 4.66*

Data presented as median (range). Healthy (HP) vs preeclamptic (PE) women. Sb; Silibinin, IL-1 β; Interleukin-1 beta; TNF- α; tumour necrosis factor-alpha; IL-10; interleukin-10. Analysed via 1-way ANOVA with multiple comparisons with Bonferroni's *post hoc* testing; Statistical significance defined as $p<0.05$; *vs PE Sb+; # vs HP Sb-.

3.5.3 Protective immuno- and redox-modulatory properties of Silibinin conferred to endothelium

In an *in vivo* model of PE, Sb treatment was demonstrated to reduce SBP, proteinuria, liver pro-inflammatory cytokine levels and improved fetal outcomes vs controls[208]. These findings stimulated us to investigate whether the anti-inflammatory effect of Sb on PE-PBMCs was associated with the previously observed beneficial cardiovascular effects.

Using an *in vitro* model, we investigated the impact PE-PBMC derived factors on HUVEC. When HUVEC were incubated with PE-PBMC vs HP-PBMC supernatant, we observed increased malondialdehyde (MDA), a major product of lipid oxidation and index of the level of oxidative stress. Exposure to supernatant from PE-PBMCs which were treated with Sb, significantly decreased the levels of MDA in HUVEC supernatant compared with non-treated PE-PBMC supernatant (Figure 29). MDA concentrations in HUVEC supernatant remained unchanged following exposure to HP-PBMC + Sb supernatants vs non treated HP-PBMC supernatants. Cell viability was not reduced in any experimental groups vs control. These data suggest that PE PBMC-derived factors elevate oxidative stress in HUVEC compared with HP PBMC-derived factors, and that Sb treatment prevents PE PBMCs from inducing oxidative stress in HUVEC.

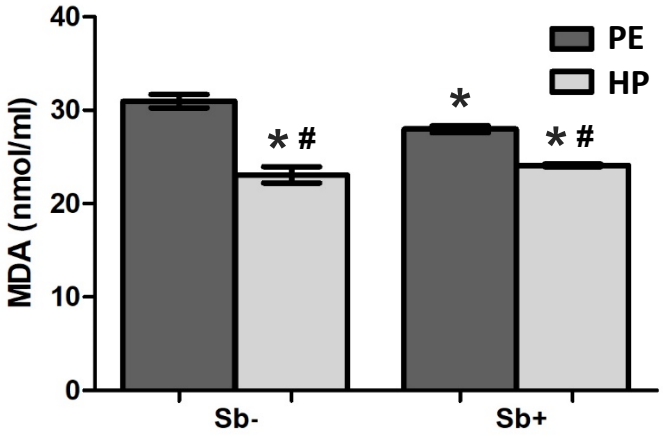

Figure 29. MDA concentration in HUVEC supernatants following 24hrs incubation with PE- and HP-PBMC supernatants. Prior to HUVEC incubation, PBMCs were incubated +/- Silibinin (Sb). PE; preeclampsia, HP; healthy pregnant women. Data presented as mean ± SD. Statistical significance defined as $p<0.05$ vs *PE Sb-; #PE Sb+.

Next, we investigated whether NO homeostasis in HUVEC was modulated by HP- vs PE-PBMC supernatants. Following 24hr incubation with HP- and PE- PBMC supernatants, HUVEC DAF-FM Diacetate fluorescence signal was comparable between groups. No changes in DAF-FM signal were observed following Sb treatment. Although it is important to consider the highly reactive properties and short-half-life of NO, as well as the known low extracellular NO output from endothelial cells, makes direct quantification of authentic local NO availability challenging[209]. We next measured nitrite and nitrate, as surrogate markers for NO. Nitrate levels in HUVEC supernatants were significantly increased when exposed to PE-vs HP-PBMC supernatants, whereas nitrite levels remained comparable. No effect of Sb treatment was observed on nitrate levels in HUVEC supernatants. Whereas Sb-treated PE-PBMC supernatants induced a significant increase in HUVEC supernatant nitrite concentration vs non-treated PE-PBMC supernatants (Figure 30). These data suggest that PBMCs have the capacity to alter NO homeostasis in the endothelium during PE. Further, that Sb treatment facilitates PE-PBMCs to mediate an increase in NO bioavailability the endothelium.

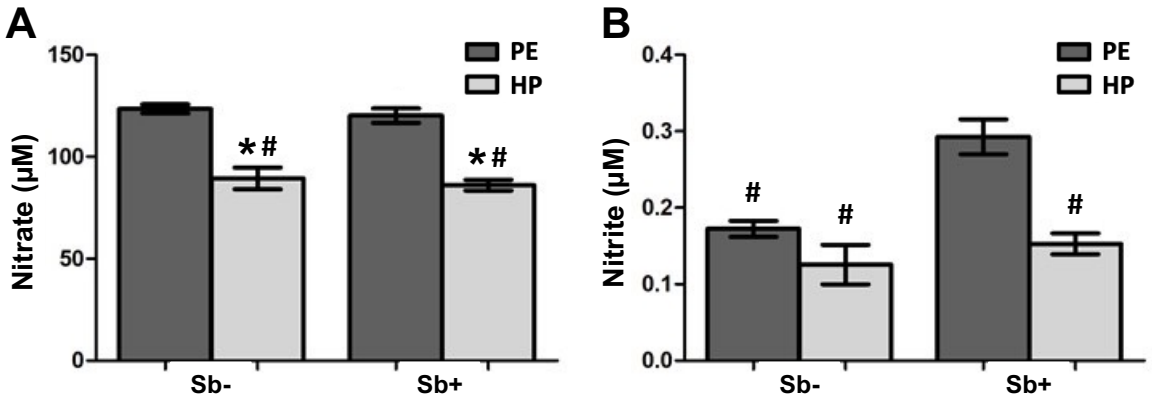

Figure 30. Nitrate (A) and nitrite (B) concentrations in HUVEC supernatants following 24hr incubation with PE and HP PBMC supernatants. Prior to HUVEC incubation, PBMCs were incubated +/- Silibinin (Sb). PE; preeclampsia, HP; healthy pregnant women. Data presented as mean ± SD. Statistical significance defined as $p<0.05$ vs *PE Sb-; #PE Sb+.

Considering that elevated oxidative stress and cytokines induce activation of HO-1, the expression of which exhibits antioxidant and anti-inflammatory properties, we next investigated if it played a role in the observed salutatory effects of Sb treatment. Indeed, higher levels of HO-1 were observed in HUVEC supernatants following incubation with Sb-treated PE-PBMCs vs non-treated PE-PBMCs (Figure 31). In accordance with our earlier findings, Sb treatment had no effect on HO-1 levels in HUVEC supernatants following incubation with HP PBMC supernatants. Based on the previous findings indicating increased oxidative stress and reduced NO bioavailability in HUVEC supernatants when incubated with PBMCs from PE vs HP women, we expected to observe a concomitant elevation of HO-1 levels. However, when PE vs HP PBMC supernatants were incubated with HUVEC, HO-1 levels were comparable (Figure 31), suggesting that Sb treatment provides a much-needed boost in HUVEC HO-1 induction in our model, following exposure to PE-PBMC supernatants.

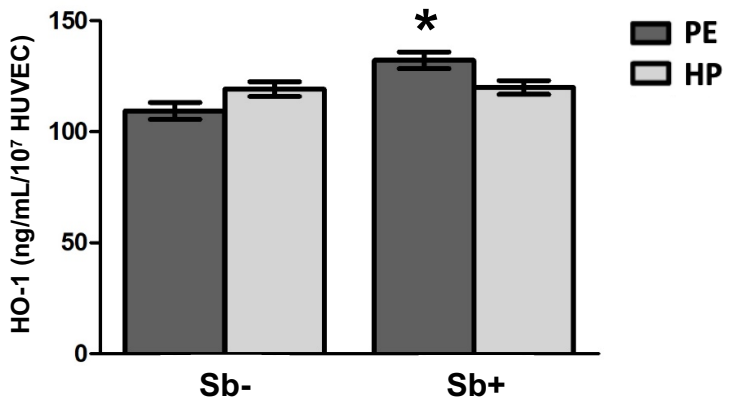

Figure 31. Heme-oxygenase 1 (HO-1) concentrations in HUVEC supernatants following 24hr incubation with PE- and HP-PBMC supernatants. Prior to HUVEC incubation, PBMCs were incubated +/- Silibinin (Sb). PE; preeclampsia, HP; healthy pregnant women. Data presented as mean ± SD. Statistical significance defined as $p<0.05$ vs *PE Sb-.

In summary, *study V* provides a glimpse into the complex interaction between monocytes and the endothelium in PE, whereby PBMCs from PE women have the capacity to mediate elevated oxidative stress and reduce NO bioavailability in HUVEC *in vitro*. Further, that the anti-inflammatory effects of Sb treatment on PBMCs alters their phenotype. This results in a less deleterious interaction between PBMC-derived factors and the endothelium, which is in part mediated via reduced secretion of pro-inflammatory cytokines and elevated endothelial HO-1 signalling. Further studies are warranted to confirm these findings, and to dissect the exact deleterious circulating factors released from PBMCs. In general, these findings support the role of monocyte-derived deleterious factors, including cytokines, in the propagation of the systemic state of oxidative stress via the endothelium. Finally, antioxidant approaches may be beneficial in reducing monocyte secretion of these factors, thus reduce this monocyte-mediation of PE pathogenesis.

4 CONCLUSIONS

Study I: Novel evidence that dietary nitrate is beneficial in the prevention of liver steatosis pathogenesis in a NOS-independent manner. These salutatory effects are mediated by modulation of AMPK signalling and reduction of NOX-derived oxidative stress. The outcome of which includes decreased synthesis of fatty acids, increased fatty acid oxidation, and ultimately decreased accumulation of lipids in the liver.

Study II: RBC eNOS *per se* is a key modulator of erythrocrine and endothelial function. A lack of RBC eNOS induces ED in adjacent vessels *ex vivo*. Mechanistically, this deleterious interaction is mediated in part via arginase and NOX-derived oxidative stress, which results in the disruption of the delicate balance between NO and ROS within the vascular microenvironment, leading to oxidative stress.

Study III: RBCs are novel mediators of the maternal systemic ED in PE. Exposure of healthy vessels to RBCs from PE induces ED via mechanisms including increased vascular oxidative stress and modulation of arginase activity. RBCs from PE patients have higher arginase activity and expression, which is correlated to disease severity, this suggests a novel association between RBC arginase and blood pressure.

Study IV: Dietary supplementation with concentrated nitrate-rich beetroot juice (~400mg nitrate) for 7-days was well accepted and considered safe in preeclamptic women, with no adverse events reported. Self-reported intake of juices aligned with plasma, saliva and urinary nitrate and nitrite levels. The findings from this pilot study will inform the planning of a larger full-scale RCT with sufficient sample sizes. Even utilising the most robust methodology, variability in blood pressure measurements in pregnant women is high. This will be addressed in future via estimation of effect size variability and by introducing other measures of vascular function, such as *in vivo* FMD, and by investigating microcirculatory function. Further research is warranted to examine the nitrate-independent effects on the interaction between RBCs and the endothelium in PE, which include appropriate controls.

Study V: Monocyte-derived deleterious factors, including cytokines, propagate the systemic state of oxidative stress via the endothelium in PE. Antioxidant approaches targeting this deleterious monocyte phenotype show therapeutic promise, resulting in reduction of monocyte-induced propagation of ED in PE.

5 POINTS OF PERSPECTIVE

The findings of the present thesis provide novel insights into the crucial intricate balance between NO signalling and oxidative stress in the ubiquitous mediation of multiple cardiometabolic sequelae. We provide further support for RBCs as important modulators of this delicate balance and potential drug targets for endothelial dysfunction, a novel observation in the context of PE. In addition, we highlighted the complexity of endothelial interactions with PBMCs in PE.

The use of dietary nitrate in the prevention of metabolic disease, specifically in the liver, is a promising therapeutic option due to its boosting of systemic NO bioavailability, and subsequent stimulation of cGMP/AMPK downstream signalling, as well as reducing NOX-derived oxidative stress. Since the publication of *study I*, our findings have been independently replicated by other groups[210,211] and further proposed mechanisms of the beneficial effects of dietary nitrate include increased adipocyte mitochondrial respiration and modulation of immune cell function[212], as well as reduced liver lipid content concomitant with decreased mitochondria-derived ROS generation[213]. In addition, dietary nitrate has been demonstrated to possess equipotent antidiabetic efficacy to metformin *in vivo*. However, nitrate was superior in the protection of vascular function and development of hypertension[214]. Importantly, the beneficial metabolic effects of inorganic nitrate and nitrite in health and disease have predominantly been observed in *in vivo* and *in vitro* experimental studies. Therefore, to assess their potential to combat the increasing global burden of metabolic diseases and associated comorbidities, clinical investigations are warranted to determine their preventative and therapeutic effects. Currently, clinical studies are recruiting for dietary nitrate intervention studies focused on T2D patients, specifically their exercise tolerance and *ex vivo* RBC function.

We provide further evidence for the RBC as a key player in the regulation of endothelial function; however much remains to be elucidated in this emerging field before they can be targeted *per se* in patients with vascular pathologies. Findings from the present thesis and other publications have begun to dissect the specific mechanisms by which RBCs and the endothelium interact, however, the identified key mechanistic players thus far are largely disease-specific, although elevated oxidative stress is commonplace. In studies investigating RBCs from T2D and COVID-19 patients, arginase has been associated with dysregulated erythrocrine function[202], the former independent from glycaemic control[132]. Similarly, we observed elevated RBC arginase activity in PE patients, which correlated with PE severity. We also demonstrated the role of RBC eNOS in this interaction, which was previously observed to independently regulate blood pressure experimentally *in vivo*[125]. Further clarification regarding the differing mechanisms between diseases is warranted before any future development of pharmacological targets focused on RBCs.

Future studies investigating the mechanistic interplay been RBCs and the endothelium should consider the following. First, further evidence is required to support RBC-induced ED *in vivo*. Although a strength of the *ex vivo* model used in the present thesis is that it facilitated the investigation of RBCs specifically on endothelial function, it is a reductionist approach when

considering the milieu of circulating factors which collectively impact the endothelium in a highly dynamic manner. This is especially true when considering the propagation of PE from stage 1 to stage 2 via the maternal circulation. However, this *ex vivo* approach will be beneficial for further mechanistic insight into the transmission of RBC-endothelial communication. We observed that the deleterious interaction between PE RBCs and the endothelium was contact-mediated, and indeed abnormal adhesion of RBCs, and in turn disruption of the cell-free zone, has been associated with vascular disorders, including sickle cell anaemia and T2Ds[215–217]. Other candidate routes of communication may include RBC export of signalling molecules via protein transport channels, diffusion of oxidative species, and RBC-derived extracellular vesicles.

During disease states RBCs are enriched with exosomes and microvesicles[218], the cargo of which has been shown to modulate arterial tone via reducing endothelial NO bioavailability and elevating oxidative stress[219]. In the context of PE, extracellular vesicles (exosomes and microvesicles) have been postulated to mediate maternal vascular dysfunction. Indeed a ~58% increase in RBC-derived microparticles in severe PE vs normotensive pregnant women was reported[220]. These have been shown to trigger the endothelium to release pro-inflammatory and pro-oxidative factors[221], reduce endothelial-dependent vasorelaxation *ex vivo* and reduce cell migration, endothelial barrier integrity and downregulate eNOS expression in human aortic ECs *in vitro*[222]. Further investigation into the characterisation of the cargo of RBC-derived extracellular vesicles and their impact on endothelial function in PE would be of interest.

Many questions remain from the findings of the current thesis regarding PE, leaving considerable scope for further investigation. A vicious cycle of systemic oxidative stress and inflammation are hallmark features of PE, however, the complex signalling relationship(s) of how RBCs and PBMC-derived factors, alongside other evidenced factors, interact to propagate them remains unknown. The lack of successful clinical studies further highlights this complexity. Further, assessment of the temporal dynamics of erythrocrine function alongside endothelial function in PE would be valuable to establish whether RBCs mainly act to initiate or propagate vascular dysfunction.

The risk factors and clinical manifestations of PE are predominately concerning the cardiovascular system, and the disease is associated with premature CVD in women[140]. ED has been demonstrated to precede the onset of the clinical manifestations and remain during pregnancy and 3 years postpartum[171]. The present thesis supports the maternal cardiovascular system being central to PE pathogenesis. It is widely accepted that circulating factors mediate PE pathogenesis between stages 1 and 2, and the studies within the present thesis expand this knowledge. Mechanistically, approaches to observing the isolated effects of these factors are valuable, however, their endothelial impact *in vivo* is the crucial next step for investigation. Although it remains a challenge to conduct robust clinical studies in this population, largely due to the heterogeneity, diagnostic challenges, and unpredictable nature of the disease, they are essential to develop much required therapeutic strategies.

6 ACKNOWLEDGEMENTS

My PhD has been an exciting, thoroughly educating, challenging journey, which would not have been possible without the following exceptional individuals.

First and foremost, thankyou to all the women who generously agreed to participate in the studies included in the thesis, this research would not have been possible without you.

A special thankyou to my principal supervisor; **Mattias Carlström**, for accepting and welcoming me into your research group, providing the opportunity to collaborate on fascinating projects, and challenging me to grow as a scientist – a truly formative experience.

Eddie Weitzberg, my co-supervisor, thank you for your support, love for scientific discussions and infectious optimism. Your kindness and expert guidance through both the highs and lows over the years has been invaluable.

Jon Lundberg, my co-supervisor, thank you for sharing your wealth of knowledge regarding NO. Your creative, enthusiastic, and down to earth approach towards scientific research has been a constant source of inspiration.

Rafael Krmar, my co-supervisor, in addition to your support and input throughout these years, thankyou for encouraging me to critically examine scientific ideological dogmas, I hope we can find time in the future for further discussions.

Josefine Naisell, thank you for the fantastic preeclampsia project collaboration – it has been a true pleasure navigating the logistics together. Thankyou for sharing your extensive knowledge of preeclampsia and clinical studies in general. Special thanks to all members (past and present) of the clinical team at Danderyd, your dedication to patient care and clinical research is greatly appreciated, it's been a privilege working with you all.

I extend my deepest gratitude to my mentor, **Eva Lindgren**. Your unwavering support throughout these years cannot be underestimated.

To all the group members past and present, thank you for fostering an inspiring and supportive lab environment, it has been a pleasure working with you all. **Drielle,** I am extremely grateful to have moved through the PhD years with you, we have been through it all and grown together – a true gift. **Michaela** (*mother nature*), thankyou for the support, wisdom, and silliness over the years – it has been a joy. **Zhuge,** thankyou for the wonderful collaborations, endless discussions regarding vascular physiology, and all the dumplings! **Tomas,** thankyou for being a consistently worthy opponent for debating every topic under the sun and, perhaps unintentionally, for always bringing levity to each day. **Annika,** thankyou for your guidance, your Swedish lessons and excellent musical taste! **Carina,** thankyou for the great collaboration within the PE projects, your technical knowledge was indispensable. **Andrei**, thankyou for the lengthy discussions next to the EPR, your enthusiasm and love for science is infectious. **Chiara**, thankyou for your guidance navigating the early PhD years, your drive and honesty.

Isa, thankyou for taking me under your wing during my first year, teaching me important techniques and allowing me to contribute to your projects.

To **Julia**, thankyou for the Ingarö days on the lake, and for the consistent support and perspective. To **Hannah** and **Mum**, thankyou for your unwavering support, love, and encouragement – I am forever grateful to have two strong women guiding me through life.

Finally, to **Alex**, my other half – thankyou. You jumped into this Swedish adventure with me and navigated it with impressive ease. You've witnessed all facets of this PhD from the outside, providing consistent unconditional love and support. I am forever grateful.

7 REFERENCES

1. Kannel WB, Hjortland M, Castelli WP. Role of diabetes in congestive heart failure: The Framingham study. *Am J Cardiol* 1974;**34**:29–34.

2. Kannel WB, McGee DL. Diabetes and cardiovascular risk factors: the Framingham study. *Circulation* 1979;**59**:8–13.

3. Wilson PWF, D'Agostino RB, Parise H, Sullivan L, Meigs JB. Metabolic Syndrome as a Precursor of Cardiovascular Disease and Type 2 Diabetes Mellitus. *Circulation* 2005;**112**:3066–3072.

4. Dagenais GR, Leong DP, Rangarajan S, Lanas F, Lopez-Jaramillo P, Gupta R, Diaz R, Avezum A, Oliveira GBF, Wielgosz A, Parambath SR, Mony P, Alhabib KF, Temizhan A, Ismail N, Chifamba J, Yeates K, Khatib R, Rahman O, Zatonska K, Kazmi K, Wei L, Zhu J, Rosengren A, Vijayakumar K, Kaur M, Mohan V, Yusufali A, Kelishadi R, Teo KK, et al. Variations in common diseases, hospital admissions, and deaths in middle-aged adults in 21 countries from five continents (PURE): a prospective cohort study. *Lancet* Elsevier Ltd; 2020;**395**:785–794.

5. Zhou B, Carrillo-Larco RM, Danaei G, Riley LM, Paciorek CJ, Stevens GA, Gregg EW, Bennett JE, Solomon B, Singleton RK, Sophiea MK, Iurilli ML, Lhoste VP, Cowan MJ, Savin S, Woodward M, Balanova Y, Cifkova R, Damasceno A, Elliott P, Farzadfar F, He J, Ikeda N, Kengne AP, Khang YH, Kim HC, Laxmaiah A, Lin HH, Margozzini Maira P, Miranda JJ, et al. Worldwide trends in hypertension prevalence and progress in treatment and control from 1990 to 2019: a pooled analysis of 1201 population-representative studies with 104 million participants. *Lancet* 2021;**398**:957–980.

6. Roth GA, Mensah GA, Johnson CO, Addolorato G, Ammirati E, Baddour LM, Barengo NC, Beaton AZ, Benjamin EJ, Benziger CP, Bonny A, Brauer M, Brodmann M, Cahill TJ, Carapetis J, Catapano AL, Chugh SS, Cooper LT, Coresh J, Criqui M, DeCleene N, Eagle KA, Emmons-Bell S, Feigin VL, Fernández-Solà J, Fowkes G, Gakidou E, Grundy SM, He FJ, Howard G, et al. Global Burden of Cardiovascular Diseases and Risk Factors, 1990–2019. *J Am Coll Cardiol* 2020;**76**:2982–3021.

7. He J, Zhu Z, Bundy JD, Dorans KS, Chen J, Hamm LL. Trends in Cardiovascular Risk Factors in US Adults by Race and Ethnicity and Socioeconomic Status, 1999-2018. *JAMA - J Am Med Assoc* 2021;**326**:1286–1298.

8. The GBD 2015 Obesity Collaborators. Health Effects of Overweight and Obesity in 195 Countries over 25 Years. *N Engl J Med* 2017;**377**:13–27.

9. Khan MAB, Hashim MJ, King JK, Govender RD, Mustafa H, Kaabi J Al. Epidemiology of Type 2 Diabetes – Global Burden of Disease and Forecasted Trends. *J Epidemiol Glob Health* 2019;**10**:107.

10. Mosenzon O, Alguwaihes A, Leon JLA, Bayram F, Darmon P, Davis TME, Dieuzeide G, Eriksen KT, Hong T, Kaltoft MS, Lengyel C, Rhee NA, Russo GT, Shirabe S, Urbancova K, Vencio S. CAPTURE: a multinational, cross-sectional study of cardiovascular disease prevalence in adults with type 2 diabetes across 13 countries. *Cardiovasc Diabetol* BioMed Central; 2021;**20**:154.

11. Jung YM, Oh GC, Noh E, Lee H-Y, Oh M-J, Park JS, Jun JK, Lee SM, Cho GJ. Pre-pregnancy blood pressure and pregnancy outcomes: a nationwide population-based study. *BMC Pregnancy Childbirth* BioMed Central; 2022;**22**:226.

12. Davidson AJF, Park AL, Berger H, Aoyama K, Harel Z, Cook JL, Ray JG. Risk of severe maternal morbidity or death in relation to elevated hemoglobin A1c preconception, and in early pregnancy: A population-based cohort study. Stock SJ, ed. *PLOS Med* 2020;**17**:e1003104.

13. Ray JG, Vermeulen MJ, Schull MJ, Redelmeier DA. Cardiovascular health after maternal placental syndromes (CHAMPS): Population-based retrospective cohort study. *Lancet* 2005;**366**:1797–1803.

14. Bellamy L, Casas J-P, Hingorani AD, Williams DJ. Pre-eclampsia and risk of cardiovascular disease and cancer in later life: systematic review and meta-analysis. *Bmj* 2007;**335**:974–974.

15. Wilson BJ, Watson MS, Prescott GJ, Sunderland S, Campbell DM, Hannaford P, Smith WCS. Hypertensive diseases of pregnancy and risk of hypertension and stroke in later life: results from cohort study. *BMJ* 2003;**326**:845.

16. Perak AM, Lancki N, Kuang A, Labarthe DR, Allen NB, Shah SH, Lowe LP, Grobman WA, Lawrence JM, Lloyd-Jones DM, Lowe WL, Scholtens DM. Associations of Maternal Cardiovascular Health in Pregnancy With Offspring Cardiovascular Health in Early Adolescence. *JAMA* 2021;**325**:658.

17. Saei Ghare Naz M, Sheidaei A, Aflatounian A, Azizi F, Ramezani Tehrani F. Does Adding Adverse Pregnancy Outcomes Improve the Framingham Cardiovascular Risk Score in Women? Data from the Tehran Lipid and Glucose Study. *J Am Heart Assoc* 2022;**11**.

18. Löhn M, Dubrovska G, Lauterbach B, Luft FC, Gollasch M, Sharma AM. Periadventitial fat releases a vascular relaxing factor. *FASEB J* 2002;**16**:1057–1063.

19. Verlohren S, Dubrovska G, Tsang S-Y, Essin K, Luft FC, Huang Y, Gollasch M. Visceral Periadventitial Adipose Tissue Regulates Arterial Tone of Mesenteric Arteries. *Hypertension* 2004;**44**:271–276.

20. Targonski P V., Bonetti PO, Pumper GM, Higano ST, Holmes DR, Lerman A. Coronary endothelial dysfunction is associated with an increased risk of cerebrovascular events. *Circulation* 2003;**107**:2805–2809.

21. Martinez-Majander N, Gordin D, Joutsi-Korhonen L, Salopuro T, Adeshara K, Sibolt G, Curtze S, Pirinen J, Liebkind R, Soinne L, Sairanen T, Sinisalo J, Lehto M, Groop PH, Tatlisumak T, Putaala J. Endothelial dysfunction is associated with early-onset cryptogenic ischemic stroke in men and with increasing age. *J Am Heart Assoc* 2021;**10**.

22. Panza JA, Quyyumi AA, Brush JE, Epstein SE. Abnormal Endothelium-Dependent Vascular Relaxation in Patients with Essential Hypertension. *N Engl J Med* Massachusetts Medical Society; 1990;**323**:22–27.

23. Brush JE, Faxon DP, Salmon S, Jacobs AK, Ryan TJ. Abnormal endothelium-dependent coronary vasomotion in hypertensive patients. *J Am Coll Cardiol* 1992;**19**:809–815.

24. Shechter M, Matetzky S, Prasad M, Goitein O, Goldkorn R, Naroditsky M, Koren-Morag N, Lerman A. Endothelial function predicts 1-year adverse clinical outcome in patients hospitalized in the emergency department chest pain unit. *Int J Cardiol* Netherlands; 2017;**240**:14–19.

25. Kubo SH, Rector TS, Bank AJ, Williams RE, Heifetz SM. Endothelium-dependent vasodilation is attenuated in patients with heart failure. *Circulation* 1991;**84**:1589–1596.

26. Taqueti VR, Solomon SD, Shah AM, Desai AS, Groarke JD, Osborne MT, Hainer J, Bibbo CF, Dorbala S, Blankstein R, Carli MF Di. Coronary microvascular dysfunction and future risk of heart failure with preserved ejection fraction. *Eur Heart J* 2018;**39**:840–849.

27. Brevetti G, Silvestro A, Schiano V, Chiariello M. Endothelial Dysfunction and Cardiovascular Risk Prediction in Peripheral Arterial Disease: Additive Value of Flow-Mediated Dilation to Ankle-Brachial Pressure Index. *Circulation* 2003;**108**:2093–2098.

28. Matsuzawa Y, Sugiyama S, Sumida H, Sugamura K, Nozaki T, Ohba K, Matsubara J, Kurokawa H, Fujisue K, Konishi M, Akiyama E, Suzuki H, Nagayoshi Y, Yamamuro M, Sakamoto K, Iwashita S, Jinnouchi H, Taguri M, Morita S, Matsui K, Kimura K, Umemura S, Ogawa H. Peripheral endothelial function and cardiovascular events in high-risk patients. *J Am Heart Assoc* 2013;**2**:1–21.

29. McVeigh GE, Brennan GM, Johnston GD, McDermott BJ, McGrath LT, Henry WR, Andrews JW, Hayes JR. Impaired endothelium-dependent and independent vasodilation in patients with Type 2 (non-insulin-dependent) diabetes mellitus. *Diabetologia* 1992;**35**:771–776.

30. Nitenberg A, Ledoux S, Valensi P, Sachs R, Attali J-R, Antony I. Impairment of Coronary Microvascular Dilation in Response to Cold Pressor–Induced Sympathetic Stimulation in Type 2 Diabetic Patients With Abnormal Stress Thallium Imaging. *Diabetes* 2001;**50**:1180–1185.

31. Al-hamoudi W, Alsadoon A, Hassanian M, Alkhalidi H, Abdo A, Nour M, Halwani R, Sanai F, Alsharaabi A, Alswat K, Hersi A, Albenmousa A, Alsaif F. Endothelial dysfunction in nonalcoholic steatohepatitis with low cardiac disease risk. *Sci Rep* Springer US; 2020;**10**:1–7.

32. Colak Y, Senates E, Yesil A, Yilmaz Y, Ozturk O, Doganay L, Coskunpinar E, Kahraman OT, Mesci B, Ulasoglu C, Tuncer I. Assessment of endothelial function in patients with nonalcoholic fatty liver disease. *Endocrine* 2013;**43**:100–107.

33. Mannaerts D, Faes E, Gielis J, Craenenbroeck E Van, Cos P, Spaanderman M, Gyselaers W, Cornette J, Jacquemyn Y. Oxidative stress and endothelial function in normal pregnancy versus pre-eclampsia, a combined longitudinal and case control study. *BMC Pregnancy Childbirth* BMC Pregnancy and Childbirth; 2018;**18**:1–9.

34. Resende Guimarães MFB de, Brandão AHF, Lima Rezende CA de, Cabral ACV, Brum AP, Leite HV, Capuruço CAB. Assessment of endothelial function in pregnant women with preeclampsia and gestational diabetes mellitus by flow-mediated dilation of brachial artery. *Arch Gynecol Obstet* 2014;**290**:441–447.

35. Aird WC. Phenotypic heterogeneity of the endothelium: II. Representative vascular beds. *Circ Res* 2007;**100**:174–190.

36. Sandoo A, Veldhuijzen van Zanten JJCS, Metsios GS, Carroll D, Kitas GD. The Endothelium and Its Role in Regulating Vascular Tone. *Open Cardiovasc Med J* 2010;**4**:302–312.

37. Furchgott R, Zawadski J V. The obligatory role of endothelial cells in the relaxation of atrial smooth muscle. *Nature* 1980;**288**:373–376.

38. Widlansky ME, Gokce N, Keaney JF, Vita JA. The clinical implications of endothelial dysfunction. *J Am Coll Cardiol* 2003;**42**:1149–1160.

39. Kalucka J, Rooij LPMH de, Goveia J, Rohlenova K, Dumas SJ, Meta E, Conchinha N V., Taverna F, Teuwen L-A, Veys K, García-Caballero M, Khan S, Geldhof V, Sokol L, Chen R, Treps L, Borri M, Zeeuw P de, Dubois C, Karakach TK, Falkenberg KD, Parys M, Yin X, Vinckier S, Du Y, Fenton RA, Schoonjans L, Dewerchin M, Eelen G, Thienpont B, et al. Single-Cell Transcriptome Atlas of Murine Endothelial Cells. *Cell* 2020;**180**:764-779.e20.

40. Pinheiro-de-Sousa I, Fonseca-Alaniz MH, Teixeira SK, Rodrigues M V., Krieger JE. Uncovering emergent phenotypes in endothelial cells by clustering of surrogates of cardiovascular risk factors. *Sci Rep* Nature Publishing Group UK; 2022;**12**:1372.

41. Moncada S, Higgs EA. The discovery of nitric oxide and its role in vascular biology. *Br J Pharmacol* 2006;**147**:S193–S201.

42. Lundberg JO, Gladwin MT, Weitzberg E. Strategies to increase nitric oxide signalling in cardiovascular disease. *Nat Rev Drug Discov* Nature Publishing Group; 2015;**14**:623–641.

43. Farah C, Michel LYM, Balligand J-L. Nitric oxide signalling in cardiovascular health and disease. *Nat Rev Cardiol* Nature Publishing Group; 2018;

44. Freedman JE, Sauter R, Battinelli EM, Ault K, Knowles C, Huang PL, Loscalzo J. Deficient Platelet-Derived Nitric Oxide and Enhanced Hemostasis in Mice Lacking the NOSIII Gene. *Circ Res* 1999;**84**:1416–1421.

45. Moroi M, Zhang L, Yasuda T, Virmani R, Gold HK, Fishman MC, Huang PL. Interaction of genetic deficiency of endothelial nitric oxide, gender, and pregnancy in vascular response to injury in mice. *J Clin Invest* 1998;**101**:1225–1232.

46. Huang PL, Huang Z, Mashimo H, Bloch KD, Moskowitz MA, Bevan JA, Fishman MC. Hypertension in mice lacking the gene for endothelial nitric oxide synthase. *Nature* 1995;**377**:239–242.

47. Kawashima S, Yokoyama M. Dysfunction of endothelial nitric oxide synthase and atherosclerosis. *Arterioscler Thromb Vasc Biol* 2004;**24**:998–1005.

48. Nakayama T, Sato W, Yoshimura A, Zhang L, Kosugi T, Campbell-Thompson M, Kojima H, Croker BP, Nakagawa T. Endothelial von Willebrand Factor Release Due to eNOS Deficiency Predisposes to Thrombotic Microangiopathy in Mouse Aging Kidney. *Am J Pathol* American Society for Investigative Pathology; 2010;**176**:2198–2208.

49. Huang Z, Huang PL, Ma J, Meng W, Ayata C, Fishman MC, Moskowitz MA. Enlarged infarcts in endothelial nitric oxide synthase knockout mice are attenuated by nitro-L-arginine. *J Cereb Blood Flow Metab* 1996;**16**:981–987.

50. Atochin DN, Wang A, Liu VWT, Critchlow JD, Dantas AP V., Looft-Wilson R, Murata T, Salomone S, Shin HK, Ayata C, Moskowitz MA, Michel T, Sessa WC, Huang PL. The phosphorylation state of eNOS modulates vascular reactivity and outcome of cerebral ischemia in vivo. *J Clin Invest* 2007;**117**:1961–1967.

51. Pannirselvam M, Verma S, Anderson TJ, Triggle CR. Cellular basis of endothelial dysfunction in small mesenteric arteries from spontaneously diabetic (db/db −/−) mice: role of decreased tetrahydrobiopterin bioavailability. *Br J Pharmacol* 2002;**136**:255–263.

52. Li Q, Atochin D, Kashiwagi S, Earle J, Wang A, Mandeville E, Hayakawa K, D'Uscio L V., Lo EH, Katusic Z, Sessa W, Huang PL. Deficient eNOS Phosphorylation Is a Mechanism for Diabetic Vascular Dysfunction Contributing to Increased Stroke Size. *Stroke* 2013;**44**:3183–3188.

53. González-Sánchez JL, Martínez-Larrad MT, Sáez ME, Zabena C, Martínez-Calatrava MJ, Serrano-Ríos M. Endothelial Nitric Oxide Synthase Haplotypes Are Associated with Features of Metabolic Syndrome. *Clin Chem* 2007;**53**:91–97.

54. Monti LD, Barlassina C, Citterio L, Galluccio E, Berzuini C, Setola E, Valsecchi G, Lucotti P, Pozza G, Bernardinelli L, Casari G, Piatti P. Endothelial Nitric Oxide Synthase Polymorphisms Are Associated With Type 2 Diabetes and the Insulin Resistance Syndrome. *Diabetes* 2003;**52**:1270–1275.

55. Nozaki Y, Fujita K, Wada K, Yoneda M, Shinohara Y, Imajo K, Ogawa Y, Kessoku T, Nakamuta M, Saito S, Masaki N, Nagashima Y, Terauchi Y, Nakajima A. Deficiency of eNOS exacerbates early-stage NAFLD pathogenesis by changing the fat distribution. *BMC Gastroenterol* BMC Gastroenterology; 2015;**15**:177.

56. Cunningham RP, Moore MP, Dashek RJ, Meers GM, Takahashi T, Sheldon RD, Wheeler AA, Diaz-Arias A, Ibdah JA, Parks EJ, Thyfault JP, Rector RS. Critical Role for Hepatocyte-Specific eNOS in NAFLD and NASH. *Diabetes* 2021;**70**:2476–2491.

57. Steinberg GR, Carling D. AMP-activated protein kinase: the current landscape for drug development. *Nat Rev Drug Discov* Springer US; 2019;**18**:527–551.

58. Mount PF, Kemp BE, Power DA. Regulation of endothelial and myocardial NO synthesis by multi-site eNOS phosphorylation. *J Mol Cell Cardiol* 2007;**42**:271–279.

59. Huang PL. eNOS, metabolic syndrome and cardiovascular disease. *Trends Endocrinol Metab* 2009;**20**:295–302.

60. Tricker AR, Preussmann R. Carcinogenic N-nitrosamines in the diet: occurrence, formation, mechanisms and carcinogenic potential. *Mutat Res Toxicol* 1991;**259**:277–289.

61. Green LC, Ruiz de Luzuriaga K, Wagner DA, Rand W, Istfan N, Young VR, Tannenbaum SR. Nitrate biosynthesis in man. *Proc Natl Acad Sci* 1981;**78**:7764–7768.

62. Moncada S, Higgs A. The L-Arginine-Nitric Oxide Pathway. *N Engl J Med* Massachusetts Medical Society; 1993;**329**:2002–2012.

63. Zweier JL, Wang P, Samouilov A, Kuppusamy P. Enzyme-independent formation of nitric oxide in biological tissues. *Nat Med* 1995;**1**:804–809.

64. Lundberg JO, Weitzberg E, Gladwin MT. The nitrate–nitrite–nitric oxide pathway in physiology and therapeutics. *Nat Rev Drug Discov* 2008;**7**:156–167.

65. Lundberg JO, Govoni M. Inorganic nitrate is a possible source for systemic generation of nitric oxide. *Free Radic Biol Med* 2004;**37**:395–400.

66. Carlström M, Liu M, Yang T, Zollbrecht C, Huang L, Peleli M, Borniquel S, Kishikawa H, Hezel M, Persson AEG, Weitzberg E, Lundberg JO. Cross-talk Between Nitrate-Nitrite-NO and NO Synthase Pathways in Control of Vascular NO Homeostasis. *Antioxid Redox Signal* 2015;**23**:295–306.

67. Larsen FJ, Ekblom B, Sahlin K, Lundberg JO, Weitzberg E. Effects of Dietary Nitrate on Blood Pressure in Healthy Volunteers. *N Engl J Med* 2006;**355**:2792–2793.

68. Webb AJ, Patel N, Loukogeorgakis S, Okorie M, Aboud Z, Misra S, Rashid R, Miall P, Deanfield J, Benjamin N, MacAllister R, Hobbs AJ, Ahluwalia A. Acute blood pressure lowering, vasoprotective, and antiplatelet properties of dietary nitrate via bioconversion to nitrite. *Hypertension* 2008;**51**:784–790.

69. Siervo M, Lara J, Ogbonmwan I, Mathers JC. Inorganic Nitrate and Beetroot Juice Supplementation Reduces Blood Pressure in Adults: A Systematic Review and Meta-Analysis. *J Nutr* 2013;**143**:818–826.

70. Ashor AW, Lara J, Siervo M. Medium-term effects of dietary nitrate supplementation on systolic and diastolic blood pressure in adults. *J Hypertens* 2017;**35**:1353–1359.

71. Kleinbongard P, Dejam A, Lauer T, Rassaf T, Schindler A, Picker O, Scheeren T, Gödecke A, Schrader J, Schulz R, Heusch G, Schaub GA, Bryan NS, Feelisch M, Kelm M. Plasma nitrite reflects constitutive nitric oxide synthase activity in mammals. *Free Radic Biol Med* 2003;**35**:790–796.

72. Heiss C, Meyer C, Totzeck M, Hendgen-Cotta UB, Heinen Y, Luedike P, Keymel S, Ayoub N, Lundberg JO, Weitzberg E, Kelm M, Rassaf T. Dietary inorganic nitrate mobilizes circulating angiogenic cells. *Free Radic Biol Med* Elsevier Inc.; 2012;**52**:1767–1772.

73. Stokes KY, Dugas TR, Tang Y, Garg H, Guidry E, Bryan NS. Dietary nitrite prevents hypercholesterolemic microvascular inflammation and reverses endothelial dysfunction. *Am J Physiol - Hear Circ Physiol* 2009;**296**:1281–1288.

74. Sindler AL, Fleenor BS, Calvert JW, Marshall KD, Zigler ML, Lefer DJ, Seals DR. Nitrite supplementation reverses vascular endothelial dysfunction and large elastic artery stiffness with aging. *Aging Cell* 2011;**10**:429–437.

75. Bahrami LS, Arabi SM, Feizy Z, Rezvani R. The effect of beetroot inorganic nitrate supplementation on cardiovascular risk factors: A systematic review and meta-regression of randomized controlled trials. *Nitric Oxide* Elsevier Inc.; 2021;**115**:8–22.

76. Gehr P. Swiss Medical Weekly Young Investigator's Award 2003: Clustering of cardiovascular risk factors mimicking the human metabolic syndrome X in eNOS null mice. *Swiss Med Wkly* Switzerland; 2004;**134**:267.

77. Balon TW, Jasman AP, Young JC. Effects of Chronic Nω-Nitro-l-arginine Methyl Ester Administration on Glucose Tolerance and Skeletal Muscle Glucose Transport in the Rat. *Nitric Oxide* 1999;**3**:312–320.

78. Carlström M, Larsen FJ, Nyström T, Hezel M, Borniquel S, Weitzberg E, Lundberg JO. Dietary inorganic nitrate reverses features of metabolic syndrome in endothelial nitric oxide synthase-deficient mice. *Proc Natl Acad Sci* 2010;**107**:17716–17720.

79. Wickman A, Klintland N, Gan L, Sakinis A, Söderling A-S, Bergström G, Caidahl K. A technique to estimate the rate of whole body nitric oxide formation in conscious mice. *Nitric Oxide* 2003;**9**:77–85.

80. Ohtake K, Nakano G, Ehara N, Sonoda K, Ito J, Uchida H, Kobayashi J. Dietary nitrite supplementation improves insulin resistance in type 2 diabetic KKAy mice. *Nitric Oxide* Elsevier Inc.; 2015;**44**:31–38.

81. Khalifi S, Rahimipour A, Jeddi S, Ghanbari M, Kazerouni F, Ghasemi A. Dietary nitrate improves glucose tolerance and lipid profile in an animal model of hyperglycemia. *Nitric Oxide* Elsevier Inc.; 2015;**44**:24–30.

82. Li T, Lu X, Sun Y, Yang X. Effects of spinach nitrate on insulin resistance, endothelial dysfunction markers and inflammation in mice with high-fat and high-fructose consumption. *Food Nutr Res* 2016;**60**:32010.

83. Gheibi S, Jeddi S, Carlström M, Gholami H, Ghasemi A. Effects of long-term nitrate supplementation on carbohydrate metabolism, lipid profiles, oxidative stress, and inflammation in male obese type 2 diabetic rats. *Nitric Oxide* Elsevier; 2018;**75**:27–41.

84. Lundberg JO, Carlström M, Weitzberg E. Metabolic Effects of Dietary Nitrate in Health and Disease. *Cell Metab* 2018;**28**:9–22.

85. Younossi ZM, Koenig AB, Abdelatif D, Fazel Y, Henry L, Wymer M. Global epidemiology of nonalcoholic fatty liver disease-Meta-analytic assessment of prevalence, incidence, and outcomes. *Hepatology* 2016;**64**:73–84.

86. Ohtake K, Ehara N, Chiba H, Nakano G, Sonoda K, Ito J, Uchida H, Kobayashi J. Dietary nitrite reverses features of postmenopausal metabolic syndrome induced by high-fat diet and ovariectomy in mice. *Am J Physiol Metab* 2017;**312**:E300–E308.

87. Wang H, Hu L, Li L, Wu X, Fan Z, Zhang C, Wang J, Jia J, Wang S. Inorganic nitrate alleviates the senescence-related decline in liver function. *Sci China Life Sci* 2018;**61**:24–34.

88. Kina-Tanada M, Sakanashi M, Tanimoto A, Kaname T, Matsuzaki T, Noguchi K, Uchida T, Nakasone J, Kozuka C, Ishida M, Kubota H, Taira Y, Totsuka Y, Kina S ichiro, Sunakawa H, Omura J, Satoh K, Shimokawa H, Yanagihara N, Maeda S, Ohya Y, Matsushita M, Masuzaki H, Arasaki A, Tsutsui M. Long-term dietary nitrite and nitrate deficiency causes the metabolic syndrome, endothelial dysfunction and cardiovascular death in mice. *Diabetologia* Diabetologia; 2017;**60**:1138–1151.

89. Gilchrist M, Winyard PG, Aizawa K, Anning C, Shore A, Benjamin N. Effect of dietary nitrate on blood pressure, endothelial function, and insulin sensitivity in type 2 diabetes. *Free Radic Biol Med* Elsevier; 2013;**60**:89–97.

90. Herzig S, Shaw RJ. AMPK: guardian of metabolism and mitochondrial homeostasis. *Nat Rev Mol Cell Biol* Nature Publishing Group; 2018;**19**:121–135.

91. Liu Y, Wan Q, Guan Q, Gao L, Zhao J. High-fat diet feeding impairs both the expression and activity of AMPKa in rats' skeletal muscle. *Biochem Biophys Res Commun* 2006;**339**:701–707.

92. Lindholm CR, Ertel RL, Bauwens JD, Schmuck EG, Mulligan JD, Saupe KW. A high-fat diet decreases AMPK activity in multiple tissues in the absence of hyperglycemia or systemic inflammation in rats. *J Physiol Biochem* 2013;**69**:165–175.

93. Peleli M, Hezel M, Zollbrecht C, Persson AEG, Lundberg JO, Weitzberg E, Fredholm BB, Carlström M. In adenosine A2B knockouts acute treatment with inorganic nitrate improves glucose disposal, oxidative stress, and AMPK signaling in the liver. *Front Physiol* Frontiers Media SA; 2015;**6**:222.

94. Lai Y-C, Tabima DM, Dube JJ, Hughan KS, Vanderpool RR, Goncharov DA, Croix CM St., Garcia-Ocaña A, Goncharova EA, Tofovic SP, Mora AL, Gladwin MT. SIRT3–AMP-Activated Protein Kinase Activation by Nitrite and Metformin Improves Hyperglycemia and Normalizes Pulmonary Hypertension Associated With Heart Failure With Preserved Ejection Fraction. *Circulation* 2016;**133**:717–731.

95. Jiang H, Torregrossa AC, Potts A, Pierini D, Aranke M, Garg HK, Bryan NS. Dietary nitrite improves insulin signaling through GLUT4 translocation. *Free Radic Biol Med* Elsevier; 2014;**67**:51–57.

96. Gheibi S, Bakhtiarzadeh F, Jeddi S, Farrokhfall K, Zardooz H, Ghasemi A. Nitrite increases glucose-stimulated insulin secretion and islet insulin content in obese type 2 diabetic male rats. *Nitric Oxide* Elsevier Inc; 2017;**64**:39–51.

97. Ohtake K, Nakano G, Ehara N, Sonoda K, Ito J, Uchida H, Kobayashi J. Dietary nitrite supplementation improves insulin resistance in type 2 diabetic KKAy mice. *Nitric Oxide - Biol Chem* Elsevier Inc.; 2015;**44**:31–38.

98. Hezel M, Peleli M, Liu M, Zollbrecht C, Jensen BL, Checa A, Giulietti A, Wheelock CE, Lundberg JO, Weitzberg E, Carlström M. Dietary nitrate improves age-related hypertension and metabolic abnormalities in rats via modulation of angiotensin II receptor signaling and inhibition of superoxide generation. *Free Radic Biol Med* Pergamon; 2016;**99**:87–98.

99. Thomas SR, Witting PK, Drummond GR. Redox Control of Endothelial Function and Dysfunction: Molecular Mechanisms and Therapeutic Opportunities. *Antioxid Redox Signal* 2008;**10**:1713–1766.

100. Drummond GR, Selemidis S, Griendling KK, Sobey CG. Combating oxidative stress in vascular disease: NADPH oxidases as therapeutic targets. *Nat Rev Drug Discov* 2011;**10**:453–471.

101. Li H, Horke S, Förstermann U. Oxidative stress in vascular disease and its pharmacological prevention. *Trends Pharmacol Sci* 2013;**34**:313–319.

102. Incalza MA, D'Oria R, Natalicchio A, Perrini S, Laviola L, Giorgino F. Oxidative stress and reactive oxygen species in endothelial dysfunction associated with cardiovascular and metabolic diseases. *Vascul Pharmacol* Elsevier; 2018;**100**:1–19.

103. Chen Q, Wang Q, Zhu J, Xiao Q, Zhang L. Reactive oxygen species: Key regulators in vascular health and diseases. *Br J Pharmacol* 2017;1279–1292.

104. Pernow J, Jung C. Arginase as a potential target in the treatment of cardiovascular disease: reversal of arginine steal? *Cardiovasc Res* 2013;**98**:334–343.

105. Daiber A, Oelze M, Daub S, Steven S, Schuff A, Kröller-Schön S, Hausding M, Wenzel P, Schulz E, Gori T, Münzel T. Vascular Redox Signaling, Redox Switches in Endothelial Nitric Oxide Synthase (eNOS Uncoupling), and Endothelial Dysfunction. In: Laher I, ed. *Systems Biology of Free Radicals and Antioxidants* Berlin, Heidelberg: Springer Berlin Heidelberg; 2014. p. 1177–1211.

106. Yachie A, Niida Y, Wada T, Igarashi N, Kaneda H, Toma T, Ohta K, Kasahara Y, Koizumi S. Oxidative stress causes enhanced endothelial cell injury in human heme oxygenase-1 deficiency. *J Clin Invest* 1999;**103**:129–135.

107. Yet S-F, Layne MD, Liu X, Chen Y-H, Ith B, Sibinga NES, Perrella MA. Absence of heme oxygenase-1 exacerbates atherosclerotic lesion formation and vascular remodeling. *FASEB J* 2003;**17**:1759–1761.

108. True AL, Olive M, Boehm M, San H, Westrick RJ, Raghavachari N, Xu X, Lynn EG, Sack MN, Munson PJ, Gladwin MT, Nabel EG. Heme oxygenase-1 deficiency accelerates formation of arterial thrombosis through oxidative damage to the endothelium, which is rescued by inhaled carbon monoxide. *Circ Res* 2007;**101**:893–901.

109. Heiss EH, Schachner D, Werner ER, Dirsch VM. Active NF-E2-related Factor (Nrf2) Contributes to Keep Endothelial NO Synthase (eNOS) in the Coupled State. *J Biol Chem* Â© 2009 ASBMB. Currently published by Elsevier Inc; originally published by American Society for Biochemistry and Molecular Biology.; 2009;**284**:31579–31586.

110. Jiang F, Roberts SJ, Datla SR, Dusting GJ. NO Modulates NADPH Oxidase Function Via Heme Oxygenase-1 in Human Endothelial Cells. *Hypertension* 2006;**48**:950–957.

111. Turkseven S, Kruger A, Mingone CJ, Kaminski P, Inaba M, Rodella LF, Ikehara S, Wolin MS, Abraham NG. Antioxidant mechanism of heme oxygenase-1 involves an increase in superoxide dismutase and catalase in experimental diabetes. *Am J Physiol Circ Physiol* 2005;**289**:H701–H707.

112. Pawloski JR, Hess DT, Stamler JS. Export by red blood cells of nitric oxide bioactivity. *Nature* 2001;**409**:622–626.

113. Dietrich HH, Ellsworth ML, Sprague RS, Dacey RG. Red blood cell regulation of microvascular tone through adenosine triphosphate. *Am J Physiol Circ Physiol* 2000;**278**:H1294–H1298.

114. Pernow J, Mahdi A, Yang J, Zhou Z. Red blood cell dysfunction: a new player in cardiovascular disease. *Cardiovasc Res* 2019;**115**:1596–1605.

115. Mahdi A, Cortese-Krott MM, Kelm M, Li N, Pernow J. Novel perspectives on redox signaling in red blood cells and platelets in cardiovascular disease. *Free Radic Biol Med* Elsevier Inc.; 2021;**168**:95–109.

116. Jia L, Bonaventura C, Bonaventura J, Stamler JS. S-nitrosohaemoglobin: a dynamic activity of blood involved in vascular control. *Nature* 1996;**380**:221–226.

117. Herold S. The outer-sphere oxidation of nitrosyliron(II)hemoglobin by peroxynitrite leads to the release of nitrogen monoxide. *Inorg Chem* 2004;**43**:3783–3785.

118. Kleschyov AL. The NO-heme signaling hypothesis. *Free Radic Biol Med* Elsevier B.V.; 2017;**112**:544–552.

119. Cosby K, Partovi KS, Crawford JH, Patel RP, Reiter CD, Martyr S, Yang BK, Waclawiw MA, Zalos G, Xu X, Huang KT, Shields H, Kim-Shapiro DB, Schechter AN, Cannon RO, Gladwin MT. Nitrite reduction to nitric oxide by deoxyhemoglobin vasodilates the human circulation. *Nat Med* 2003;**9**:1498–1505.

120. Nagababu E, Ramasamy S, Abernethy DR, Rifkind JM. Active Nitric Oxide Produced in the Red Cell under Hypoxic Conditions by Deoxyhemoglobin-mediated Nitrite Reduction. *J Biol Chem* 2003;**278**:46349–46356.

121. Aamand R, Dalsgaard T, Jensen FB, Simonsen U, Roepstorff A, Fago A. Generation of nitric oxide from nitrite by carbonic anhydrase: A possible link between metabolic activity and vasodilation. *Am J Physiol - Hear Circ Physiol* 2009;**297**:2068–2074.

122. Kleinbongard P, Schulz R, Rassaf T, Lauer T, Dejam A, Jax T, Kumara I, Gharini P, Kabanova S, Özüyaman B, Schnürch HG, Gödecke A, Weber AA, Robenek M, Robenek H, Bloch W, Rösen P, Kelm M. Red blood cells express a functional endothelial nitric oxide synthase. *Blood* 2006;**107**:2943–2951.

123. Cortese-Krott MM, Kelm M. Endothelial nitric oxide synthase in red blood cells: Key to a new erythrocrine function? *Redox Biol* Elsevier; 2014;**2**:251–258.

124. Wood KC, Cortese-Krott MM, Kovacic JC, Noguchi A, Liu VB, Wang X, Raghavachari N, Boehm M, Kato GJ, Kelm M, Gladwin MT. Circulating blood endothelial nitric oxide synthase contributes to the regulation of systemic blood pressure and nitrite homeostasis. *Arterioscler Thromb Vasc Biol* 2013;**33**:1861–1871.

125. Leo F, Suvorava T, Heuser SK, Li J, LoBue A, Barbarino F, Piragine E, Schneckmann R, Hutzler B, Good ME, Fernandez BO, Vornholz L, Rogers S, Doctor A, Grandoch M, Stegbauer J, Weitzberg E, Feelisch M, Lundberg JO, Isakson BE, Kelm M, Cortese-Krott MM. Red Blood Cell and Endothelial eNOS Independently Regulate Circulating Nitric Oxide Metabolites and Blood Pressure. *Circulation* 2021;**144**:870–889.

126. Yang J, Gonon AT, Sjoquist P-O, Lundberg JO, Pernow J. Arginase regulates red blood cell nitric oxide synthase and export of cardioprotective nitric oxide bioactivity. *Proc Natl Acad Sci* 2013;**110**:15049–15054.

127. Merx MW, Gorressen S, Sandt AM Van De, Cortese-Krott MM, Ohlig J, Stern M, Rassaf T, Gödecke A, Gladwin MT, Kelm M. Depletion of circulating blood NOS3 increases severity of myocardial infarction and left ventricular dysfunction. *Basic Res Cardiol* 2014;**109**:1–10.

128. Silva DGH, Belini Junior E, Almeida EA de, Bonini-Domingos CR. Oxidative stress in sickle cell disease: An overview of erythrocyte redox metabolism and current antioxidant therapeutic strategies. *Free Radic Biol Med* Elsevier; 2013;**65**:1101–1109.

129. George A, Pushkaran S, Konstantinidis DG, Koochaki S, Malik P, Mohandas N, Zheng Y, Joiner CH, Kalfa TA. Erythrocyte NADPH oxidase activity modulated by Rac GTPases, PKC, and plasma cytokines contributes to oxidative stress in sickle cell disease. *Blood* 2013;**121**:2099–2107.

130. Devrim E, Ergüder İB, Özbek H, Durak İ. High-cholesterol diet increases xanthine oxidase and decreases nitric oxide synthase activities in erythrocytes from rats. *Nutr Res* 2008;**28**:212–215.

131. Yang J, Zheng X, Mahdi A, Zhou Z, Tratsiakovich Y, Jiao T, Kiss A, Kövamees O, Alvarsson M, Catrina SB, Lundberg JO, Brismar K, Pernow J. Red Blood Cells in Type 2 Diabetes Impair Cardiac Post-Ischemic Recovery Through an Arginase-Dependent Modulation of Nitric Oxide Synthase and Reactive Oxygen Species. *JACC Basic to Transl Sci* 2018;**3**:450–463.

132. Zhou Z, Kövamees O, Zahorán S, Hedin U, Alvarsson M, Hermesz E, Tratsiakovich Y, Nordin F, Mahdi A, Lundberg JO, Yang J, Östenson C-G, Pernow J, Uribe Gonzalez AE, Andersson DC. Erythrocytes From Patients With Type 2 Diabetes Induce Endothelial Dysfunction Via Arginase I. *J Am Coll Cardiol* 2018;**72**:769–780.

133. Mahdi A, Tengbom J, Alvarsson M, Wernly B, Zhou Z, Pernow J. Red Blood Cell Peroxynitrite Causes Endothelial Dysfunction in Type 2 Diabetes Mellitus via Arginase. *Cells* 2020;**9**.

134. Pernow J, Jung C. The Emerging Role of Arginase in Endothelial Dysfunction in Diabetes. *Curr Vasc Pharmacol* 2016;**14**:155–162.

135. ACOG. Gestational Hypertension and Preeclampsia. *Obstet Gynecol* 2020;**135**:e237–e260.

136. Abalos E, Cuesta C, Grosso AL, Chou D, Say L. Global and regional estimates of preeclampsia and eclampsia: A systematic review. *Eur J Obstet Gynecol Reprod Biol* Elsevier Ireland Ltd; 2013;**170**:1–7.

137. Ananth C V., Keyes KM, Wapner RJ. Pre-eclampsia rates in the United States, 1980-2010: Age-period-cohort analysis. *BMJ* 2013;**347**:1–9.

138. Say L, Chou D, Gemmill A, Tunçalp Ö, Moller AB, Daniels J, Gülmezoglu AM, Temmerman M, Alkema L. Global causes of maternal death: A WHO systematic analysis. *Lancet Glob Heal* 2014;**2**:323–333.

139. Souza JP, Gülmezoglu AM, Vogel J, Carroli G, Lumbiganon P, Qureshi Z, Costa MJ, Fawole B, Mugerwa Y, Nafiou I, Neves I, Wolomby-Molondo J-J, Bang HT, Cheang K, Chuyun K, Jayaratne K, Jayathilaka CA, Mazhar SB, Mori R, Mustafa ML, Pathak LR, Perera D, Rathavy T, Recidoro Z, Roy M, Ruyan P, Shrestha N, Taneepanichsku S, Tien NV, Ganchimeg T, et al. Moving beyond essential interventions for reduction of maternal mortality (the WHO Multicountry Survey on Maternal and Newborn Health): a cross-sectional study. *Lancet* 2013;**381**:1747–1755.

140. Grandi SM, Filion KB, Yoon S, Ayele HT, Doyle CM, Hutcheon JA, Smith GN, Gore GC, Ray JG, Nerenberg K, Platt RW. Cardiovascular Disease-Related Morbidity and Mortality in Women With a History of Pregnancy Complications. *Circulation* 2019;**139**:1069–1079.

141. Parikh NI, Gonzalez JM, Anderson CAM, Judd SE, Rexrode KM, Hlatky MA, Gunderson EP, Stuart JJ, Vaidya D. Adverse Pregnancy Outcomes and Cardiovascular Disease Risk: Unique Opportunities for Cardiovascular Disease Prevention in Women: A Scientific Statement From the American Heart Association. *Circulation* 2021;**143**:E902–E916.

142. Brown MC, Best KE, Pearce MS, Waugh J, Robson SC, Bell R. Cardiovascular disease risk in women with pre-eclampsia: systematic review and meta-analysis. *Eur J Epidemiol* 2013;**28**:1–19.

143. Wang Z, Wang Z, Wang L, Qiu M, Wang Y, Hou X, Guo Z, Wang B. Hypertensive disorders during pregnancy and risk of type 2 diabetes in later life: a systematic review and meta-analysis. *Endocrine* Springer US; 2017;**55**:809–821.

144. Davis EF, Lazdam M, Lewandowski AJ, Worton SA, Kelly B, Kenworthy Y, Adwani S, Wilkinson AR, McCormick K, Sargent I, Redman C, Leeson P. Cardiovascular Risk Factors in Children and Young Adults Born to Preeclamptic Pregnancies: A Systematic Review. *Pediatrics* 2012;**129**:e1552–e1561.

145. Lazdam M, la Horra A de, Pitcher A, Mannie Z, Diesch J, Trevitt C, Kylintireas I, Contractor H, Singhal A, Lucas A, Neubauer S, Kharbanda R, Alp N, Kelly B, Leeson P. Elevated Blood Pressure in Offspring Born Premature to Hypertensive Pregnancy. *Hypertension* 2010;**56**:159–165.

146. Redman CWG. Pre-eclampsia and the placenta. *Placenta* 1991;**12**:301–308.

147. Staff AC. The two-stage placental model of preeclampsia: An update. *J Reprod Immunol* 2019;**134**–**135**:1–10.

148. Chaiworapongsa T, Chaemsaithong P, Yeo L, Romero R. Pre-eclampsia part 1: Current understanding of its pathophysiology. *Nat Rev Nephrol* Nature Publishing Group; 2014;**10**:466–480.

149. Duley L, Meher S, Hunter KE, Seidler AL, Askie LM. Antiplatelet agents for preventing pre-eclampsia and its complications. *Cochrane Database Syst Rev* 2019;**2019**.

150. Chaiworapongsa T, Chaemsaithong P, Korzeniewski SJ, Yeo L, Romero R. Pre-eclampsia part 2: Prediction, prevention and management. *Nat Rev Nephrol* Nature Publishing Group; 2014;**10**:531–540.

151. Chappell LC, Cluver CA, Kingdom J, Tong S. Pre-Eclampsia. 2021;13–15.

152. Malha L, August P. Safety of Antihypertensive Medications in Pregnancy: Living With Uncertainty. *J Am Heart Assoc* 2019;**8**:1–3.

153. Webster LM, Conti-Ramsden F, Seed PT, Webb AJ, Nelson-Piercy C, Chappell LC. Impact of antihypertensive treatment on maternal and perinatal outcomes in pregnancy complicated by chronic hypertension: A systematic review and meta-analysis. *J Am Heart Assoc* 2017;**6**.

154. Magee LA, Dadelszen P von, Rey E, Ross S, Asztalos E, Murphy KE, Menzies J, Sanchez J, Singer J, Gafni A, Gruslin A, Helewa M, Hutton E, Lee SK, Lee T, Logan AG, Ganzevoort W, Welch R, Thornton JG, Moutquin J-M. Less-Tight versus Tight Control of Hypertension in Pregnancy. *N Engl J Med* 2015;**372**:407–417.

155. Garovic VD, Dechend R, Easterling T, Karumanchi SA, Baird SMM, Magee LA, Rana S, Vermunt J V., August P. Hypertension in Pregnancy: Diagnosis, Blood Pressure Goals, and Pharmacotherapy: A Scientific Statement From the American Heart Association. *Hypertension* 2022;**79**:E21–E41.

156. Wang Y, Walsh SW. Placental mitochondria as a source of oxidative stress in pre-eclampsia. *Placenta* 1998;**19**:581–586.

157. Cui* X-L, Brockman D, Campos B, L. Myatt. Expression of NADPH Oxidase Isoform 1 (Nox1) in Human Placenta: Involvement in Preeclampsia. *Placenta* 2006;**27**:422–431.

158. Myatt L, Cui X. Oxidative stress in the placenta. *Histochem Cell Biol* 2004;**122**:369–382.

159. González-Garrido Chem JA, Olivares-Corichi IM, Tovar-Rodriguez JM, Hernández-Santana NA, Méndez-Bolaina E, Ceballos-Reyes GM, García-Sánchez JR. Influence of the at 2 receptor on the L-arginine-nitric oxide pathway and effects of (-)-epicatechin on HUVECs from women with preeclampsia. *J Hum Hypertens* 2013;**27**:355–361.

160. Many A, Hubel CA, Fisher SJ, Roberts JM, Zhou Y. Invasive cytotrophoblasts manifest evidence of oxidative stress in preeclampsia. *Am J Pathol* 2000;**156**:321–331.

161. Mitchell B, Cook L, Danchuk S, Puschett J. Uncoupled Endothelial Nitric Oxide Synthase and Oxidative Stress in a Rat Model of Pregnancy-Induced Hypertension. *Am J Hypertens* 2007;**20**:1297–1304.

162. Uzun H, Benian A, Madazli R, Topçuoğlu MA, Aydin S, Albayrak M. Circulating oxidized low-density lipoprotein and paraoxonase activity in preeclampsia. *Gynecol Obstet Invest* 2005;**60**:195–200.

163. Hubel CA. Oxidative Stress in the Pathogenesis of Preeclampsia. *Soc Exp Biol Med* 1999;

164. Vaughan JE, Walsh SW. Oxidative stress reproduces placental abnormalities of preeclampsia. *Hypertens Pregnancy* 2002;**21**:205–223.

165. Vadillo-Ortega F, Perichart-Perera O, Espino S, Avila-Vergara MA, Ibarra I, Ahued R, Godines M, Parry S, MacOnes G, Strauss JF. Effect of supplementation during pregnancy with l-arginine and antioxidant vitamins in medical food on preeclampsia in high-risk population: Randomized controlled trial. *Obstet Gynecol Surv* 2011;**66**:537–539.

166. Conde-Agudelo A, Romero R. Supplementation with vitamins C and E during pregnancy for the prevention of preeclampsia: a systematic review and meta-analysis. *Am J Obstet Gynecol* Elsevier Inc.; 2009;**201**:S285.

167. Zullino S, Buzzella F, Simoncini T. Nitric oxide and the biology of pregnancy. *Vascul Pharmacol* Elsevier; 2018;**110**:71–74.

168. Schiessl B, Strasburger C, Bidlingmaier M, Mylonas I, Jeschke U, Kainer F, Friese K. Plasma- and urine concentrations of nitrite/nitrate and cyclic Guanosinemonophosphate in intrauterine growth restricted and preeclamptic pregnancies. *Arch Gynecol Obstet* 2006;**274**:150–154.

169. Choi JW, Im MW, Pai SH. Nitric oxide production increases during normal pregnancy and decreases in preeclampsia. *Ann Clin Lab Sci* 2002;**32**:257–263.

170. Sandrim VC, Montenegro MF, Palei ACT, Metzger IF, Sertorio JTC, Cavalli RC, Tanus-Santos JE. Increased circulating cell-free hemoglobin levels reduce nitric oxide bioavailability in preeclampsia. *Free Radic Biol Med* Elsevier Inc.; 2010;**49**:493–500.

171. Weissgerber TL, Milic NM, Milin-Lazovic JS, Garovic VD. Impaired Flow-Mediated Dilation Before, During, and After Preeclampsia. *Hypertension* 2016;**67**:415–423.

172. Burke SD, Zsengellér ZK, Khankin E V., Lo AS, Rajakumar A, DuPont JJ, McCurley A, Moss ME, Zhang D, Clark CD, Wang A, Seely EW, Kang PM, Stillman IE, Jaffe IZ, Karumanchi SA. Soluble FMS-like Tyrosine Kinase 1 promotes angiotensin II sensitivity in preeclampsia. *J Clin Invest* 2016;**126**:2561–2574.

173. Myers J, Mires G, Macleod M, Baker P. In Preeclampsia, the Circulating Factors Capable of Altering In Vitro Endothelial Function Precede Clinical Disease. *Hypertension* 2005;**45**:258–263.

174. Hayman R, Warren A, Brockelsby J, Johnson I, Baker P. Plasma from women with pre-eclampsia induces an in vitro alteration in the endothelium-dependent behaviour of myometrial resistance arteries. *BJOG An Int J Obstet Gynaecol* 2000;**107**:108–115.

175. Konijnenberg A, Stokkers EW, Post JAM Van der, Schaap MCL, Boer K, Bleker OP, Sturk A. Extensive platelet activation in preeclampsia compared with normal pregnancy: Enhanced expression of cell adhesion molecules. *Am J Obstet Gynecol* 1997;**176**:461–469.

176. Khalil A, Hardman L, O'Brien P. The role of arginine, homoarginine and nitric oxide in pregnancy. *Amino Acids* Springer Vienna; 2015;**47**:1715–1727.

177. Groten T, Lehmann T, Schleußner E. Does Pentaerytrithyltetranitrate reduce fetal growth restriction in pregnancies complicated by uterine mal-perfusion? Study protocol of the PETN-study: a randomized controlled multicenter-trial. *BMC Pregnancy Childbirth* BMC Pregnancy and Childbirth; 2019;**19**:336.

178. Meher S, Duley L. Nitric oxide for preventing pre-eclampsia and its complications. *Cochrane Database Syst Rev* 2007;**2010**.

179. Ferreira RD da S, Negrini R, Bernardo WM, Simões R, Piato S. The effects of sildenafil in maternal and fetal outcomes in pregnancy: A systematic review and meta-analysis. Rosenfeld CS, ed. *PLoS One* 2019;**14**:e0219732.

180. Sharp A, Cornforth C, Jackson R, Harrold J, Turner MA, Kenny LC, Baker PN, Johnstone ED, Khalil A, Dadelszen P von, Papageorghiou AT, Alfirevic Z, Agarwal U, Willis E, Mammarella S, Masson G, Aquilina J, Greco E, Higgins S, Vinayagam D, Shaw L, Stephens L, Howe D, Rand A, Patni S, Mousa T, Rabab A, Russell H, Hannon T, Fenn A, et al. Maternal sildenafil for severe fetal growth restriction (STRIDER): a multicentre, randomised, placebo-controlled, double-blind trial. *Lancet Child Adolesc Heal* 2018;**2**:93–102.

181. Hawkes N. Trial of Viagra for fetal growth restriction is halted after baby deaths. *BMJ* BMJ Publishing Group Ltd; 2018;**362**.

182. Grosser N, Abate A, Oberle S, Vreman HJ, Dennery PA, Becker JC, Pohle T, Seidman DS, Schröder H. Heme oxygenase-1 induction may explain the antioxidant profile of aspirin. *Biochem Biophys Res Commun* 2003;**308**:956–960.

183. Helgadottir H, Tropea T, Gizurarson S, Meiri H, Mandalà M. Aspirin causes endothelium-dependent vasodilation of resistance arteries from non-gravid and gravid rats. *Pregnancy Hypertens* Elsevier; 2019;**15**:141–145.

184. Gonçalves-Rizzi VH, Possomato-Vieira JS, Sales Graça TU, Nascimento RA, Dias-Junior CA. Sodium nitrite attenuates hypertension-in-pregnancy and blunts increases in soluble fms-like tyrosine kinase-1 and in vascular endothelial growth factor. *Nitric Oxide - Biol Chem* Academic Press; 2016;**57**:71–78.

185. Bosch M van den, Wijnen J, Linde I van de, Wesel A van, Melchior D, Kemp B, Clouard C, Brand H van den. Effects of maternal dietary nitrate supplementation during the perinatal period on piglet survival, body weight, and litter uniformity. *Transl Anim Sci* Elsevier Ltd; 2019;**129**:1–7.

186. Volino-Souza M, Oliveira GV De, Alvares TS. A single dose of beetroot juice improves endothelial function but not tissue oxygenation in pregnant women: A randomised clinical trial. *Br J Nutr* 2018;**120**:1006–1013.

187. Ormesher L, Myers JE, Chmiel C, Wareing M, Greenwood SL, Tropea T, Lundberg JO, Weitzberg E, Nihlen C, Sibley CP, Johnstone ED, Cottrell EC. Effects of dietary nitrate supplementation, from beetroot juice, on blood pressure in hypertensive pregnant women: A randomised, double-blind, placebo-controlled feasibility trial. *Nitric Oxide - Biol Chem* Elsevier; 2018;**80**:37–44.

188. Tropea T, Renshall LJ, Nihlen C, Weitzberg E, Lundberg JO, David AL, Tsatsaris V, Stuckey DJ, Wareing M, Greenwood SL, Sibley CP, Cottrell EC. Beetroot juice lowers blood pressure and improves endothelial function in pregnant eNOS−/− mice: importance of nitrate-independent effects. *J Physiol* 2020;**598**:4079–4092.

189. Brown MA, Magee LA, Kenny LC, Karumanchi SA, McCarthy FP, Saito S, Hall DR, Warren CE, Adoyi G, Ishaku S. The hypertensive disorders of pregnancy: ISSHP classification, diagnosis; management recommendations for international practice. *Pregnancy Hypertens* 2018;**13**:291–310.

190. Yang T, Zollbrecht C, Winerdal ME, Zhuge Z, Zhang X, Terrando N, Checa A, Sällström J, Wheelock CE, Winqvist O, Harris RA, Larsson E, Persson AEG, Fredholm BB, Carlström M. Genetic Abrogation of Adenosine A 3 Receptor Prevents Uninephrectomy and High Salt–Induced Hypertension. *J Am Heart Assoc* 2016;**5**.

191. Montenegro MF, Sundqvist ML, Nihlén C, Hezel M, Carlström M, Weitzberg E, Lundberg JO. Profound differences between humans and rodents in the ability to concentrate salivary nitrate: Implications for translational research. *Redox Biol* Elsevier; 2016;**10**:206–210.

192. Berkowitz DE, White R, Li D, Minhas KM, Cernetich A, Kim S, Burke S, Shoukas AA, Nyhan D, Champion HC, Hare JM. Arginase Reciprocally Regulates Nitric Oxide Synthase Activity and Contributes to Endothelial Dysfunction in Aging Blood Vessels. *Circulation* 2003;**108**:2000–2006.

193. Kapil V, Khambata RS, Robertson A, Caulfield MJ, Ahluwalia A. Dietary Nitrate Provides Sustained Blood Pressure Lowering in Hypertensive Patients: A Randomized, Phase 2, Double-Blind, Placebo-Controlled Study. *Hypertension* 2015;**65**:320–327.

194. Bondonno CP, Liu AH, Croft KD, Considine MJ, Puddey IB, Woodman RJ, Hodgson JM. Antibacterial mouthwash blunts oral nitrate reduction and increases blood pressure in treated hypertensive men and women. *Am J Hypertens* 2015;**28**:572–575.

195. Lara J, Ashor AW, Oggioni C, Ahluwalia A, Mathers JC, Siervo M. Effects of inorganic nitrate and beetroot supplementation on endothelial function: a systematic review and meta-analysis. *Eur J Nutr* Springer Berlin Heidelberg; 2016;**55**:451–459.

196. Diehl AM, Day C. Cause, Pathogenesis, and Treatment of Nonalcoholic Steatohepatitis. Longo DL, ed. *N Engl J Med* 2017;**377**:2063–2072.

197. Gao X, Yang T, Liu M, Peleli M, Zollbrecht C, Weitzberg E, Lundberg JO, Persson AEG, Carlstrom M. NADPH oxidase in the renal microvasculature is a primary target for blood pressure-lowering effects by inorganic nitrate and nitrite. *Hypertension* 2015;**65**:161–170.

198. Montenegro MF, Amaral JH, Pinheiro LC, Sakamoto EK, Ferreira GC, Reis RI, Marçal DMO, Pereira RP, Tanus-Santos JE. Sodium nitrite downregulates vascular NADPH oxidase and exerts antihypertensive effects in hypertension. *Free Radic Biol Med* 2011;**51**:144–152.

199. Choudhury M, Qadri I, Rahman SM, Schroeder-Gloeckler J, Janssen RC, Friedman JE. C/EBPβ is AMP kinase sensitive and up-regulates PEPCK in response to ER stress in hepatoma cells. *Mol Cell Endocrinol* 2011;**331**:102–108.

200. Donadee C, Raat NJH, Kanias T, Tejero J, Lee JS, Kelley EE, Zhao X, Liu C, Reynolds H, Azarov I, Frizzell S, Meyer EM, Donnenberg AD, Qu L, Triulzi D, Kim-Shapiro DB, Gladwin MT. Nitric oxide scavenging by red blood cell microparticles and cell-free hemoglobin as a mechanism for the red cell storage lesion. *Circulation* 2011;**124**:465–476.

201. Smeds E, Romantsik O, Jungner Å, Erlandsson L, Gram M. Pathophysiology of extracellular haemoglobin: use of animal models to translate molecular mechanisms into clinical significance. *ISBT Sci Ser* 2017;**12**:134–141.

202. Mahdi A, Collado A, Tengbom J, Jiao T, Wodaje T, Johansson N, Farnebo F, Färnert A, Yang J, Lundberg JO, Zhou Z, Pernow J. Erythrocytes Induce Vascular Dysfunction in COVID-19. *JACC Basic to Transl Sci* 2022;**7**.

203. Roberts JM, Taylor RN, Musci TJ, Rodgers GM, Hubel CA, McLaughlin MK. Preeclampsia: An endothelial cell disorder. *Am J Obstet Gynecol* 1989;**161**:1200–1204.

204. Faas MM, Vos P de. Maternal monocytes in pregnancy and preeclampsia in humans and in rats. *J Reprod Immunol* Elsevier Ireland Ltd; 2017;**119**:91–97.

205. Harmon AC, Cornelius DC, Amaral LM, Faulkner JL, Cunningham MW, Wallace K, LaMarca B. The role of inflammation in the pathology of preeclampsia. *Clin Sci* 2016;**130**:409–419.

206. Abenavoli L, Izzo AA, Milić N, Cicala C, Santini A, Capasso R. Milk thistle (Silybum marianum): A concise overview on its chemistry, pharmacological, and nutraceutical uses in liver diseases. *Phyther Res* 2018;**32**:2202–2213.

207. Matias ML, Gomes VJ, Romao-Veiga M, Ribeiro VR, Nunes PR, Romagnoli GG, Peracoli JC, Peracoli MTS. Silibinin Downregulates the NF-κB Pathway and NLRP1/NLRP3 Inflammasomes in Monocytes from Pregnant Women with Preeclampsia. *Molecules* 2019;**24**:1548.

208. Souza CO de, Peraçoli MTS, Weel IC, Bannwart CF, Romão M, Nakaira-Takahagi É, Medeiros LTL de, Silva MG da, Peraçoli JC. Hepatoprotective and anti-inflammatory effects of silibinin on experimental preeclampsia induced by l-NAME in rats. *Life Sci* Elsevier Inc.; 2012;**91**:159–165.

209. Leikert JF, Räthel TR, Müller C, Vollmar AM, Dirsch VM. Reliable in vitro measurement of nitric oxide released from endothelial cells using low concentrations of the fluorescent probe 4,5-diaminofluorescein. *FEBS Lett* 2001;**506**:131–134.

210. Liu Y, Croft KD, Caparros-Martin J, O'Gara F, Mori TA, Ward NC. Beneficial effects of inorganic nitrate in non-alcoholic fatty liver disease. *Arch Biochem Biophys* Elsevier Inc.; 2021;**711**:109032.

211. Sonoda K, Kono Y, Kitamori K, Ohtake K, Shiba S, Kasono K, Kobayashi J. Beneficial Effects of Dietary Nitrite on a Model of Nonalcoholic Steatohepatitis Induced by High-Fat/High-Cholesterol Diets in SHRSP5/Dmcr Rats: A Preliminary Study. *Int J Mol Sci* 2022;**23**:2931.

212. Peleli M, Ferreira DMS, Tarnawski L, McCann Haworth S, Xuechen L, Zhuge Z, Newton PT, Massart J, Chagin AS, Olofsson PS, Ruas JL, Weitzberg E, Lundberg JO, Carlström M. Dietary nitrate attenuates high-fat diet-induced obesity via mechanisms involving higher adipocyte respiration and alterations in inflammatory status. *Redox Biol* Elsevier B.V.; 2020;**28**:101–387.

213. DesOrmeaux GJ, Petrick HL, Brunetta HS, Holloway GP. Independent of mitochondrial respiratory function, dietary nitrate attenuates HFD-induced lipid accumulation and mitochondrial ROS emission within the liver. *Am J Physiol Metab* 2021;**321**:E217–E228.

214. Cordero-Herrera I, Guimarães DD, Moretti C, Zhuge Z, Han H, McCann Haworth S, Uribe Gonzalez AE, Andersson DC, Weitzberg E, Lundberg JO, Carlström M. Head-to-head comparison of inorganic nitrate and metformin in a mouse model of cardiometabolic disease. *Nitric Oxide* Elsevier; 2020;**97**:48–56.

215. Hebbel RP, Boogaerts MAB, Eaton JW, Steinberg MH. Erythrocyte Adherence to Endothelium in Sickle-Cell Anemia. *N Engl J Med* 1980;**302**:992–995.

216. Wautier J-L, Paton RC, Wautier M-P, Pintigny D, Abadie E, Passa P, Caen JP. Increased Adhesion of Erythrocytes to Endothelial Cells in Diabetes Mellitus and Its Relation to Vascular Complications. *N Engl J Med* 1981;**305**:237–242.

217. Kaliyaperumal R, Deng X, Meiselman HJ, Song H, Dalan R, Leow MK-S, Neu B. Depletion interaction forces contribute to erythrocyte-endothelial adhesion in diabetes. *Biochem Biophys Res Commun* 2019;**516**:144–148.

218. Thangaraju K, Neerukonda SN, Katneni U, Buehler PW. Extracellular Vesicles from Red Blood Cells and Their Evolving Roles in Health, Coagulopathy and Therapy. *Int J Mol Sci* 2020;**22**:153.

219. Poisson J, Tanguy M, Davy H, Camara F, Mdawar M-B El, Kheloufi M, Dagher T, Devue C, Lasselin J, Plessier A, Merchant S, Blanc-Brude O, Souyri M, Mougenot N, Dingli F, Loew D, Hatem SN, James C, Villeval J-L, Boulanger CM, Rautou P-E. Erythrocyte-derived microvesicles induce arterial spasms in JAK2V617F myeloproliferative neoplasm. *J Clin Invest* 2020;**130**:2630–2643.

220. Thangaraju K, Neerukonda SN, Katneni U, Buehler PW. Extracellular Vesicles from Red Blood Cells and Their Evolving Roles in Health, Coagulopathy and Therapy. *Int J Mol Sci* Elsevier B.V.; 2020;**22**:153.

221. Tannetta D, Collett G, Vatish M, Redman C, Sargent I. Syncytiotrophoblast extracellular vesicles – Circulating biopsies reflecting placental health. *Placenta* Elsevier Ltd; 2017;**52**:134–138.

222. Murugesan S, Hussey H, Saravanakumar L, Sinkey RG, Sturdivant AB, Powell MF, Berkowitz DE. Extracellular Vesicles From Women With Severe Preeclampsia Impair Vascular Endothelial Function. *Anesth Analg* 2022;**134**:713–723.